Inaugural dissertation

for

obtaining the doctoral degree

of the

Combined Faculty of Mathematics, Engineering and Natural Sciences

of the

Ruprecht - Karls – University

Heidelberg

Presented by

M.Sc. Sarah Richtmann

born in: Remscheid, Germany
Oral examination: 24.10.2022

The role of the pregnancy-associated protein glycodelin and its influence on the immune system in non-small-cell lung cancer

Referees:
Prof. Dr. Ursula Klingmüller
Prof. Dr. Holger Sültmann

Content

List of figures

List of tables

List of abbreviations

ADC	Adenocarcinoma
BSA	Bovine serum albumin
C	Control
CD	Cluster of differentiation
cDNA	complementary deoxyribonucleic acid
cRNA	complementary ribonucleic acid
C_T	Threshold cycle
CTLA-4	Cytotoxic T lymphocyte associated protein 4
CXCL	C-X-C motif chemokine
ddH_20	Double-distilled water
ECOG	Eastern Cooperative Oncology Group
EGFR	Epidermal growth factor receptor
EMT	Epithelial to mesenchymal transition
ESD	Esterase D
Gd	Glycodelin
GrzB	Granzyme B
hCG	human choriogonadotropin
HR	Hazard ratio
HRP	Horseradish peroxidase
Ig	Immunoglobulin
IL	Interleukin
iNOS	Inducible nitric oxide synthase
IPA	Ingenuity Pathway Analysis
LCC	Large cell carcinoma
MIQE	Minimum information for publication of qPCR data
N/A	Not available
NK	Natural killer
ns	Not significant
NSCLC	Non-small cell lung cancer
OS	Overall survival
qPCR	Quantitative Polymerase Chain Reaction
RPS18	40S Ribosomal Protein S18
PAEP	Progesterone-associated endometrial protein

PAGE	Polyacrylamide gel electrophoresis
PD-L1	Programmed death ligand 1
PFS	Progression-free survival
RIN	RNA integrity number
RPS18	40S ribosomal protein S18
SCLC	Small cell lung cancer
siRNA	Small interfering RNA
SQCC	Squamous cell carcinoma
TGF-β	Transforming growth factor β
Th1	Type 1 helper T cells
Th2	Type 2 helper T cells
TSA	Tyramide-signal amplification
TKI	Tyrosine kinase inhibitor
UPL	Universal probe library
v/v	volume/volume
VEGF	Vascular endothelial growth factor
w/v	weight/volume

Zusammenfassung

Lungenkrebs ist nach wie vor die Hauptursache für krebsbedingte Todesfälle weltweit. Jüngste Entwicklungen in der Immuntherapie versprechen eine Wende bei frühen und fortgeschrittenen Erkrankungen, indem sie das Immunsystem reaktivieren. Die derzeitigen immuntherapeutischen Ansätze können jedoch nicht bei allen Patienten angewandt werden. Insbesondere Frauen leiden häufig unter schweren Nebenwirkungen oder sprechen nicht erfolgreich auf die Behandlung an.

Glycodelin ist ein Glykoprotein, das für die Entstehung und Aufrechterhaltung einer Schwangerschaft entscheidend ist. Glycodelin A, eine von vier Glykosylierungsformen, unterdrückt das mütterliche Immunsystem und ermöglicht es der befruchteten Eizelle, in das Dezidualgewebe einzudringen. Während der Schwangerschaft moduliert es die Immunumgebung an der feto-maternalen Schnittstelle, um Abwehrmechanismen gegenüber dem Fötus als Semi-Allotransplantat zu verhindern. Interessanterweise wurde in Lungentumoren im Vergleich zu normalem Lungengewebe auch eine hohe Glycodelin-Proteinkonzentration und entsprechende *progesterone-associated endometrial protein* (*PAEP*)-Genexpression entdeckt.

Im Rahmen dieses Projekts habe ich untersucht, ob Glycodelin in nicht-kleinzelligem Lungenkarzinom (NSCLC) die aus der Schwangerschaft bekannte immunsuppressive Funktion von Glycodelin A teilt und daher als neues Ziel für zukünftige Immuntherapien dienen könnte.

Für meine Studie habe ich die primären Zelllinien 4950T und 170162T verwendet, die zwischen 20-100 ng/ml Glycodelin in den Zellkulturüberstand sezernieren. Die Glykosylierungsstruktur wurde durch Lektin-basierte Anreicherung analysiert und konnte zeigen, dass das von NSCLC stammende Glykodelin dem Glykosylierungsmuster des aus Fruchtwasser isolierten Glykodelin A ähnelt. Die Proteine wiesen eine hohe Sialylierung auf, die bekanntermaßen für die Immunsuppression entscheidend ist. Hier waren die Sialylketten in Glycodelin aus 170162T schwächer ausgeprägt, einer NSCLC-Zelllinie, die von einem männlichen Patienten stammt. Somit könnte das Protein geschlechtsspezifische Strukturen und Funktionen haben. *In vitro* wurde das NSCLC assoziierte Glycodelin von Immunzellen gebunden und internalisiert. Es löste keine Apoptose aus, beeinflusste aber die Genexpression in Monozyten-ähnlichen Zellen und natürlichen Killerzellen, die an der Mikroumgebung des Tumors und an Entzündungsvorgängen beteiligt sind. Durch Multiplex-Immunfluoreszenz und räumliche Analyse von 700 Gewebeproben konnte ich nachweisen, dass Glycodelin an CD8+ T-Zellen und CD163+ (M2) Makrophagen im Tumor und Stroma bindet. Somit interagiert Glycodelin beim NSCLC eindeutig mit den umgebenden Immunzellen und könnte ein tumor-freundliches Umfeld modulieren. Die Analyse von Glycodelin im Serum

von inoperablen, immuntherapierten NSCLC-Patienten (n = 139) vor der Immuntherapie zeigte, dass hohe Glycodelin-Konzentrationen im Serum mit einem verringerten progressionsfreien Überleben ($p < 0,001$) von Patientinnen verbunden waren, die eine Anti-PD-1/PD-L1-Therapie erhielten. Die Glycodelinwerte korrelierten nicht mit den Hormonen Progesteron, Östradiol, humanes Choriongonadotropin (hCG) oder Testosteron im Serum. Daher könnte es als prädiktiver Biomarker dienen und bessere Therapieentscheidungen für weibliche Patientinnen ermöglichen. In einem ersten Ansatz *in vitro* konnte ich zeigen, dass die Bindung von Glycodelin an Immunzellen durch die Verwendung eines monoklonalen Anti-Glycodelin-Antikörpers gehemmt werden kann.

Abschließend konnte ich zeigen, dass Glycodelin das Potenzial hat, ein neuartiges Ziel in der Immunonkologie und ein Prädiktor für das Ansprechen auf eine Therapie bei NSCLC-Patienten zu sein.

Abstract

Lung cancer remains the major cause of cancer related death worldwide. Recent developments in immunotherapy promise to be a gamechanger in early and advanced disease by overcoming the tumor immune escape. However, current immunotherapeutic approaches cannot be implemented for every patient, some lack a benefit and especially women often suffer from severe side effects or fail to respond to the treatment successfully.

Glycodelin is a glycoprotein which is crucial for the establishment and maintenance of pregnancy. Glycodelin A, one of four glycosylation forms, suppresses the maternal immune system and allows the fertilized egg to invade into the decidual tissue. During pregnancy, it modulates the immune environment at the feto-maternal interface to prevent defense mechanisms towards the fetus as a semi-allograft. Interestingly, high glycodelin protein and corresponding *progesterone-associated endometrial protein* (*PAEP)* gene expression were also discovered in lung tumors compared to normal lung tissue.

In the frame of this project I have investigated whether glycodelin in non-small cell lung cancer (NSCLC) shares the immunosuppressive function of glycodelin A known from pregnancy and could therefore serve as a novel target for future immunotherapies.

For my study, I have used the primary cell lines 4950T and 170162T that secrete between 20-100 ng/ml glycodelin into the cell culture supernatant. The glycosylation structure was analyzed by lectin-based enrichment and could show that NSCLC derived glycodelin resembles the glycosylation pattern of glycodelin A isolated from amniotic fluid. The proteins shared high sialylation which is known to be crucial for immunosuppression. It is important to point out that sialic residues were detected weaker in glycodelin derived from 170162T, a NSCLC cell line that originates from a male patient. Thus, the protein might have sex-specific structures and functions. *In vitro*, NSCLC-derived glycodelin was bound and internalized by immune cells. It did not induce apoptosis but affected gene expression in monocytic and natural killer cells involved in tumor microenvironment and inflammation pathways. By using multiplex immunofluorescence and spatial analysis on 700 tissue samples, I could demonstrate that glycodelin binds to CD8+ T cells and CD163+ (M2) macrophages in tumor and stroma. Thus, glycodelin in NSCLC clearly interacts with surrounding immune cells and might modulate a pro-tumorigenic environment. The analysis of glycodelin in the serum of inoperable immunotherapy-treated NSCLC patients (n = 139) prior to immunotherapy showed that high serum concentrations of glycodelin were associated with a decreased progression-free survival ($p < 0.001$) of female patients receiving an anti-PD-1 / PD-L1 therapy. Glycodelin levels did not correlate with the hormones progesterone, estradiol, human chorionic gonadotropin (hCG), or testosterone in the serum. Consequently, it could serve as a predictive biomarker and enable better therapy decisions for female patients. As a first approach *in vitro*,

I showed that glycodelin is targetable and that glycodelin binding to immune cells can be inhibited by using a monoclonal anti-glycodelin antibody.

In conclusion, I could demonstrate that glycodelin has high potential of being a novel target in immuno-oncology and predictor of therapy response for NSCLC patients.

1 Introduction

1.1 Lung cancer – Epidemiology, Diagnosis, and Histology

Lung cancer remains one of the most common and deadliest cancers worldwide, with an incidence of 2.2 million new cases per year and 1.8 million deaths [1], [2]. With smoking being the main risk factor for lung cancer, the global distribution of incidence and mortality is closely linked to smoking patterns. More than 80 % of all lung tumors are directly caused by smoking [3]. Since the introduction of comprehensive tobacco control programs, numbers have declined steadily [4]–[6]. However, rates in women are still rising in central and eastern European countries and there is a high discrepancy in incidence and mortality rates related to earlier stages of tobacco trends, socioeconomic and educational inequalities, and diagnosis at later stages of the disease [7], [8].

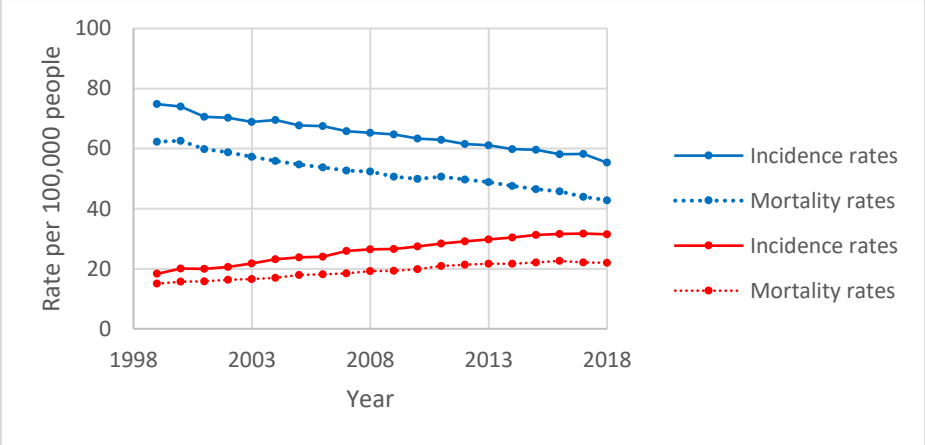

Figure 1.1. Age-standardised incidence and mortality rates in Germany by sex (blue = male, red = female), ICD-10 C33-C34, Germany 1999 – 2018, per 100,000 (old European standard population) [9]

Besides, secondhand smoking, asbestos exposure, hereditary disposition, exposure to toxic substances like polycyclic aromatic hydrocarbons, heavy metals, and radon gas are risk factors for developing lung cancer [10]. Nowadays, electronic cigarettes are becoming more popular, especially in the young population [11]. Long term effects are still unknown, but it could be shown that electronic cigarettes have a significant potential for serious lung toxicity [12].

The diagnosis of lung cancer is mostly done in symptomatic patients with cough, fatigue, dyspnea, chest pain, weight loss, and/or hemoptysis [13]. For diagnosis and staging, imaging tests like computer tomography (CT) scans are required as well as tissue samples to ensure a pathological review for PD-L1 testing and molecular analysis [14]. The staging is based on the 8th edition of the tumor, node, metastasis (TNM) classification of thoracic tumors which includes 100,000 patients in an international database [15]. It is crucial in selecting the best therapy option for each patient. In addition, liquid biopsies have shown to assist in the detection

of lung cancer and specific genetic aberrations by analyzing circulating tumor DNA (ctDNA), micro-RNA, and circulating tumor cells (CTCs) in the plasma, serum, or urine of patients [14]. The main histological groups are small cell lung cancer (SCLC) and non-small cell lung (NSCLC), the latter being the more prevalent type with 85 % of all lung cancers. For NSCLC, three major subtypes are further distinguished: adenocarcinoma (ADC), squamous cell carcinoma (SQCC), and large cell carcinoma among other very rare types like sarcomatoid carcinomas and adenosquamous carcinomas [16], [17]. Despite the classification, it is important to mention that lung cancer is a highly heterogeneous disease histologically and molecularly, which impedes therapies that can be effectively applied universally [18].

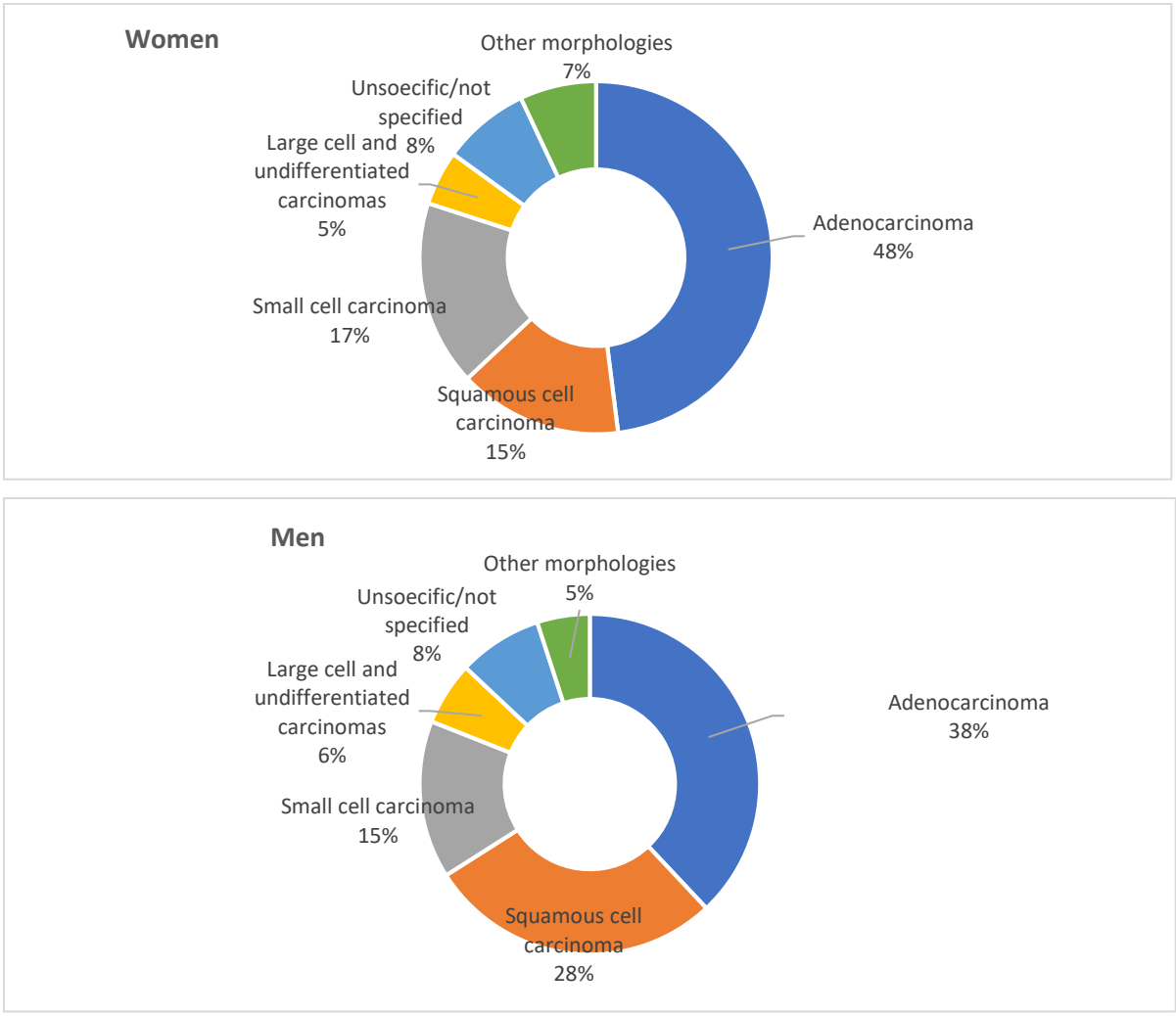

Figure 1.2: Distribution of malignant neoplasms of the lung by histological type and sex, ICD-10 C33–C34, Germany 2015–2016 [9]

1.2 Treatment of non-small cell lung cancer

The optimal treatment of NSCLC depends on several factors and can be applied alone or in multimodal therapy options. In general, it includes surgery, radiotherapy, chemotherapy, molecularly targeted therapy, and/or immunotherapy depending on stage, histology, genetic alterations, and the patient's fitness. For early stages of NSCLC (stage I-IIIA), curative surgical resection is recommended for medically fit patients. In addition, for stages II-IIIA adjuvant platinum-based chemotherapy can be used [19]. 5-year survival reaches up to 90 % in stage IA and decreases over stages to 56 % for stage IIB [20]. Nonetheless, around half of patients with stage IB (tumor > 4 cm) and more than 70 % of patients with stage IIIA will have tumor relapse [19]. If surgery is not an option due to the patients' refuse or medical contraindications, high-dose stereotactic body radiation therapy can be applied. Further options involve radiofrequency ablation, standard radiotherapy, and chemotherapy, which have all shown to have more than 85 % local tumor-control rates over 5 years [21], [22]. However, over 60 % of lung tumors are diagnosed at an advanced stage and are not resectable [17]. Despite major developments in novel treatment approaches, the 5-year survival rate for late stages with distant metastases is only 6 % [23].

In order to further improve treatment response and survival of late-stage patients and to overcome relapse in early stages, it is important to identify targetable genetic alterations. Several tyrosine kinase inhibitors (TKIs) are approved for the treatment of NSCLC subtypes, targeting epidermal growth factor receptor (*EGFR)*, *ALK*, *ROS1*, *RET*, *BRAF V600E*, *MET* Exon 14, and *NTRK* mutations [14]. These mutations in receptors or other kinases can stimulate a complex cascade of cross signaling pathways leading to uncontrolled proliferation, growth, and survival. The third-generation oral EGFR-TKI Osimertinib binds EGFR driver mutations as well as EGFR T790M resistance mutations [24]. Adjuvant application of Osimertinib *vs* placebo in patients after complete resection of a stage IB to IIIA NSCLC led to an absolute improvement in two-year disease-free survival (DFS) of 37 % in a phase III trial [25]. Several clinical trials are ongoing, that further investigate a possible advantage of adjuvant oral TKI or immunotherapy. Adjuvant therapies, apart from chemotherapy, are thus becoming more important to reach the goal of a fully curative lung cancer [26].

Stage III NSCLC is a highly heterogeneous disease which comprises about 20 % of cases in Germany [9]. It includes tumors that have metastasized to mediastinal lymph nodes or large tumors that may involve local lymph nodes [20]. Many patients with stage III NSCLC are not eligible for surgery. Trials that incorporated immunotherapy for patients who have completed a concurrent chemotherapy and radiotherapy showed promising results [27]. If surgery is possible, novel neoadjuvant strategies are of increasing interest to improve the therapy outcome and overcome the high rate of local relapse. In general, neoadjuvant chemotherapy

and radiotherapy followed by surgery can be considered for a specific group of patients [28]. The benefit of immunotherapy as a neoadjuvant approach is under current investigation in many studies. First results already showed major pathological response and complete pathological response in a significant amount of patients receiving durvalumab and chemotherapy, representing the high potential of this combination therapy [29].

More than 50 % of patients are diagnosed with metastatic (stage IV) NSCLC in Germany [9]. In addition, a high proportion of patients that suffered from early stage before or from a locally advanced disease eventually relapse and/or progress into the metastatic condition. The main treatment focus in stage IV NSCLC includes the management or improvement of the quality of life, and the overall survival. Here, palliative care has a positive effect on both [30]. Systemic therapy options depend on several clinical parameters and patients should be tested for driver mutations to evaluate the application of targeted therapy. For patients lacking any driver mutations, treatment can include single-agent immunotherapy, combination immunotherapy regimens or chemotherapy [31]. Here, PD-L1 expression analysis is the most important value in deciding the best therapy option.

1.3 Immunotherapies in the treatment of NSCLC

Immunotherapies have revolutionized the landscape of cancer treatment and have shown to enable long-term survival in patients with metastatic NSCLC. The basis of immune checkpoint inhibitors (ICIs) is the interaction of tumor cells with surrounding immune cells and immune escape mechanisms that result in tumor growth. One mechanism of tumor cells to avoid immune recognition is the reduction of their immunogenicity. The immunoinhibitory molecule PD-L1 can be upregulated in cancer cells by IFN-γ that is produced and secreted by tumor infiltrating lymphocytes [32]. Across various cancer types, PD-L1 could be found on the membrane of tumor cells and the expression correlated with lymphocyte-rich regions. In these tumors, anti-PD-1 therapy has shown a corresponding objective response [33]. These findings might suggest that PD-L1 expression could serve as an efficient biomarker for the immunotherapy responsiveness of a tumor. However, not all tumors that are positive for PD-L1 show immune infiltrates and some do not respond to anti-PD-1 therapies [32], [33]. Consequently, additional markers will be needed that cover other immune checkpoint molecules expressed on tumor cells and surrounding cells in the tumor microenvironment. Moreover, negative regulatory markers on tumor-infiltrating lymphocytes could serve as markers, e.g. LAG-3, TIM-3, VISTA, CD244, CD160, and BTLA [34], [35]. Similar to the interaction of PD-1 and PD-L1, the corresponding molecular pathways regulate the cellular fate of tumor-infiltrating T cells. It might be possible, that these immunoinhibitory pathways and the PD-1/PD-L1 signaling axis share some level of redundancy. Thus, by targeting them in

combination therapies, a decrease of immunoinhibitory signaling might increase T cell activating signals and result in an efficient anti-tumor T cell immunity [36]. Nevertheless, the main challenge will remain how to identify and select patients for a particular immunotherapy as the combination will inevitably lead to increased toxicity [37].

The most relevant role of immunotherapy in the treatment of NSCLC is regarding patients with an advanced disease. Several studies in the recent years could demonstrate the high benefit of monotherapies, as well as combination therapies with chemotherapy or double immunotherapy. Combining chemotherapy and immune checkpoint inhibitors (ICIs) aims to induce immunological effects with the chemotherapy and by this increase efficacy of PD-1/PD-L1 inhibition [38]. Another combination is represented by the dual inhibition of PD-1 and CTLA-4 which has been studied in different trial including NSCLC patients. By this, the immune response could be enhanced in the tumor microenvironment through PD-1/PD-L1 blockade and at the same time, recruitment of anti-tumorigenic T cells could be increased through CTLA-4 [39], [40]. However, in a clinical study this setting led to a higher number of treatment withdrawals due to toxicity in the dual ICI arm [41]. Due to very promising results that were seen in advanced stages, in the recent years studies were performed that also included immunotherapy at earlier stages. It was applied in neoadjuvant and adjuvant settings. The most promising results were shown in the phase II NADIM trial, with 83 % of the patients presenting a major pathological response of which 71 % were a pathological complete response after neoadjuvant immunotherapy and subsequent surgery [42].

Numerous studies are ongoing that aim to further exploit the high potential of ICIs in the treatment of NSCLC. The main obstacles are to identify suitable biomarkers and additional immune related targets which are both questions of current research.

1.4 **Glycodelin – a major lipocalin in pregnancy**

In the 1970s and 1980s several investigators could identify a protein at the same time that they found in the human placenta, in amniotic fluid, the pregnancy decidua, and seminal plasma. Independent of each other, they named the protein based on the origin of isolation, such as placental-α2-globulin, progestogen-dependent endometrial protein (PEP), human lactoglobulin homolog, among other suggestions [43]–[47]. The identified proteins highly differed in their glycosylation, which was also depending on the tissue that has been used to isolate it. Therefore, researchers who have performed and published pioneering work related to this glycoprotein agreed upon the name “glycodelin” [48]. Glycodelin is encoded by its gene *progesterone-associated endometrial protein* (*PAEP*) and a 900 bp mRNA which shares high homology with bovine β-lactoglobulin and other lipocalins [49]. Glycodelin isolated from amniotic fluid has a molecular mass of 28 kDa and forms homodimeric complexes [44], [45], [50]. It is known to be involved in immunosuppression, angiogenesis, and apoptosis signaling during the first trimester of pregnancy [51] and regulates fertilization and implantation [52]–[54]. As indicated by the gene name, glycodelin expression is regulated by progesterone, while a connection with levels of human chorionic gonadotropin (hCG) were observed, as well [55]–[57]. Four different glycosylation forms are known, which share the same protein backbone but highly differ in their sugar structure. Glycodelin A is found in amniotic fluid, in the secretory and decidualized endometrium and can also be detected in the serum of women who are pre-menopausal [57], [58]. Glycodelin C is related with the cumulus matrix and glycodelin F can be found in follicular fluid and oviduct [53], [59]. Glyodelin S is the only form found in men, more precisely in seminal plasma [56], [60]. The different functions are based on the specific glycosylation residues at Asn28 and Asn63, both located in a conformational loop [61]. While most of the interactions are specific to the distinct glycosylation, some activities were reported to be based on the protein backbone [62]–[65]. The distinct distribution of glycodelin underlines the possible relation between its function and the immunological and hormonal regulation of reproduction [56].

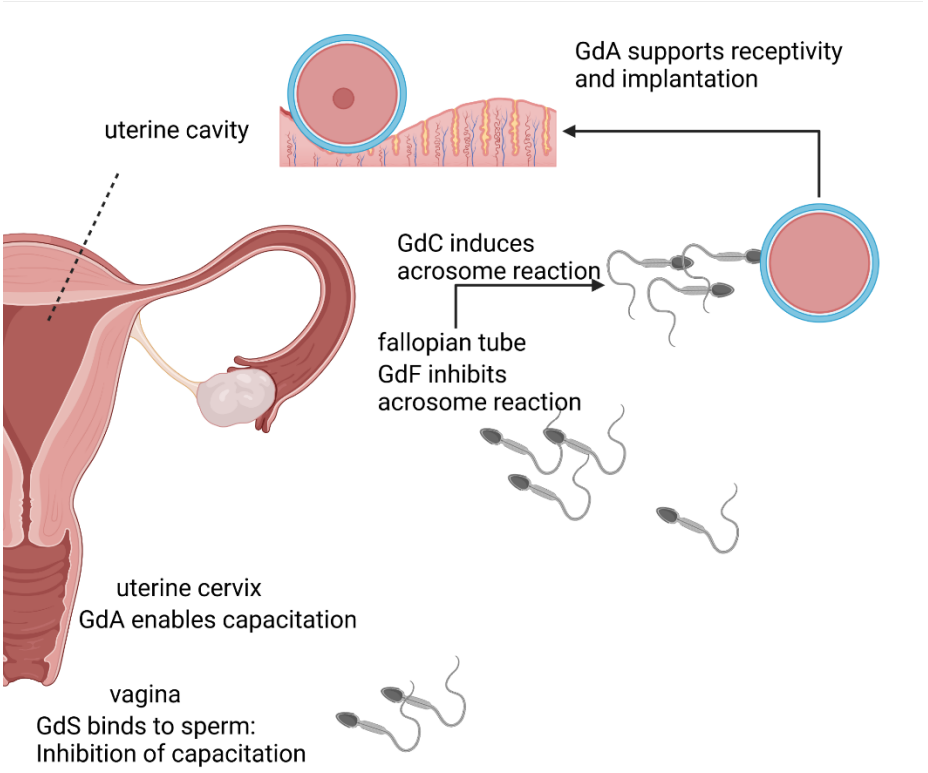

Figure 1.3: Schematic process of the different glycodelin forms in reproduction. Adapted from [56].

In the process of a successful pregnancy, each glycosylation form performs a specific task (**Figure *1.3***). After ejaculation into the vagina, glycodelin S rapidly binds to spermatozoa to inhibit capacitation through inhibition of albumin-induced cholesterol efflux [66], [67]. In the uterine cervix, glycodelin A competes with GdS binding and enables capacitation after removal of glycodelin S. Thereupon, in the fallopian tube, glycodelin F is expressed which inhibits the progesterone-induced acrosome reaction until apposition of the sperm and oocyte [68], [69]. Finally, glycodelin C replaces GdF and A and induces the acrosome reaction. Glycodelin A modulates the endometrial epithelial cells and the surrounding immune environment to support, apposition, adhesion, and embryo penetration [56].

1.5 Glycodelin A as a modulator of the immune environment

Pregnancy is similar to a semi-allograft implantation. Consequently, the maternal immune response needs to be repressed to allow a successful pregnancy. Glycodelin A is the major immunomodulator among the different glycosylation forms and acts on various levels. It suppresses the cytotoxicity of natural killer cells [70], [71] and induces apoptosis of Th1 cells through activation of caspase-3, -8, and -9 [72]. Furthermore, it stimulates hCG production and leads to progesterone secretion from the trophoblast [73], [74]. Moreover, glycodelin suppresses Th1 cytokines IFN-γ and IL-2 secretion and expression of the chemokine receptor CXCR3 in naïve CD4+ T cells [75]. Regarding CD8+ T cells, it was shown that glycodelin impairs cytotoxicity, involving reduced expression of granzyme B and perforin. However,

apoptosis induction could not be observed in the study of Soni and Karande [76]. IL-2/IL-2R signaling in T cells is altered by glycodelin A which leads to proliferation inhibition of T cells and impairs immune responses including CD8+ T cell cytotoxicity and CD4+ T cell apoptosis [77].

In monocytes, the chemotaxis ability is suppressed by glycodelin. Here, the glycosylation did not play a part in the functionality [78], [79]. It could be shown, that glycodelin binds CD14 in monocytes which does not exist on T or B cells [80]. When the mechanism of the functions was further explored, it was revealed that glycodelin regulates apoptotic-related genes in monocytes, like the decrease of Bcl-2A1 and APRIL and the increase of TNF-R1, Bad, and Bax which have a pro-apoptotic effect. Similar to the regulation in T cells, activation of caspase -2, -3, and -8 could be identified [78], [81].

Decidual natural killer cells are the most abundant leucocytes in the decidua [82]. They are characterized by a lower cytotoxicity and higher cytokine secretion. Glycodelin A treatment of peripheral blood NK cells enhanced the expression of CD9 and CD49a which are both markers of decidual NK cells. It further led to the ERK-activation dependent production of VEGF and IGFBP-1 by the NK cells. This function was based on the sialylation of glycodelin A and binding to L-selectin [70].

In addition, interaction of glycodelin A with dendritic cells and B cells was reported, underlining the pleiotropic effects of the glycoprotein [81], [83].

1.6 **Glycodelin in NSCLC**

In the first investigations with glycodelin, the protein was found mainly in secretory endometrium, pregnancy decidua, and amniotic fluid [50]. It was further characterized as an immunoregulator at the feto-maternal interface. A connection of aberrant glycodelin expressions was reported with diseases that are related to the reproductive system, including premature ovarian failure [84], recurrent spontaneous abortion [85], and endometriosis [86]. Now, a connection of glycodelin and various cancer types is known, as well. Expression could be validated in female-specific malignancies, like endometrial cancer and ovarian cancer [87]–[89]. But also, non-gender specific cancers were found to express the pregnancy-associated protein, among them lung cancer [90], [91].

In NSCLC, both *PAEP* gene expression as well as glycodelin protein detection were increased in lung ADC and SQCC compared to normal lung tissues [90], [91]. Another study could confirm these findings and revealed elevated glycodelin expression in NSCLC as well as lung metastases of colon cancer [92]. As glycodelin is secreted, it could be measured in the serum of NSCLC patients where levels were higher than in the comparison group without cancer.

Female patients suffering from NSCLC secrete more glycodelin when lymph node metastases are present. Interestingly, complete resection of the tumor led to a significant reduction of glycodelin serum levels which increased again in case of tumor recurrence or metastasis. Besides, higher PAEP gene expression resulted in a significantly worse overall survival in female patients only [91]. A case report from one of the investigated patients revealed a concomitant change of glycodelin expression along with the cancer status, beginning at the initial diagnosis, lobectomy, chemotherapy, cancer progression, and death [93]. The upregulation of glycodelin in NSCLC is also reflected in metastases and could serve as a monitoring biomarker [90]. In NSCLC cell lines and patient samples, regulatory pathways could be detected that affect glycodelin expression. In SQCC, TGF-β led to an increase in *PAEP* gene and glycodelin protein expression, while in SQCC and ADC the PKC-signaling led to induction [94].

In the past years, immunotherapy in the treatment of NSCLC has represented a major breakthrough in cancer therapy. It might be possible, that glycodelin plays an important role in the regulation of immunosuppressive pathways [94]. The potential of various regulatory mechanisms is enormous and could be exploited in future therapeutic applications. For this, it is needed to further investigate the role of aberrantly expressed glycodelin in malignant cells.

2 Objective

Lung cancer patients suffering from an advanced disease still face a poor 5-year survival. Immunotherapies have recently reached promising results and response in a subset of NSCLC patients, while others fail to benefit. Especially women seem to be more prone to severe side effects or treatment failure. Through immunotherapeutic approaches, immune escape mechanisms of the tumor are tackled and the immune system is reactivated to recognize cancer cells. However, some tumors seem to adapt and are not targetable by common antibody treatments like anti-PD1, anti-PD-L1, or CTLA4. Glycodelin is a glycoprotein well known from pregnancy, enabling successful fertilization, trophoblast invasion, and pregnancy maintenance by modulating the endometrial environment. One of the four glycosylation forms, namely Glycodelin A, acts as an immunosuppressor through the highly sialylated glycosylation structure. It binds to various immune cells and drives them towards a decidual phenotype, modulating the immune environment into a tolerant state.

Gene expression of the encoding gene *PAEP* and protein expression of Glycodelin was recently described in several tumor types, including NSCLC. The main question that is addressed in the herein presented thesis is therefore, whether glycodelin secreted by NSCLC cells might have similar immunosuppressive characteristics as glycodelin A in pregnancy and modulates the tumor microenvironment to be pro-tumorigenic. In order to investigate this hypothesis, I will investigate the protein from three perspectives:

1. Characterization of the glycosylation of NSCLC derived glycodelin

The glycosylation and especially a high sialylation drive the immunosuppressive function of glycodelin A in pregnancy and at the feto-maternal interface. Immune cell receptors specific for sialyl residues are known to activate inhibitory downstream pathways, leading to inhibition/reduction of cytotoxicity and modelling the phenotype towards a tolerating state [60], [95].

2. Functional analysis of NSCLC derived glycodelin *in vitro*

The actual binding ability and specific functionality will be further explored *in vitro.* If glycodelin is detectable in the immune cells after treatment, I will examine whether it has a functional effect by analyzing differences in gene expression upon glycodelin addition.

3. Investigation of the immune microenvironment *in vivo* and the influence on immunotherapy

In the third part, I will focus on the interaction of glycodelin with the surrounding immune environment *in vivo* and whether it might impact the response to immunotherapy. I will apply multiplex immunofluorescence in tumor microarrays from patients with NSCLC. The analysis can be used to investigate specific immune cell subtypes that interact or do not interact with

glycodelin. By this, possible targetable interactions might be identified that can be exploited in future therapeutic approaches.

To obtain an idea about the functionality of glycodelin in NSCLC patients, I will measure glycodelin serum levels via ELISA in patients suffering from advanced NSCLC who will be treated with PD-1or PD-L1 immunotherapy. I will then analyze progression-free survival in these patients to determine whether glycodelin might influence a therapy response and benefit.

To sum up, the project shall characterize glycodelin in NSCLC, shed light on the functionality, and reveal whether it might be a marker for immunotherapy response prediction or even a novel target for future therapies.

3 Material and Methods

3.1 **Material**

3.1.1 Equipment

Table 3.1: List of equipment used during the project.

Name	**Manufacturer**
Agilent 2100 Bioanalyzer	Agilent Technologies
Agilent RNA 6000 Nano Kit	Agilent Technologies
Amersham Hyperfilm™ ECL	GE Healthcare
Amersham Protran Premium 0.2 NC nitrocellulose membrane	GE Healthcare
Centrifuge 5415R	Eppendorf
GeneChipTM 3' IVT PLUS Reagent Kit	Thermo Fisher Scientific
GeneChipTM Human Genome U133 Plus	Thermo Fisher Scientific
GeneChipTM Fluidics Station 450	Thermo Fisher Scientific
GeneChipTM Scanner 3000	Thermo Fisher Scientific
Hoefer SE 600 standard vertical electrophoresis unit	Thermo Fisher
Cytotoxicity Detection Kit (LDH)	Roche
LightCycler® 480 Real-Time PCR Instrument	Roche
Microplate Reader	Tecan
NanoDrop ND-1000 Spectrophotometer	NanoDrop Technologies
PMR-100 Rocker-Shaker	Grant-bio
RNeasy Mini Kit	Qiagen
Rotina 420 R	Hettich Zentrifugen
Thermomixer comfort	Eppendorf
Transcriptor First Strand cDNA Synthesis Kit	Roche
Transfer Electroblotting Unit LKB 2005	LKB
Vectra Polaris	Akoya Biosciences

3.1.2 Chemicals and reagents

Table 3.2: List of chemicals and reagents used during the project.

Name	Manufacturer	Article No.
Accutase®	Sigma Aldrich	#A6964-100ML
Acidic Acid	Riedel de Haën	#R10-35
Acrylamide Solution (30 %)	AppliChem	#A3626,1000
Agar	Sigma Aldrich	#05040-250G
APS (Ammoniumperoxodisulfate)	AppliChem	#A2941,0100
BSA (Bovine Serum Albumin)	PAA	#K15-020
Chemiluminescence Reagents:		
Solution A – Luminol and Enhancer Solution CheLuminate-HRP PicoDetect	PanReac AppliChem	#A3417,5000A
Solution B – Stable peroxide Solution CheLuminate-HRP PicoDetect	PanReac AppliChem	#A3417,5000B
DAPI/Hoechst 33342	Sigma Aldrich	# 14533-100MG
Developer and Replenisher	Carestream Dental	#1900943
DMEM/F-12 (Dulbecco's Modified Eagle Medium)	Life Technologies	#21331-020 (1 Bottle) #21331-046 (10 Bottles)
DMSO (Dimethylsulfoxide)	Carl Roth	#A994.2
DPBS (Dulbecco's Phosphate Buffered Saline)	Life Technologies	#14190-094
Epithelial airway growth factors	Promocell	#C-39160
Ethanol	Carl Roth	#9065.2
FBS (Fetal Bovine Serum)	Invitrogen	#10500-064
Fixer and Replenisher	Carestream Dental	#1901875
D(+)-Glucose	Carl Roth	#HN06.1
stable Glutamine	Life Technologies	#35050038
Glycine	AppliChem	#A1067,5000
HCl	Carl Roth	#4625.1
HEPES	Life Technologies	#15630-056
Lipofectamine™ RNAiMax	Invitrogen	#13778-150
Methanol	Carl Roth	#8388.4
Nonfat dried milk powder	AppliChem	#A0830,0500

PBS (Phosphate Buffered Saline)	AppliChem	#A0965,9010
PFA (Paraformaldehyde)	Sigma Aldrich	#16005-1KG-R
Ponceau	AppliChem	#A2935,0100
PrimaQuant 2 x qPCR Probe-MasterMix – no-ROX	Steinbrenner Laborsysteme	#SL-9802-50ML
ProLong™ Diamond Antifade Mountant	Life Technologies	#P36961
ROCK inhibitor Y-27632	Stemcell Technologies	#72308
SDS (Sodiumdodecylsulfate)	AppliChem	#A7249,1000
Trichloroacetic acid	AppliChem	
TEMED (Tetramethylethylendiamine)	AppliChem	#A1148,0025
Tris	Sigma Aldrich	#T1503-1KG
Triton X-100	AppliChem	#A4975,0100
Trypan blue	Sigma Aldrich	#T8154-20ML
Tween20	AppliChem	#A4974,0250

3.1.3 Buffers

Table 3.3: Overview of buffers and their respective composition.

Buffer and Composition	**Amount**
Running Buffer (1x)	
10x Tank Buffer	100 ml
10 % (w/v) SDS	10 ml
Desalted Water	to 1 l
Tank Buffer (10x), autoclaved	
Tris	30 g
Glycine	144 g
Water	to 1 l
Transfer Buffer	
10x Tank Buffer	100 ml
Methanol	200 ml

Desalted Water	to 1 l
Separation Gel Buffer	
1.5 M Tris-HCl, pH 8.8	variable
Stacking Gel Buffer	
0.5 M Tris-HCl, pH 6.8	variable
Sample Buffer (2x)	
Stacking Gel Buffer	2.5 ml
10 % (w/v) SDS	4 ml
Glycerin	2 ml
β-Mercaptoethanol	1 ml
1 % (w/v) Pyronin	0.2 ml

3.1.4 Cell culture medium

Table 3.4: Cell lines and respective cell culture media with detailed composition.

Cell line	Basal medium	Media supplement	Final concentration
170162T **4950T**	DMEM/HAMs F12	Bovine Pituitary Extract	13 µg/ml
		Insulin	5 µg/ml
		Hydrocortisone	0.5 µg/ml
		Triiodothyronine	6.7 ng/ml
		Transferrin	0.01 mg/ml
		L-glutamine	2 mM
		ROCK inhibitor	10 µM
4950T-F **2427T**	DMEM/HAMs F12	L-glutamine	2 mM
		FBS	10 % (v/v)

Jurkat	RPMI 1640	D-glucose	4.5 mg/ml
THP1		HEPES	10 mM
KHYG-1		L-glutamine	2 mM
		Sodium bicarbonate	1.5 mg/ml
		Sodium pyruvate	1 mM
		FBS	10 % (v/v)

3.1.5 Small interfering RNAs

Table 3.5: List of siRNAs used during the project.

Name	Manufacturer	Catalog No.
AllStars Negative Control siRNA	Qiagen	SI03650318
Hs_PAEP_1	Qiagen	SI00039704
Hs_PAEP_2	Qiagen	SI00039711
Hs_PAEP_3	Qiagen	SI00039718
Hs_PAEP_5	Qiagen	SI03102659

Efficiency was confirmed by quantitative *Real Time* PCR and suitable siRNAs were pooled. siRNA pools are generated by mixing equal volumes of siRNAs.

3.1.6 Antibodies

Table 3.6: List of antibodies used during the project.

Name	Dilution	Manufacturer	Article No./Clone
Rabbit anti-goat HRP conjugated	1:5,000	Sigma Aldrich	#5420
Goat anti-rabbit IgG		Sigma Aldrich	#A6154
Goat anti mouse IgG HRP conjugated	1:10,000	Sigma Aldrich	#A 4416
Mouse anti β-Actin	1:10,000	Sigma Aldrich	#A5441
Goat anti-Glycodelin	1:300 WB 1:1,000 mIF	Santa Cruz	N-20
Mouse anti-CD68	1:100	Dako	PG-M1
Mouse anti-panCK	1:300	Zytomed	AE1/AE3
Rabbit anti-CD163	1:300	Cell Signaling	#D6U1J
Rabbit anti-iNOS	1:300	Abcam	SP126
Mouse anti-D8	1:100	Abcam	SP16
Rabbit anti-CD4	1:100	Cell Signaling	EP204
Rabbit anti-Granzyme B	1:300	Cell Signaling	D6e9W

3.1.7 Universal Probe Library Primers

Table 3.7: List of UPL forward (for) and reverse (rev) Primers used in this project. Probes and primers were purchased from Roche Life Science.

Name	Primer sequence 5'-3'	UPL #
ESD_for	TCAGTCTGCTTCAGAACATGG	50
ESD_rev	CCTTTAATATTGCAGCCACGA	50
RPS18_for	CTTCCACAGGAGGCCTACAC	46
RPS18_rev	CGCAAAATATGCTGGAACTTT	46
PAEP_for	CCTGTTTCTCTGCCTACAGGA	77
PAEP_rev	CGTCCTCCACCAGGACTCT	77
CXCL10_for	GAAAGCAGTTAGCAAGGAAAGGT	34
CXCL10_rev	GACATATACTCCATGTAGGGAAGTGA	34

NFKB_for	CCTGGAACCACGCCTCTA	49
NFKB_rev	GGCTCATATGGTTTCCCATTTA	49
TNF_for	CAGCCTCTTCTCCTTCCTGAT	29
TNF_rev	GCCAGAGGGCTGATTAGAGA	29
PDGFA_for	GATGAGGACCTTGGCTTGC	68
PDGFA_rev	CCAGCCTCTCGATCACCTC	68
THBS1_for	GCAGGAAGACTATGACAA	-
THBS1_rev	CTGTCATCTGGAATTTTATCA	-
MMP9_for	GAACCAATCTCACCGACAGG	21
MMP9_rev	GCCACCCGAGTGTAACCATA	21

3.2 **Methods**

3.2.1 Cultivation of cells

The protocol is adapted from my Master's thesis:

Cells were cultivated under humidified conditions at 37 °C and 5 % CO_2. The fibroblast cell line 4950T-F and the squamous cell carcinoma (SQCC) cell line 2427T were cultivated in DMEM/HAMs F12 with 10 % FBS and 1 x stable glutamine. For Jurkat, THP1, and KHYG-1 RPMI 1640 added with 10 % FBS was used (+ 10 ng/ml IL-2 for KHYG-1). The patient derived primary cell lines 4950T and 170162T were cultivated in serum-free DMEM/HAMs F12 with epithelial airway growth factors and ROCK inhibitor (Rho associated, coiled-coil containing protein kinase inhibitor). A detailed summary of all cell lines and the respective culture media is shown in the material section. Cultivation was performed in T175 or T75 culture flasks with a minimal medium volume of 25 ml and 15 ml, respectively. The cells were passed when a confluency of 80-90 % was reached to ensure further cell growth and survival.

Therefore, the adherent cells were washed with 1 x DPBS and treated with 1.5 ml (T75) or 3 ml (T175) accutase at 37 °C and 5 % CO_2 for 5-10 min. After they have detached, the accutase was neutralized by adding 8.5 ml (T75) or 7 ml (T175) culture medium and the cell suspension was transferred into a 50 ml tube. The suspension was centrifuged for 5 min at 300 x g and room temperature, the supernatant was discarded and the cell pellet was resuspended in 10 ml fresh culture medium. Depending on the desired period of cultivation and on the doubling time of the specific cell lines, an appropriate amount of cell suspension was dispensed into a new culture flask and further cultivated in the incubator until needed. A maximum amount of 20 passages was not exceeded.

3.2.2 Thawing and freezing cells

The protocol is adapted from my Master's thesis:

Cells were thawed rapidly in the water bath at 37 °C by gentle agitation, transferred into a 50 ml tube containing 9 ml prewarmed complete growth medium and centrifuged at 300 x g for 5 min at room temperature. The supernatant was discarded and the cell pellet was resuspended in complete growth medium before being dispensed into a T75 culture flask. The minimum volume of culture medium should amount 15 ml.

In order to freeze cells, they were first harvested as described above. 10 µl of the cell suspension were mixed with an equal amount of trypan blue and viable cells were counted in

a Neubauer counting chamber. The suspension was centrifuged at 300 x g for 5 min at room temperature and resuspended in the respective amount of cryo medium to obtain the desired cell number /ml. For cryopreservation, the full growth medium was supplemented with 5-10 % DMSO. Cells were divided into aliquot portions of 1 ml per vial and slowly cooled down in a Cryo 1 ° Freezing Container at -80 °C for 24 h. For long-term storage, the vials were transferred into a -150 °C freezer.

3.2.3 Transient gene knockdown by siRNA transfection

The standard protocol was performed as follows: Cells were seeded in 12 well plates with cell numbers of 2.5 x 10^5 cells/well and kept in the incubator at 37 °C and 5 % CO_2 overnight. For one reaction, 1.2 µl of siRNA (c = 10 µM) were diluted in 100 µl culture medium without FBS. 2 µl RNAiMax were added and the solution was incubated for 10-20 min at room temperature. The cell culture medium was exchanged to a final volume of 1.1 ml/well and 100 µl siRNA solution were carefully dripped onto the cells, resulting in a final siRNA concentration of 10 nM. Treated cells were incubated for 72 h at 37 °C and 5 % CO_2.

For transfection approaches in another dish, the amount was adapted respectively.

As a control, AllStars Negative Control siRNA was used.

3.2.4 Total RNA isolation and cDNA synthesis

The protocol is adopted from my Master's thesis:

For RNA isolation from cell lines, the RNeasy Mini Kit was used. The quantity of RNA was measured with a NanoDrop ND-1000 Spectrophotometer. The quality of total RNA was assessed with an Agilent 2100 Bioanalyzer and Agilent RNA 6000 Nano Kit. Total RNA was considered to be sufficient for further analyses if it had an RNA integrity number (RIN) of at least 8.0. Total RNA was transcribed to sscDNA with a Transcriptor First Strand cDNA Synthesis Kit in three independent reactions. Complementary DNA synthesis was performed with anchored oligo(dT)18 primers and random hexamer primers. To ensure denaturation of possible secondary RNA structures, 2 µg total RNA, 1 µl oligo(dT)18 and 2 µl random hexamer were incubated in a total volume of 13 µl for 10 min at 65°C, followed by a cooling step for 5 min at 4°C. The final concentrations of oligo(dT)18 and random hexamers were 2.5 µM and 60 µM, respectively. The reactions were completed with 4 µl 5x reaction buffer, 0.5 µl RNase

inhibitor (20 U), 2 µl dNTPs (1 mM each) and 0.5 µl reverse transcriptase (10 U) with water to a final volume of 20 µl. Reverse transcription was performed by incubating the reaction mixture for 10 min at 25°C, 60 min at 50°C and 5 min at 85°C. In addition, a reaction without RNA (no RT control) was performed as a control for possible contamination by genomic DNA. The three independent sscDNA reaction mixtures were pooled, mixed by pipetting and separately stored in 20 µl aliquots at -20°C until further analyses.

3.2.5 Quantitative *Real Time* Polymerase Chain Reaction (qPCR)

The protocol is adopted from my Master's thesis:

Real-time quantitative PCR (qPCR) was performed in accordance with MIQE-guidelines [96] using a LightCycler® 480 Real-Time PCR Instrument in a 384-well plate format. Gene-specific primers and probes (Universal ProbeLibrary, Roche) were used in combination with qPCR Probe-MasterMix. Table 13 shows the composition of one qPCR reaction.

Table 3.8: Composition of one qPCR reaction. Total volume equals 12 µl.

Reagent	**Amount**	**Final concentration**
Template	5 µl	Corresponds to 5 ng total RNA
2 x qPCR master mix	6 µl	1 x
Primer Forward	0.12 µl	0.2 µM
Primer Reverse	0.12 µl	0.2 µM
Universal Probe	0.12 µl	0.1 µM
PCR-grade H_20	0.64 µl	

Technical triplicates as well as a non-template control were used to increase the validity of the measurements. The qPCR conditions were applied as follows: activation of the Taq polymerase at 95°C for 15 min, followed by 45 cycles of 10 sec at 95°C (denaturation), 30 sec at 60°C (annealing) and 1 sec at 72°C (elongation). C_T values were calculated with LightCycler® 480 software version 1.5 using the 2nd derivative maximum method. To evaluate differences in gene expression, a relative quantification method based on the $\Delta\Delta C_T$ -method was performed. Target genes were normalized with the mean of two housekeeping genes (ESD, Esterase D and RPS18, 40S Ribosomal Protein S18). To calculate the siRNA knockdown efficiency in cell culture experiments, *PAEP* siRNA treated cells were compared

with control siRNA treated cells. A maximum standard deviation of 0.3 was set for all measurements.

Prior to this work, a PCR efficiency calculation was performed for all applied primer pairs. Therefore, five dilutions (corresponding to total RNA amounts from 50 ng to 5 pg (1:10 dilutions)) of cDNA from QPCR Human Reference Total RNA (Agilent Technologies) were used to amplify target genes. GenEx 5 software (multid Analyses) was used for PCR efficiency calculation of the utilized primers. The primer-probe set was only used when the PCR efficiency was within the range from 0.9 to 1.1.

To ensure the correct amplification of the targets, amplicons from qPCR efficiency calculations (5 ng dilutions) were cloned into the pJet 1.2 cloning vector with the CloneJET PCR Cloning Kit (Thermo Scientific) and confirmed by sequencing (Eurofins MWG GmbH).

3.2.6 Tissue sample collection, characterization and preparation

Tissue samples and TMAs were provided by the Lung Biobank Heidelberg, a member of the accredited Tissue Bank of the National Center for Tumor Diseases (NCT) Heidelberg, the BioMaterialBank Heidelberg, and the Biobank platform of the German Center for Lung Research (DZL). All diagnoses were made according to the 2015 WHO classification for lung cancer by at least two experienced pathologists [16]. Tumor stage was designated according to the 8th edition of the UICC tumor, node, and metastasis [97]. Tissues were snap-frozen within 30 minutes after resection and stored at -80°C until the time of analysis.

3.2.7 Statistical analyses

Survival and PFS data were statistically analyzed using REMARK criteria with SPSS 22.0 for Windows and kindly performed by Dr. Marc Schneider. The primary endpoint of the study was progression-free survival. PFS time is calculated from the date of surgery until the day of diagnosed tumor progression. Univariate analysis of survival data was performed according to Kaplan and Meier and using the Cox proportional hazards model. The cut-off between high and low expression was identified by CutOff Finder version 2.1 (Translational Tumor Research Team, Institute of Pathology, Charité – Universitätsmedizin Berlin). Significance between the groups was examined by the log-rank test. A p-value of less than 0.05 was considered significant. Multivariate survival analysis was performed using the Cox proportional hazards model. The non-parametric Mann-Whitney U test was used to investigate significant

differences between non-parametric datasets (patient related data). The Spearman ranked correlation coefficient test was performed for correlation analyses. Paired t-test was applied for *in vitro* experiments with at least three biological replicates. Visualization of the data was made by GraphPad Prism 5.

3.2.8 multiplex Immunofluorescence

The multiplex immunofluorescence was performed with two different panels including either T cell related markers or macrophage related markers. The corresponding antibodies are depicted in **Table *3.6***. The staining was performed in alternating steps, starting with antigen retrieval in AR6 buffer by microwaving for 1 x 1 min at 1250 W, followed by 10 min at 125 W. In the first round, remaining peroxidase reactivity was removed by incubation with 3 % peroxide for 10 min. The slides were washed in 1 x Tris/Tween20 0.1 % wash buffer and blocked in Akoya blocking buffer for 10 min at room temperature. Primary antibody was added in Renaissance Background Reducing Diluent (Biocare Medical) for 45 min at room temperature in the dark with gentle shaking. The slides were washed and anti-mouse/anti-rabbit HRP polymer (Akoya Biosciences) was added for 10 min at room temperature. Finally, the respective Tyramide-signal amplification (TSA) reaction with OPAL fluorochromes was performed with each OPAL-TSA conjugate diluted 1:150 in TSA plus reaction buffer with 10 min of enzyme reaction time. The next staining step was again initiated by antigen retrieval. panCK staining was performed by using an OPAL TSA-DIG antibody in combination with an OPAL 780 fluorophore conjugated anti-DIG antibody. Cell nuclei were stained with spectral DAPI in PBS for 5 min and the slides were mounted with Hard-set Vectashield mounting medium (Vector Laboratories, Burlingame, California, USA). Mounted slides were allowed to harden prior to scanning. The following fluorophores were used:

Table 3.9: OPAL TSA-Fluorophores with respective protein

Fluorophore	Macrophage panel	T cell panel
520	CD68	CD4
570	iNOS	Granzyme B
620	Glycodelin	Glycodelin
690	CD163	CD8
780	panCK	panCK

For image acquisition, the mIF stained slides were scanned on a Vectra Polaris (Akoya Biosciences) as a .qptiff file at 0.5 µm pixel resolution using the 20× objective with saturation

protection as a whole-slide overview. TMA cores were annotated using the TMA function of the Phenochart software (Akoya Biosciences) by setting a grid with 1.2 mm punch diameter.

3.2.9 Image selection and analysis

InForm V.2.4.1 and the *PhenoptR* R package were used for subsequent image analysis. Slides stained with the same panel were also included in the same inForm project. Multiple representative images representing the observed variability for each protein marker were selected for training purposes within inForm software. User-guided training for tissue segmentation or phenotyping was performed. When the test analysis resulted in satisfying classification regarding tissue segmentation, cell segmentation, and phenotyping, the algorithm was used for batch analysis among all images. Consistently misclassified images and results were omitted rigorously.

3.2.10 Tissue segmentation

Machine learning-based tissue segmentation was applied using inForm software with the three different tissue categories ‘Tumor’, ‘Stroma’ and ‘Other’. User-annotated training regions for tumor identification included regions with a low expression of panCK or glycodelin and different histological subtypes to cover tissue heterogeneity. Overall tissue segmentation accuracy among the different staining panels was at least 95%.

3.2.11 Cell segmentation

The cell segmentation algorithm from the inForm software V.2.4.1 was used and improved manually.

3.2.12 Phenotyping

Machine learning-based classification and counting of cellular phenotypes was performed by the use of inForm software on the protein markers used in the project. Selection of representative cellular phenotypes was done by manual annotation.

3.2.13 Immunoblot

Samples were prepared with SDS sample buffer and loaded onto a 15 % SDS polyacrylamide gel to separate the proteins according to their size. The proteins were transferred onto a nitrocellulose membrane (pore size 0.2 µm) and transfer was confirmed by ponceau red staining. The membrane was blocked with 5 % skim milk in 1 x PBS/Tween20 0.1 % (v/v) for 1 h at room temperature. Primary antibodies were added in skim milk overnight at 4 °C. The membrane was washed 4 times for 5 min with 1 x PBS/Tween20 0.1 % (v/v) and the HRP conjugated secondary antibody was added for 1 h at room temperature. The membrane was washed, ECL substrate was added to initiate a chemiluminescent reaction and the signal was either detected by film exposure or by chemiluminescence imaging system.

3.2.14 Lectin-based pull-down assay

A set of 22 different lectins were used that bind to different glycosylation structures. Biotinylated lectins were incubated with strep-coupled magnetic beads for 45 min on the overhead shaker. Cell culture supernatant from 4950T or 170162T was condensed using an Amicon 100 kDa cutoff filter. Concentrated supernatant or glycodelin A isolated from amniotic fluid (kindly provided by Hannu Koistinen) was added to the lectin coupled beads and incubated overnight on a overhead shaker at 4 °C. Non-bound flowthrough was collected, the beads were thoroughly washed 3 x and bound proteins were eluted by adding hot SDS sample buffer and boiling for 5 min at 99 °C. Samples were analyzed via immunoblot.

3.2.15 ELISA

Glycodelin levels in serum were measured using a glycodelin ELISA from Bioserv according to the manufacturers' instructions. As the commercial ELISA was not available anymore, further measurements of glycodelin in cell culture supernatant were kindly provided by Hannu Koistinen and Annikki Ljöfhelm. The corresponding protocol was provided previously [88].

3.2.16 In vitro binding assays

The cell line 4950T secretes glycodelin into the culture supernatant in high amounts compared to other cell lines (average of 100 ng/ml). For cell-based assays, cell culture supernatant was condensed using Amicon filter columns with either 30 kDa or 100 kDa cutoff, retaining glycodelin in the concentrated part. For time course binding assays, the condensed supernatant was diluted to the initial concentration with cell culture medium without FBS. For binding assays with deglycosylated glycodelin, the condensed supernatant was first incubated with PNGase F, heat inactivated and then diluted to the initial concentration.

3.2.17 Affymetrix gene expression analysis

Control or knockdown 4950T cell culture supernatant was concentrated using an Amicon filter column with 30 kDa cutoff and glycodelin levels were measured via ELISA. The supernatants were diluted to final glycodelin concentrations of 200 ng/ml (control) and 60 ng/ml (knockdown) in RPMI without FBS (+ 10 ng/ml IL-2 for KHYG-1 treatment). The immune cell lines Jurkat, THP1, and KHYG-1 were washed and 5 x 10^5 cells were treated with 1 ml of condensed supernatant for 3, 8, or 24 h. Cells were collected, washed with PBS and RNA was isolated as described above.

For Affymetrix gene chip analysis, total RNA was processed following the instructions of GeneChip™ 3' IVT PLUS Reagent Kit User Guide (Manual Target Preparation for GeneChip™ 3' Expression Arrays). Chips covering the Human Genome Array Type: HG-U133_Plus_2 were prepared by Elizabeth Xu Meister and used to assess the gene expression. Data was analyzed using the Transcriptome Analysis Console and Ingenuity Pathway Analysis Software (QIAGEN Inc., https://digitalinsights.qiagen.com/IPA). The canonical pathway analysis and networks were generated through the use of QIAGEN IPA (QIAGEN Inc., https://digitalinsights.qiagen.com/IPA)[98].

4 Results

4.1 Comparison of the glycosylation pattern of NSCLC-derived glycodelin and immunosuppressive glycodelin A

The immunosuppressive function of glycodelin A is mediated mainly by its high sialylation and the distinct glycosylation pattern at the two asparagine sites N46 and N81 [99], [100]. In order to characterize the sugar structure in NSCLC-derived glycodelin, a lectin based pull-down assay was performed investigating 22 different binding specificities.

For the herein presented project, the cell culture supernatant of two NSCLC primary cell lines was used that secrete high amounts of glycodelin, i.e. around 20-100 ng/ml. The adenocarcinoma cell line 4950T was derived from a female NSCLC patient, while 170162T was established from the tumor tissue of a male patient. Both cell lines are cultivated without of fetal bovine serum. In order to prepare the cell culture supernatants for the subsequent pull-down assay, they were processed through a centrifugal filter with a mass cutoff of 100 kDa. Glycodelin has a molecular mass of 28 kDa when fully glycosylated and is known to form homodimeric complexes [48]. In addition, it seems to either form larger complexes or to bind to other proteins in the solution as it was efficiently retained in the concentrate (**Figure *4.1*** A).

The condensed supernatants were then incubated with different lectins and binding was assessed by detecting glycodelin using western blot analysis (**Figure *4.1*** B). As a comparison, glycodelin A was used that was isolated from amniotic fluid and kindly provided by my cooperation partners Hannu Koistinen and Annikki Löfhjelm (University of Helsinki, Department of Clinical Chemistry and Hematology, Finland). An exemplary immunoblot for glycodelin A is shown in **Figure *4.1*** C, the respective results for glycodelin in 4950T and 170162T supernatant are displayed as representative blots in **Figure *4.1*** D and E. For each lectin, the flowthrough or non-binding signal was compared to the signal of bound protein and scored according to the relative signal intensity in the bound fraction. Scoring was divided from very strong (>70 % signal detection in bound fraction compared to flowthrough), over strong (40-69 % signal detection), weak (10-39 % signal detection), to no detectable binding (0-9 %). For 170162T derived glycodelin, only eight lectins were implied that would enable a comparison of the most interesting glycosylation features. The results of three independent experiments are summarized and presented in **Table *4.1***.

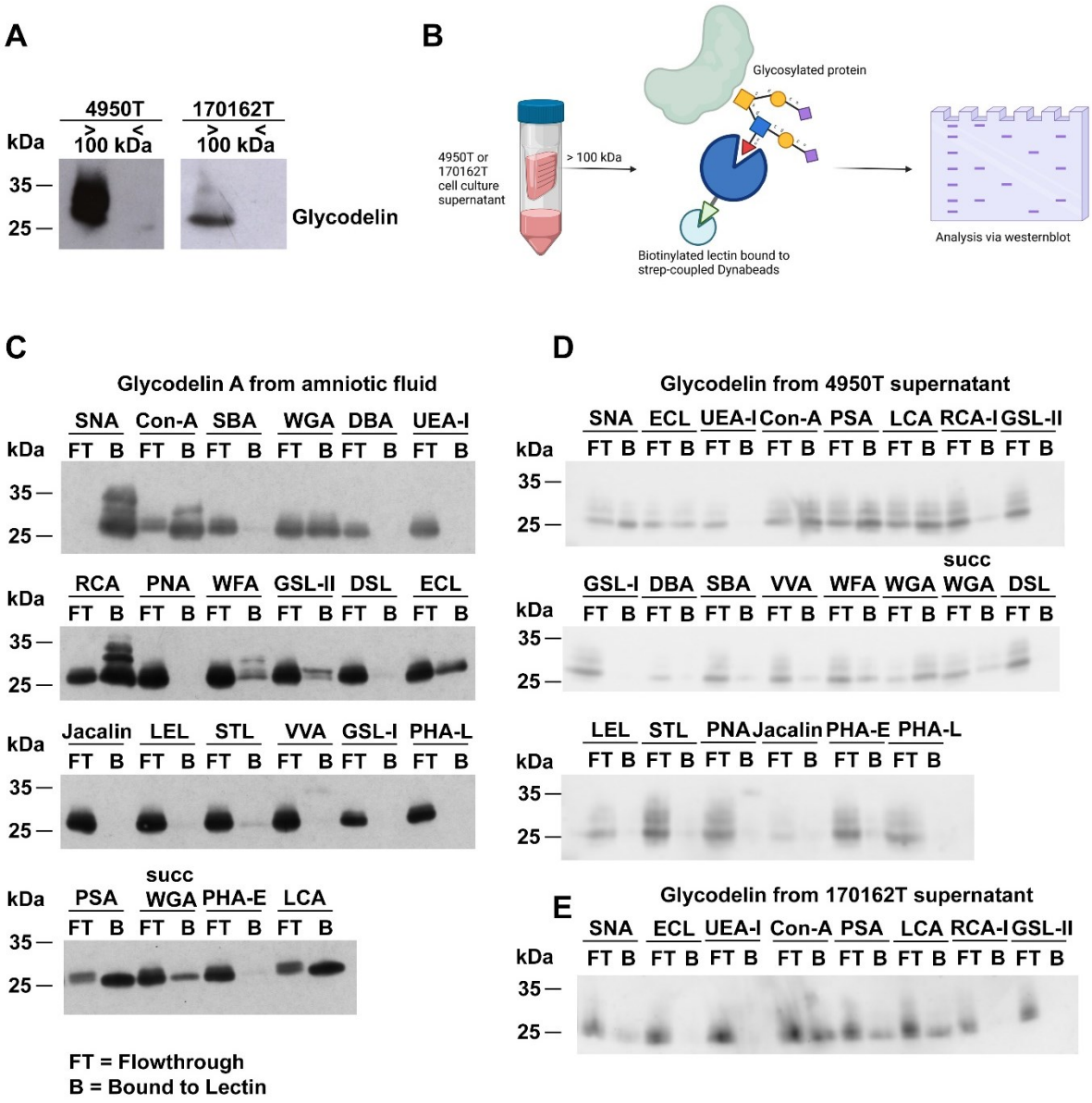

Figure 4.1: Characterization of NSCLC-derived glycodelin using lectin-based enrichment. A) Western blot showing cell culture supernatant from 4950T and 170162T before and after filter centrifugation with a 100 kDa cutoff. B) Schematic workflow of lectin-based enrichment and subsequent analysis. C-E) Representative western blot images depicting the flowthrough (FT) and bound (B) glycodelin to the distinct lectins of glycodelin A from amniotic fluid, 4950T supernatant, and 170162T supernatant.

An overview of the table reveals that glycodelin derived from the NSCLC cell lines supernatants and immunosuppressive glycodelin A from amniotic fluid share many similarities. All proteins were bound by *Sambucus Nigra Agglutinin* (SNA) which is specific for sialic acid, the major glycosylation residue in glycodelin A and driver of its immunosuppressive function [53], [101]. However, the signal for glycodelin from 170162T supernatant was weaker compared to the other analyzed glycoproteins. Another difference exclusively found in 170162T could be observed in the binding capacity of ECL that did not bind any protein, while the other signals match with glycodelin in 4950T supernatant. All three proteins were bound by *Concanavalin-A* (Con-A), *Pisum sativum* agglutinin (PSA), and *Lens culinaris* agglutinin (LCA)

and thus seem to share the typical sugar backbone consisting of mannose and glucose [60]. Some differences were observed between glycodelin A and 4950T-derived glycodelin. In contrast to the protein from the NSCLC cell line, glycodelin A was strongly bound by *Ricinus communis* agglutinin (RCA I), and to a slightly weaker extend by *Griffonia (Bandeiraea) Simplicifolia* Lectin II (GSL II), and succinylated *Triticum vulgaris* agglutinin (succ. WGA).

To summarize, glycodelin secreted by NSCLC cell lines share basic and functional glycosylation residues with immunosuppressive glycodelin A. Differences were observed between the NSCLC cell lines, that might be based on the sex difference of the patients but need further investigation.

Table 4.1: Results of the lectin based pull-down assay. 22 different lectins were used and incubated with glycodelin A from amniotic fluid, 4950T supernatant or 170162T supernatant. The binding specificity of each lectin is described in the right column. Binding was scored from very strong (dark red), over strong and weak (pale red to white), to no detectable binding (blue). Scoring is based on three independent experiments.

Lectin	GdA	4950T SN	170162T	Binding Specificity
SNA				Sialic acid
ECL				Galactose, N-Acetylgalactosamine, Lactose
UEA I				Fucose, Arabinose
Con-A				Mannose, Glucose
PSA				Mannose, Glucose
LCA				Mannose, Glucose
RCA I				Galactose, Lactose
GSL II				N-Acetylglucosamine
GSL I			N/A	Galactose, N-Acetylgalactosamine
DBA			N/A	N-Acetylgalactosamine
SBA			N/A	Galactose, N-Acetylgalactosamine
VVA			N/A	N-Acetylgalactosamine (Tn antigen)
WFA			N/A	N-Acetylgalactosamine
WGA			N/A	N-Acetylglucosamine, Sialic acid
WGA_{succ}			N/A	N-Acetylglucosamine
DSL			N/A	[GlcNAc]1-3, N-Acetylglucosamine
LEL			N/A	[GlcNAc]1-3, N-Acetylglucosamine
STL			N/A	N-Acetylglucosamine
PNA			N/A	Galactose
Jacalin			N/A	Galactose, O-glycosylation
PHA-E			N/A	Galactose, Complex Structures
PHA-L			N/A	Galactose, Complex Structures

4.2 **Binding of NSCLC-derived glycodelin to immune cells *in vitro***

After revealing the structural similarities of glycodelin A and NSCLC-derived glycodelin, I proceeded to investigate its capability to bind to immune cells in order to achieve a regulation.

Hence, I have established several different tests with immortalized leukocytes that were treated with cell culture supernatant from 4950T containing glycodelin. The *in vitro* experiments were performed with the immune cell lines Jurkat (T lymphocyte), THP1 (monocyte derived), and KHYG-1 (natural killer cell) and cell lysates were analyzed *via* western blot after glycodelin treatment (***Figure 4.2*** A). In a first attempt, I tested whether glycodelin will be exclusively detected in the immune cell lysates after treatment for 24 h compared to a control sample that was cultivated in the corresponding cell culture medium (***Figure 4.2*** B). The immunoblot revealed that the immune cells do not express glycodelin and are capable of binding the protein when it was present in the culture medium.

Furthermore, I could validate that the signal which was detected with the anti-glycodelin antibody was specific as no protein was detected in cell lysates that were cultivated with medium containing FBS (***Figure 4.2*** C). In FBS, β-lactoglobulin can be found which shares genetic homology with the human *PAEP*/glycodelin and has a closely related sequence and structure [102]. However, it did not interfere with the *in vitro* evaluation by immunoblots.

In addition to the experiments using unprocessed cell culture supernatant and thus the native form of NSCLC-derived glycodelin, I performed a complete digest of N-glycosylation by using PNGase F (**Figure *4.2*** D). As a control of a fully successful digest, one sample was treated under denaturing conditions, while the non-denatured protein was used for subsequent binding experiments. After treatment for 24 h, the cell lysates were analyzed by western blot. It demonstrated that deglycosylated glycodelin is also capable of binding to the examined leukocytes. Thus, the interaction of NSCLC-derived glycodelin and immune cells is not dependent on its glycosylation structure.

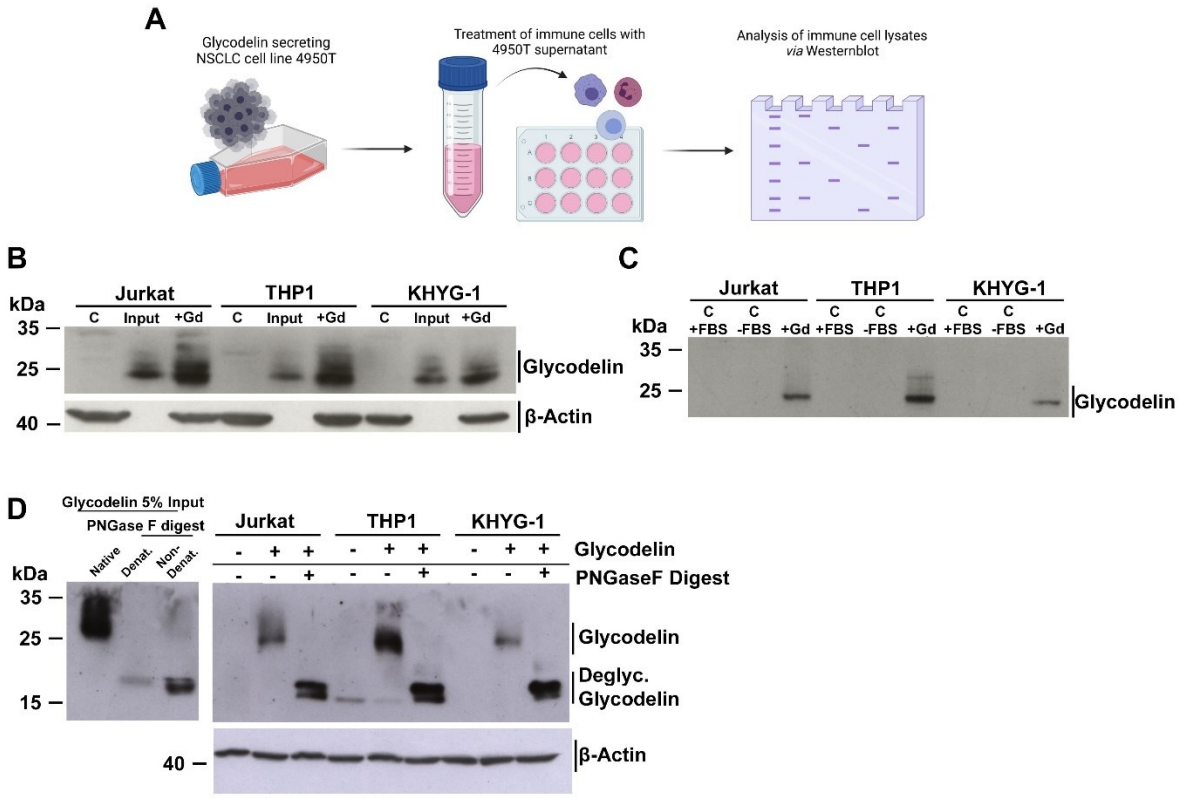

Figure 4.2: Immune cells bind glycodelin from 4950T supernatant. A) Schematic workflow of immune cell treatment with 4950T cell culture supernatant and subsequent analysis via western blot. B) Western blot detecting glycodelin in immune cell lysates. C are the control lysates that were treated only with culture medium, the input represents the 4950T supernatant that was used for the treatment (corresponds to 5 % of the final amount added), +Gd represents the sample that was incubated with glycodelin in 4950T supernatant. C) Western blot depicting control samples that were pre-treated with and without FBS. D) Western blot of native glycodelin or deglycosylated glycodelin immune cells. Successful deglycosylation under non-denaturing condition was confirmed by comparison with reaction of fully denatured protein (Denat.).

Following the first approaches to investigate binding of NSCLC-derived glycodelin to leukocytes, I attempted to further identify whether the detected interaction was efficient and specific for the immune cell lines. Therefore, I have performed time course experiments where the immune cells were incubated with glycodelin containing supernatant for 10-120 min (**Figure *4.3*** A). The glycoprotein could be detected in the cell lysates after the shortest incubation time of 10 min, suggesting a fast binding ability. The same conclusion could be drawn with deglycosylated glycodelin, that was detected in the investigated immune cell lines after 10 min incubation (**Figure *4.3*** B).

To assess whether the observed binding might be specific for leukocytes, two other cell lines were treated with 4950T cell culture supernatant as a comparison to Jurkat (**Figure *4.3*** C). I have cultivated the fibroblast cell line 4950T-F from tumor tissue corresponding to patient 4950 and used it as one comparison cell line. Another cell line that I used for this assay were the 2427T, which is a squamous cell lung cancer derived cell line negative for glycodelin expression. Neither the cell lysates of the fibroblast cell line 4950T-F nor the tumor cell line 2427T could bind glycodelin from the cell culture medium as effective as the Jurkat cells.

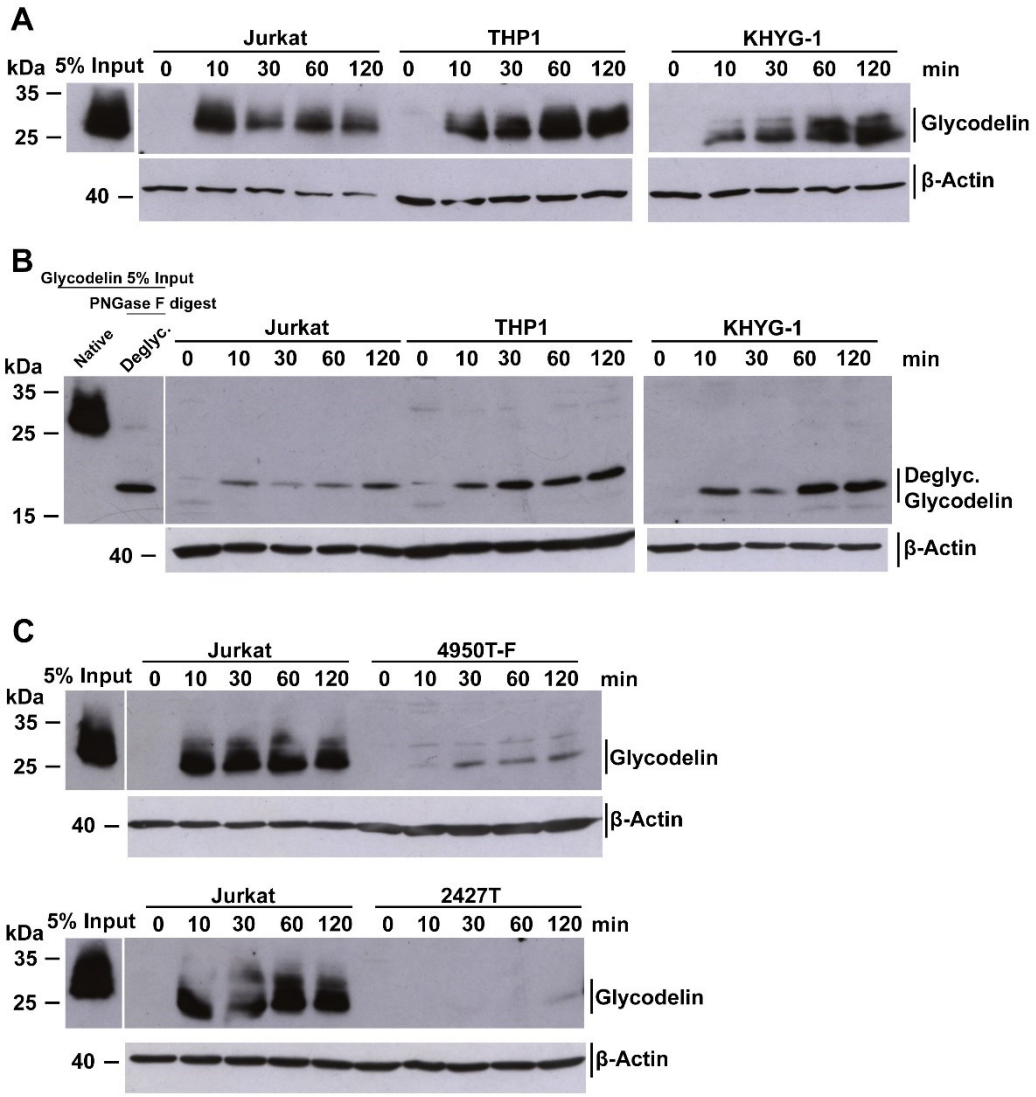

Figure 4.3: Glycodelin is specifically detectable on immune cells after short incubation. A+) Time course experiments of glycodelin binding to immune cells with natice (A) and deglycosylated (B) glycodelin. C) Glycodelin signal detection in Jurkat cell lysates compared to the fibroblast cell line 4950T-F and the tumor cell line 2427T.

The presented *in vitro* assays could not yet distinguish between glycodelin being bound to the membrane of immune cells or being internalized either by endocytosis or receptor-mediated uptake. Previous immunofluorescence experiments failed to give robust results due to unspecific signals independent of glycodelin treatment. Thus, I have performed several approaches to be able to differentiate between the possible interactions (**Figure *4.4*** A-F). The immune cell lines were treated with 4950T supernatant for 10 min and 2 h at different temperatures, as receptor internalization is strongly diminished at lower temperatures [103]–[106]. After incubation with glycodelin, the cells were either washed with DPBS or with an acidic glycine solution at pH 3. Washing the cells at a low pH removes proteins that are bound to the cell membrane. In addition, I have performed a TCA precipitation in the acidic wash solution after the cell wash to check for glycodelin that might have been removed from the cell surface.

The immunoblots and the corresponding signal quantification revealed that glycodelin can be detected in every cell lysate sample independent of the time, temperature or sample acquisition procedure that was applied. The TCA precipitation did not result in any detectable levels of glycodelin, indicating that the majority of available protein was internalized.

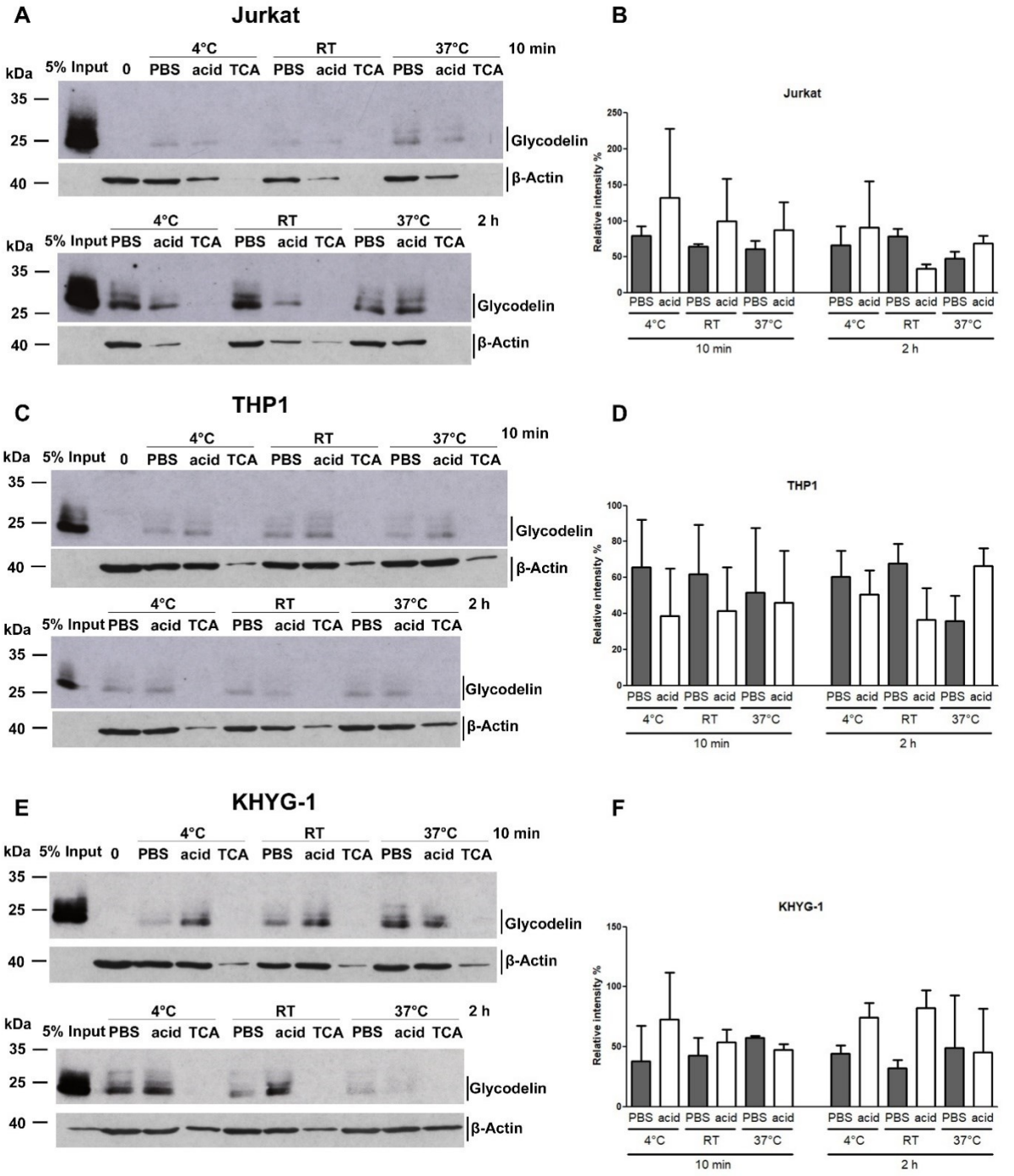

Figure 4.4: Investigating glycodelin binding and uptake by immune cells. A) Western blot and B) corresponding signal quantification of Jurkat cell lysates after treatment with glycodelin for 10 min and 2 h at different temperatures. Cells were either washed with PBS or with glycine at pH 3 after glycodelin treatment. TCA precipitation was performed on the acidic wash solution to check for glycodelin. C) and D) represent the respective results for THP1, E) and F) for KHYG-1.

The various binding assays *in vitro* have shown that glycodelin which is secreted by the NSCLC cell line 4950T is capable of binding to immune cells in a fast and specific manner, and that it is internalized independent of receptor binding. While protein uptake could also be observed for the de-glycosylated backbone, previous studies indicate that the distinct glycosylation pattern is crucial for functionality [60]. Consequently, native NSCLC-derived glycodelin was used for further experiments.

4.3 Functionality of glycodelin from NSCLC cell line - gene expression regulation in monocytic and natural killer cells

The function of glycodelin A in the endometrium, during the menstrual cycle, and before or during pregnancy is well characterized [51], [58]. Numerous studies have investigated the highly pleiotropic effects and the modulation of different leukocytes upon glycodelin interaction [56], [95], [107].

In NSCLC, the function of glycodelin is not known, yet. While it was shown to be highly expressed in lung tumor tissue compared to normal lung [90], the functionality and possible immunomodulating characteristics remain to be described.

4.3.1 Establishment of a robust *PAEP* knockdown procedure

To examine the functionality of NSCLC glycodelin, it was first necessary to establish a comparable, reproducible, and robust method. The NSCLC cell line 4950T secretes high amounts of glycodelin compared to other cell lines. In addition, the primary cell line is cultivated without FBS thus enabling a procedure that might not be biased by the presence of β-lactoglobulin. To treat the immune cells with comparable solutions, i.e. cancer cell supernatant with and without glycodelin, a gene knockdown using small interfering RNAs (siRNAs) was performed that target the encoding gene *PAEP*. I have therefore developed the optimal experimental conditions to achieve a high difference in glycodelin concentration while obtaining cancer cell viability.

Several concentrations of a mixture of siRNAs that were validated before were included and successful gene knockdown was analyzed by qRT-PCR and western blot (**Figure *4.5*** A and B). *PAEP* knockdown efficiency was highly significant when using a final concentration of 5 and 1 nM siRNA. 4950T cell lysates were processed for SDS-PAGE and western blot, which confirmed the strong downregulation of the protein when using final siRNA concentrations of 1 nM and above. In addition, cell viability upon gene knockdown was examined by light microscopy (**Figure *4.5*** C). The cell morphology of 4950T cells was highly altered with siRNA concentrations of 5 and 10 nM when compared to the control cells that were incubated with 10 nM negative control siRNA. Moreover, I performed an LDH activity assay to measure the cell viability (**Figure *4.5*** D). The experiment confirmed that lower siRNA concentrations result in a higher cell viability and consequently would not change the composition of the supernatant due to a change of cell morphology, fitness, and viability.

As a result, I decided to use a final siRNA concentration of 1 nM pooled *PAEP* siRNA to perform knockdown experiments and yield supernatants with high and low concentrations of NSCLC derived glycodelin.

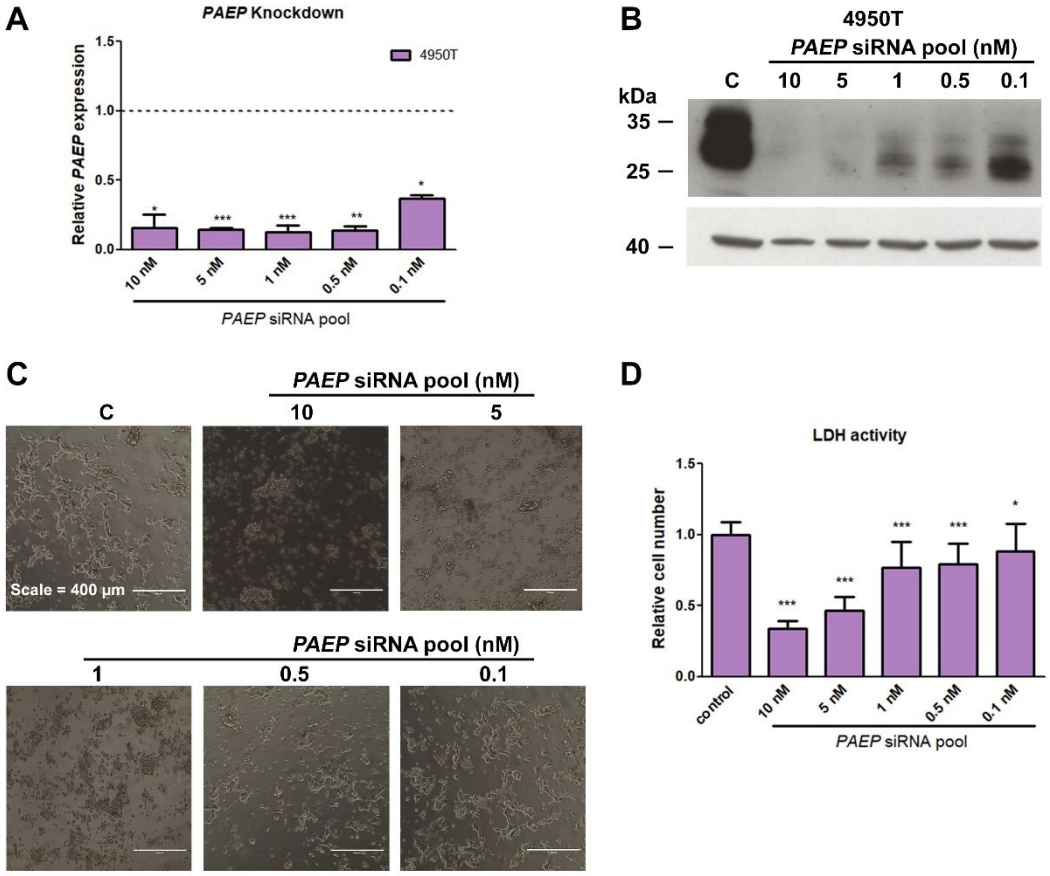

Figure 4.5 : *PAEP* Knockdown experiments in 4950T to assess the optimal siRNA concentration for further approaches. A) PAEP gene knockdown efficiency analyzed by qRT-PCR (dotted line represents the control) and B) glycodelin protein knockdown validated by western blot. Cell viability upon 72 h siRNA incubation was examined by C) light microscopy and D) LDH activity measurement. C = control

4.3.2 Gene expression analysis after glycodelin treatment using GeneChip® and Transcriptome Analysis Console (TAC)

I investigated a possible impact of NSCLC-derived glycodelin on the gene expression in immune cells as displayed in **Figure *4.6*** A. After the establishment of a sufficient knockdown protocol, I have prepared the control and knockdown cell culture supernatants by centrifugal filtration using a 30 kDa filter. Under physiological conditions in pregnancy, glycodelin concentrations reach up to more than 100 µg/ml in the amniotic fluid [50]. To increase the amount of glycodelin that can be obtained from the NSCLC cell culture, supernatants were condensed and kindly measured by Hannu Koistinen and Annikki Löfhjelm who have a robust ELISA to predict glycodelin concentrations [108]. A control analysis *via* western blot confirmed the high difference in the amount of glycodelin (**Figure *4.6*** B). Hence, the immune cell lines Jurkat, THP1, and KHYG-1 were treated with condensed cell culture supernatant containing either 200 ng/ml glycodelin for the control or 60 ng/ml glycodelin for the knockdown samples. The leukocytes were incubated for 3, 8, and 24 h to cover possible early and late gene

expression responses. After sample processing, the gene expression was analyzed by using the Affymetrix Human Genome U133 2.0 array. Furthermore, cell viability of the treated immune cells after 24 h glycodelin treatment was examined with an AO/PI assay revealing no impact of the applied supernatants on the viability in general (**Figure *4.6*** C). RNA integrity throughout the process and successful fragmentation was controlled by gel electrophoresis of the cRNA and the fragmented cRNA by using a Bioanalyzer (**Figure *4.6*** D-G).

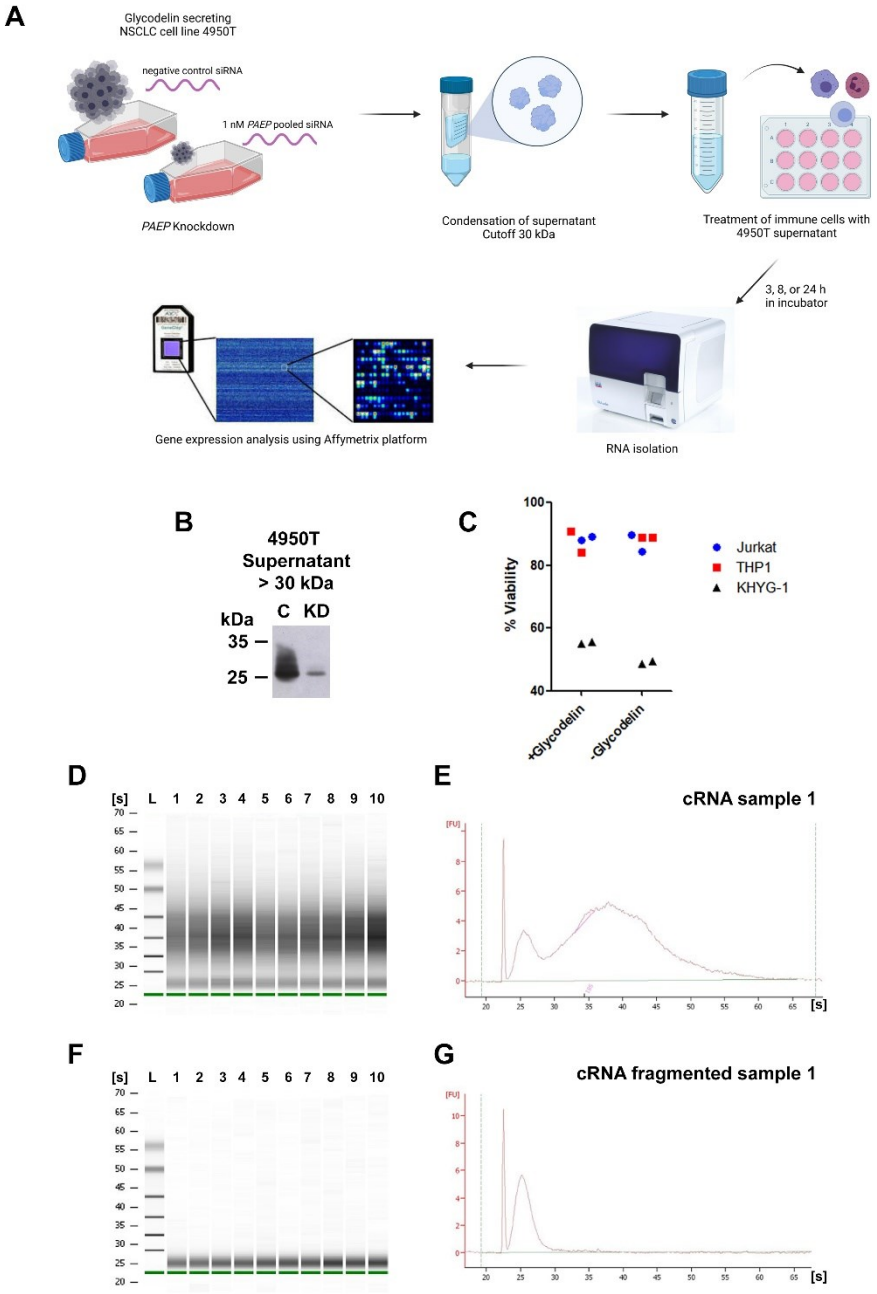

Figure 4.6: Investigating the impact of glycodelin on the gene expression of immune cells. A) Schematic workflow depicts the single steps of the approach. Control and knockdown supernatant of the NSCLC cell line 4950T was condensed over a 30 kDa filter and applied onto the immune cells for different time points. Total RNA was isolated and gene expression was measured with a GeneChip® 3' Expression Array. B) Western blot validating the glycodelin knockdown (KD) compared to the control (C) sample. C) AO/PI viability assay of immune cells after treatment with 4950T control and knockdown supernatant for 24 h. D) Representative gel electrophoresis of cRNA

as quality control and E) corresponding electropherogram of sample 1. F) and G) represent the results for fragmented cRNA.

The obtained data was analyzed by using the Transcriptome Analysis Console and the groups glycodelin *vs*. no glycodelin were compared with regard to a significantly altered gene expression. Genes with a fold change expression of < -2 or > 2 and a p-value < 0.05 were included in subsequent analyses. For the T lymphocyte cell line Jurkat, no differential gene expression was observed after any of the time points in the range of the applied glycodelin concentrations. Treatment of THP1 across all time points and of KHYG-1 after 24 h resulted in the significant up- or downregulation of several genes. For KHYG-1 only two replicates were suitable for analysis due to a low RNA quality in previous processing steps. An overview is displayed in the heat maps in **Figure *4.7***. The samples clearly clustered according to the condition of treatment with or without glycodelin. In THP1 cells, an effect on the gene expression of 138 genes (95 upregulated, 43 downregulated) could already be observed after 3 h (**Figure *4.7*** A), while for the NK cell line the incubation lasted 24 h to generate a significant difference in 58 genes (54 upregulated, 4 downregulated) (**Figure *4.7*** D). After 8 h, 61 genes (45 upregulated, 16 downregulated) showed a differential expression in THP1 (**Figure *4.7*** B), while after 24 h, 106 genes were significantly upregulated and only the gene *AKR1C2* showed a lower expression(**Figure *4.7*** C). Gene expression alteration was validated by qPCR of several selected genes, while in KHYG-1 the variability in sample quality after glycodelin treatment led to high standard deviations (**Figure *4.7*** E and F).

Among the top upregulated genes in THP1, several inflammatory related genes could be found like *TNF*, *CXC10*, *CCL4*, and *ICAM1*. In contrast, the gene *THBS1* was downregulated in most analyzed samples which is important for cell-to-cell and cell-to-matrix interactions. In KHYG-1, similar to the findings in THP1, the inflammatory related genes *TNF*, *CCL4*, and *IFNG* were upregulated among cell-cycle induction associated genes like *CCNE2*, *CDC6*, or *E2F8*.

The analysis revealed, that even the comparably low concentration of glycodelin derived from the NSCLC cell line supernatant has a significant effect on the gene expression in the monocyte like and the natural killer cell line used in this project. The data generated by the TAC software was further analyzed to obtain a global view on pathways and associated networks that might be affected in the immune cells by the glycodelin treatment.

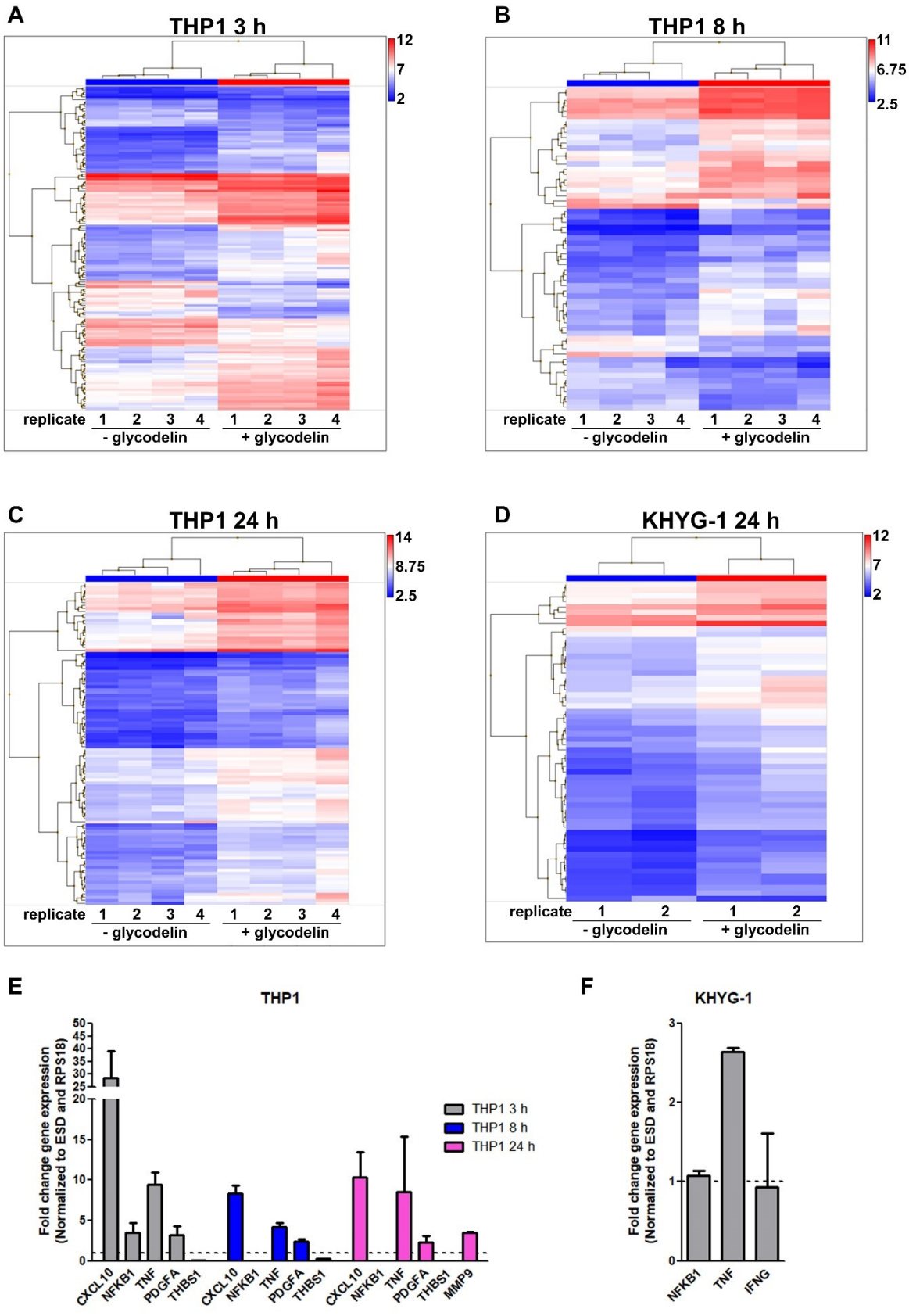

Figure 4.7: Results from the transcriptome analysis displayed in hierarchical clusters. Gene expression profiles of A)-C) THP1 and D) KHYG-1 with glycodelin containing supernatant. Signal intensity is shown as color scale ranging from high (red) to low (blue). E) qPCR validation of selected genes in THP1 and F) KHYG-1.

4.3.3 Pathways and networks in THP1 and KHYG-1 that are affected by glycodelin treatment

By investigating genetic alterations in treated samples using an array like the Affymetrix platform, a broad overview is generated that can be further analyzed. For this, I have used the Ingenuity Pathway Analysis software that can be used to evaluate affected pathways and create gene networks to visualize transcriptional regulations and effects.

First, I have investigated the canonical pathways that were affected by glycodelin treatment due to the up- or downregulation of significant genes (**Figure *4.8***). In THP1, inflammatory pathways were highly affected like the TREM1 signaling pathway or Neuroinflammation Signaling Pathway. Related to the pulmonary region, all time points revealed the alteration of genes leading to hypercytokinemia/hyperchemokinemia in the pathogenesis of Influenza (**Figure *4.8*** A-C). In addition, the tumor microenvironment pathway was affected in all samples and the pathway regarding the regulation of epithelial mesenchymal transition by growth factors was influenced in the early time points of 3 and 8 h treatment.

In KHYG-1 similar inflammatory pathways were influenced by the treatment with glycodelin, leading to significant effects in the role of hypercytokinemia/hyperchemokinemia in the pathogenesis of Influenza and the Neuroinflammation Signaling Pathway (**Figure *4.8*** D). Furthermore, a cell-to-cell interaction pathway between dendritic cells and natural killer cells and a cell-cycle related pathway were affected.

The canonical pathway analysis revealed a highly inflammatory response of THP1 and KHYG-1 to the treatment with NSCLC-derived glycodelin. In THP1, a cancer related impact could be detected, as well.

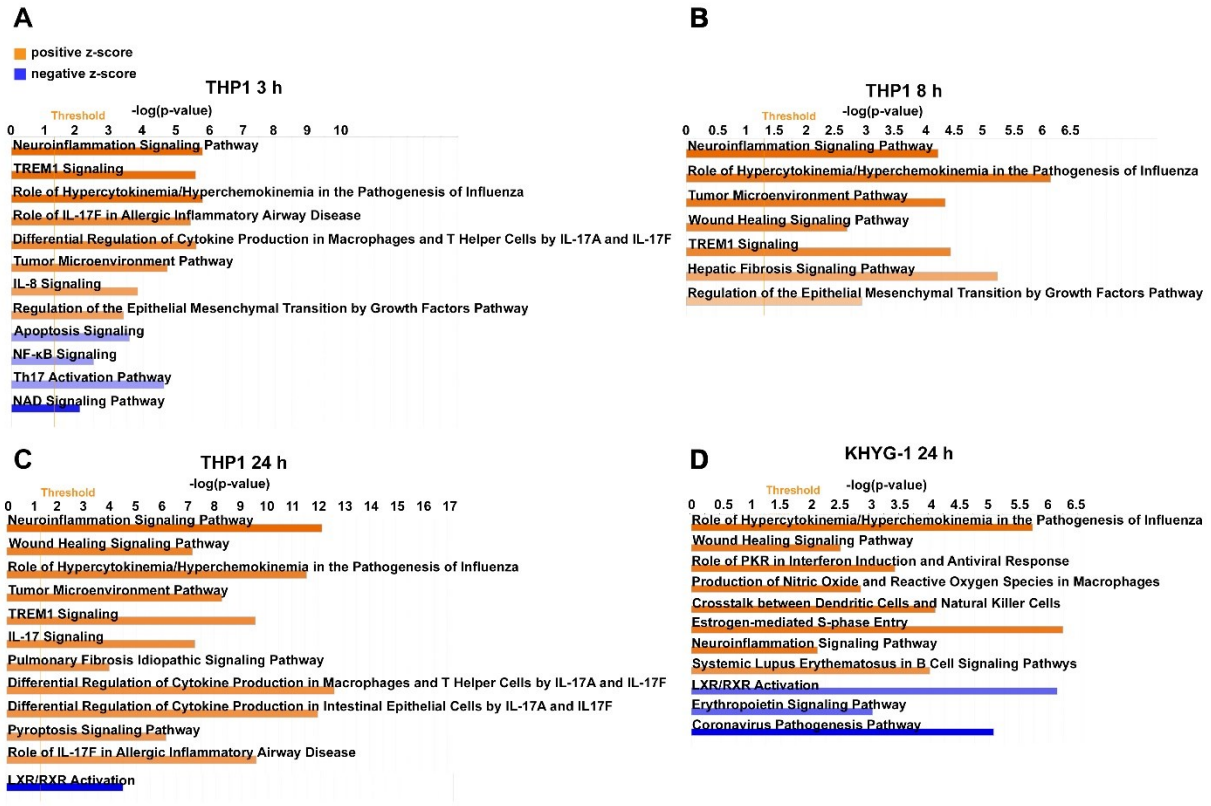

Figure 4.8: Major canonical pathways affected by treating THP1 and KHYG-1 with glycodelin. The charts depict representative canonical pathways sorted by the z-scores of the contained genes. Positive (orange) z-scores denote upregulation of genes, negative (blue) z-scores denote downregulation. A)-C) Results for the monocytic cell line THP1 after treatment with glycodelin for 3, 8, and 24 h. D) Results for the natural killer cell line KHYG-1 after 24 h treatment.

Following the evaluation of canonical pathways upon glycodelin treatment, I have applied a transcriptional network analysis to investigate and visualize signaling effects of aberrantly up- or downregulated genes. The software adds and connects genes that are predicted to be regulated and part of the signaling network based on the data of the imported experiment.

In THP1, the significant increase of *TNF* expression built the center of the network, along with additional immune response related genes (**Figure *4.9***). The network composition after 3 h of incubation mainly consisted of genes that are known to regulate inflammatory response, hematological system development and function, and tissue morphology (**Figure *4.9*** A). After 8 h, connective tissue disorders, and inflammatory disease and response represented the mainly affected diseases and functions (**Figure *4.9*** B). The longest incubation of 24 h led to network and signaling conditions that are important for cellular movement, immune cell trafficking, and hematological system development and function (**Figure *4.9*** C). The functions that are influenced by the aberrant expression of related genes thus change over time from a highly inflammatory response to the regulation of cell mobility in THP1 cells.

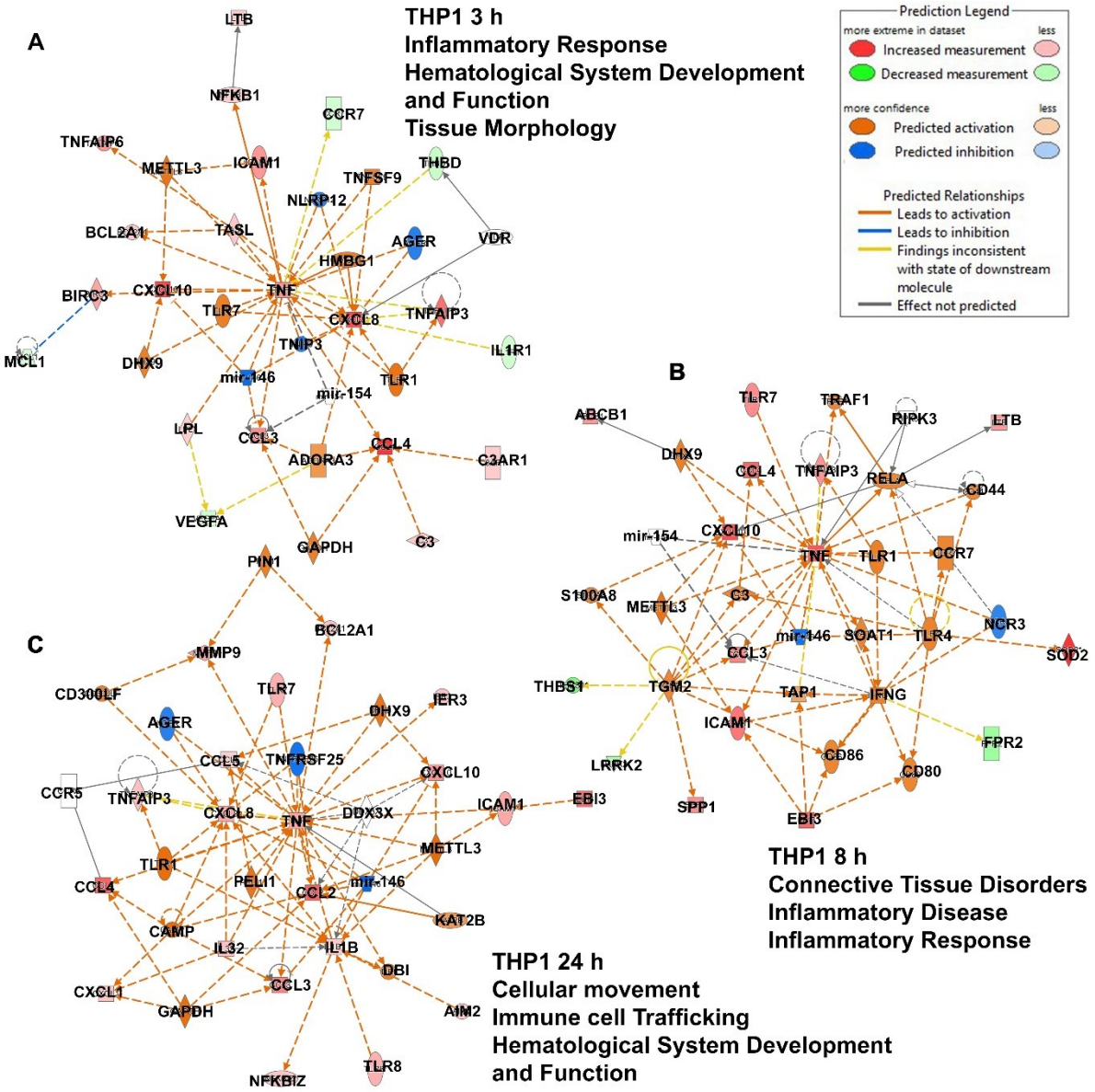

Figure 4.9: Ingenuity Pathway network analysis of up- and downregulated genes in THP1 after glycodelin treatment. The corresponding top three related diseases and functions are described next to the network maps after A)-C) 3, 8, and 24 h treatment of THP1 with glycodelin.

The analysis in KHYG-1 revealed a major transcriptional interaction network that is important in cancer, hematological, and immunological disease (**Figure *4.10***). Again, upregulation of *TNF* built the center among *CCL4*, both genes being major regulators in various signaling pathways. In comparison to the networks in THP1, several predicted relationships between the genes are inconsistent with the actual state of the respective genes, which is depicted by the yellow connecting lines.

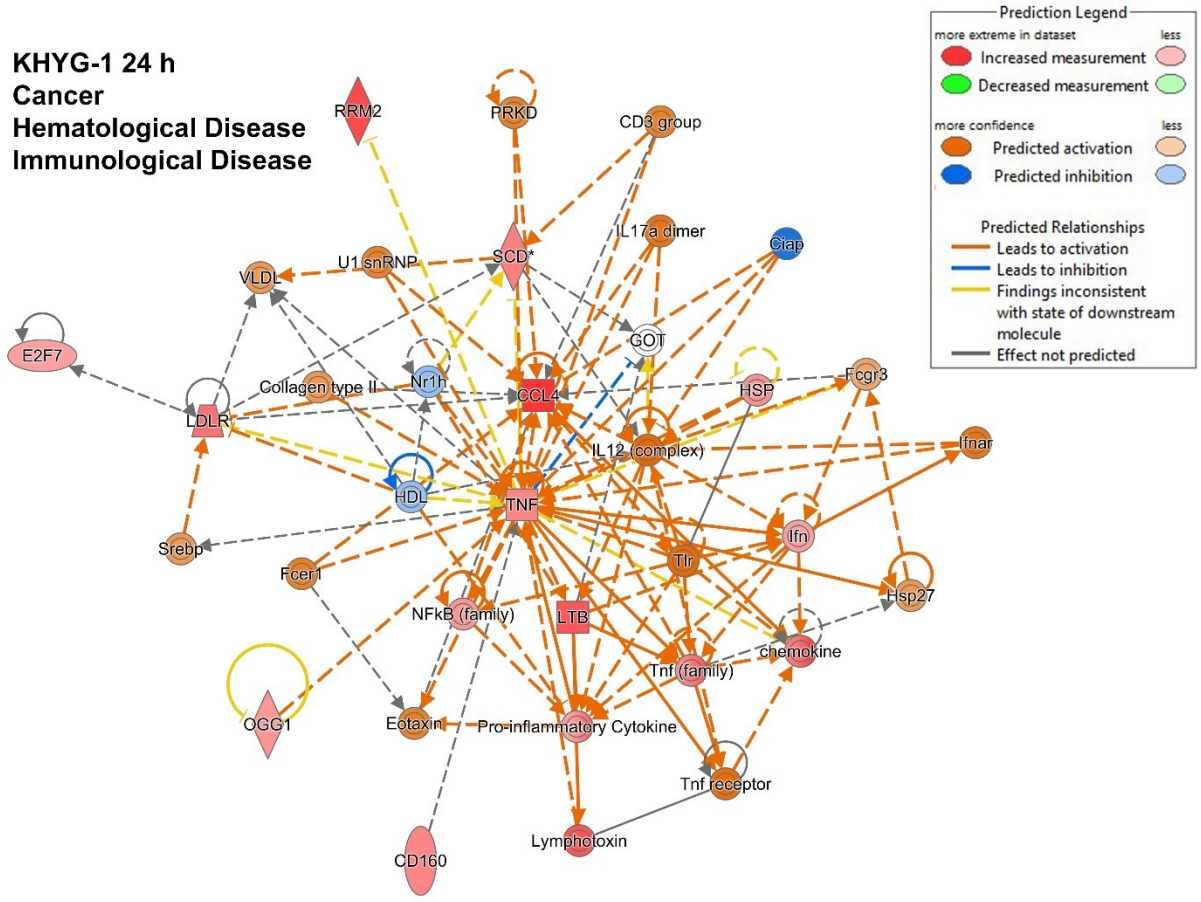

Figure 4.10: Ingenuity Pathway network analysis of up- and downregulated genes in KHYG-1 after glycodelin treatment. The corresponding top three related diseases and functions are described next to the network map.

To sum up, the gene expression analysis of THP1 and KHYG-1 after treatment with NSCLC-derived glycodelin was performed to evaluate whether a functionality and a transcriptional regulation can be observed. Moreover, related pathways and genetic networks were of interest that might give information on the impact of glycodelin in the different immune cell lines.

For the monocyte like cell line THP1 and the natural killer cell line KHYG-1 the analysis resulted in valuable data indicating a major inflammatory response. Important pathways related to tumor microenvironment, airway hyperinflammation, or cell-cycle control are affected due to the significant upregulation of genes like *TNF*, *CCL4*, or *ICAM1,* among others. Consequently, NSCLC-derived glycodelin from cell culture supernatant indeed shows significant characteristics in the modulation of distinct immune cells.

4.4 **Spatial analysis of glycodelin and leukocyte markers in NSCLC tissue**

4.4.1 Heterogeneous expression and binding to CD45+ leukocytes of glycodelin in NSCLC tissue

The *in vitro* experiments showed that glycodelin in NSCLC cell culture medium shares the immunosuppressive glycosylation structure with glycodelin A from pregnancy and is capable of binding to immune cells functionally. In the next step, I aimed to investigate whether these findings can be recapitulated *in vivo* by analyzing FFPE tissue and multiplex immunofluorescence staining.

To check for any possible interaction with immune cells in tissue sections, FFPE samples corresponding to the patients 4950T and 170162T were used, thus glycodelin in the same patients was investigated as during the *in vitro* experiments. Staining was kindly performed by our cooperation partners in Borstel, Torsten Goldmann and Sebastian Marwitz (Research Center Borstel, Germany). The results are depicted in **Figure *4.11***.

The tissues were stained with antibodies against glycodelin and CD45, a common marker for leukocytes. DAPI was applied for cell nuclei staining. The staining revealed several major points. First, glycodelin is heterogeneously expressed across the tumor and glycodelin signal can be detected in various regions ranging from the tumor center to the rim or only single cells scattered throughout the tumor tissue. In addition, signals were also detected in the tumor surrounding stroma. Here, distinct cells were found to be double positive for glycodelin and CD45 as underlined by the white arrows in the enlarged images. Thus, some leukocytes seem to interact with the tumor derived glycodelin.

The results confirmed that glycodelin secreted by the tumor cells of the patients 4950T and 170162T binds to leukocytes *in vivo*. However, not all of the tumor surrounding immune cells showed a glycodelin signal, therefore a more detailed analysis of the respective cell phenotypes was needed.

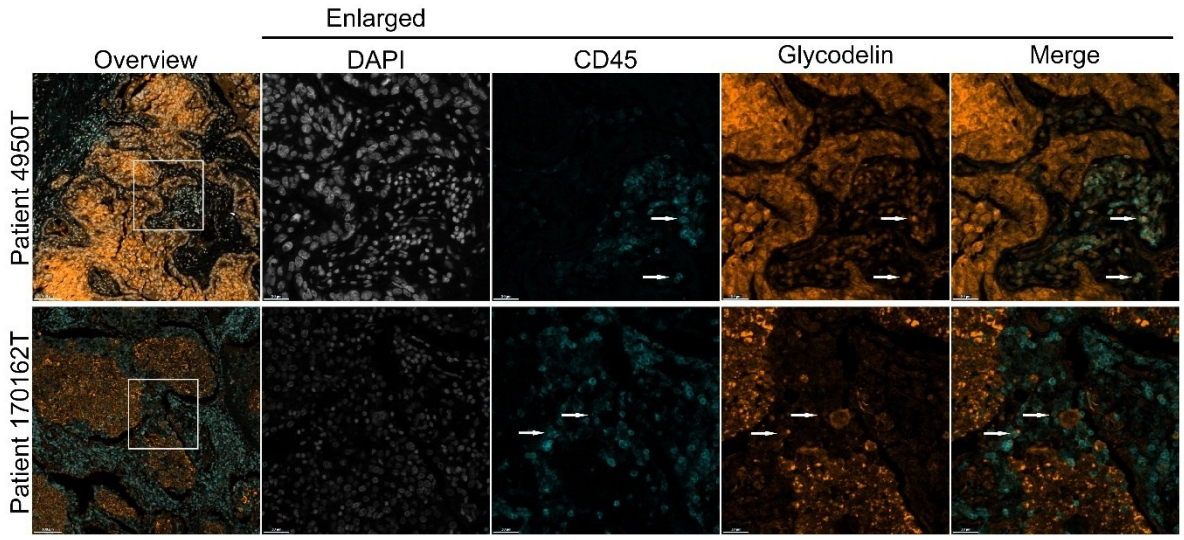

Figure 4.11: Multiplex immunofluorescence staining of tumor tissue from the patients 4950T and 170162T. FFPE tissue was stained for the leukocyte marker CD45 and glycodelin. Overview scale = 100 µm, enlarged images scale = 30 µm.

4.4.2 Algorithm based analysis of a multiplex immunofluorescence assay

To gain a broad and reliable insight into the properties of glycodelin in NSCLC regarding the interaction with immune cells, spatial analysis was performed on 12 tissue microarrays (TMAs) which covered tumor punches of around 700 patients. I performed the stainings and the subsequent analysis based on the Vectra Polaris™ System and inForm® software.

The technique behind the multiplex staining is based on the tyramide signal amplification system as displayed in **Figure *4.12*** A. In detail, antigen retrieval is induced by heat, followed by blocking and incubation with the primary antibody that targets the desired epitope. Thereupon, a polymer is added that binds to the primary antibodies and is conjugated to HRP. OPAL fluorophores with a specific excitation wavelength and coupled to inactive tyramide are incubated, leading to the activation of tyramide through HRP and hydrogen peroxide. Activated tyramide residues with conjugated fluorophores covalently bind to tyrosine residues in close proximity to the primary antibodies and consequently to the epitope of interest. The antibodies are stripped by repeating heat induced antigen retrieval and the procedure can be performed for the next labeling round. Finally, I have stained the TMAs with two different 5-plex panels and DAPI for cell nuclei staining. An example of a successfully stained TMA is shown in **Figure *4.12*** B.

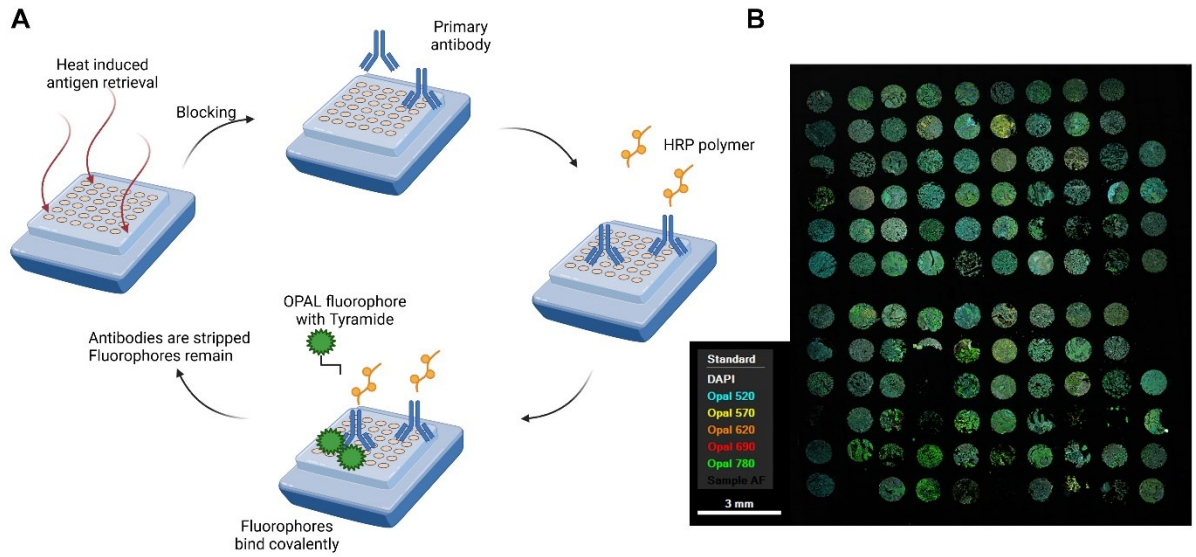

Figure 4.12: Multiplex Immunofluorescence technique to stain FFPE tissue with 5-plex. A) Schematic workflow describes the principle behind the OPAL TSA fluorophore staining procedure. B) Whole slide image of a TMA stained with a 5-plex including OPAL 520 (cyan), 570 (yellow), 620 (orange), 690 (red), and 780 (green). DAPI is used for nucleus staining. Scale = 3 mm.

The slides were then scanned and each tissue punch was analyzed regarding the type of tissue, the number of cells, and the specific phenotypes apparent in the section. For this, I have chosen distinct punches that I have used to train an algorithm in the inForm® software for the following analysis (**Figure *4.13*** A). First, I have marked regions in the training punches that are either tumor tissue (red), stroma (green) or other (background in blue). I have used a variety of histologies and staining qualities to ensure proper batch analysis. After verification of efficient tissue segmentation, I have optimized cell segmentation. The recognition of single cells is based on nucleus staining and further improved by several parameters like signal intensity, nucleus size, cytoplasmic and membrane markers, and splitting strength. In the next step, phenotypes were classified by machine-learning after manual annotation of examples based on fluorescent labeling, cell morphology, and signal intensity above threshold. (**Figure *4.13*** B).

The trained algorithm was applied onto the whole batch and enabled a fast and efficient analysis of nearly 700 tissue samples stained with two different multiplex panels.

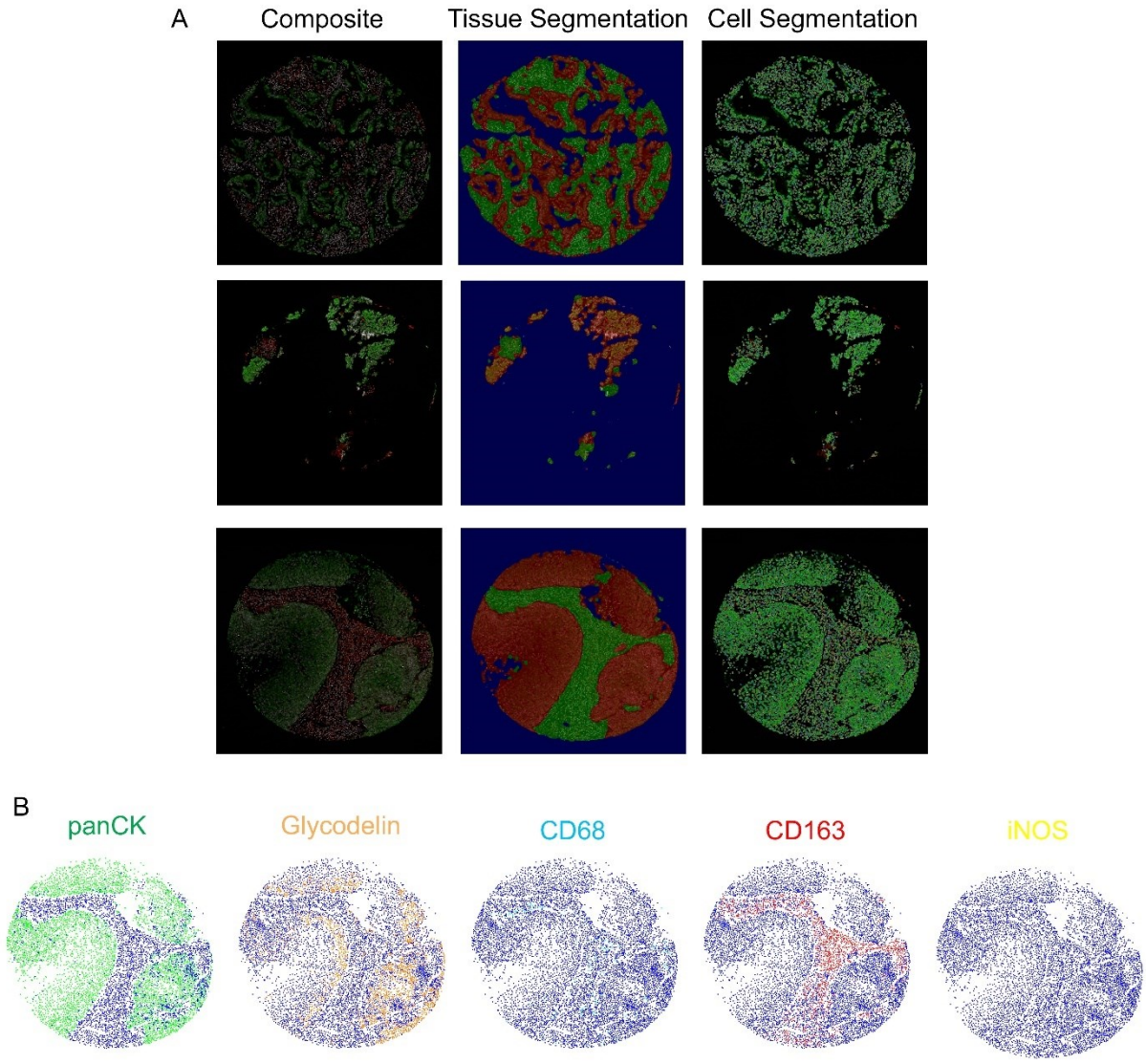

Figure 4.13: Algorithm based analysis of tissue samples. A) Representative tissue punches are used to train the algorithm in order to distinguish between tumor (red), stroma (green), and other (blue) areas. Three different examples of punches are depicted here. DAPI staining as well as additional parameters are used to enable single cell segmentation which is the basis for the subsequent phenotyping. B) Example of phenotyping based on fluorescent labeling, cell morphology, signal intensity, etc. of specific targets.

4.4.3 Spatial analysis of glycodelin and macrophages in NSCLC tumor microarrays

The tissue samples were analyzed for glycodelin and specific immune cell subsets. One of the panels that was used to stain the TMAs covered different macrophage markers. It included CD68, a universal marker for macrophages, iNOS, a M1 macrophage marker, and CD163, representing M2 macrophages. Besides, pan-cytokeratin (panCK) was used to selectively stain tumor tissue.

In-line with the previous findings in tumor tissue, glycodelin expression was heterogeneous, with some samples being highly positive (**Figure *4.14*** A), while in others hardly any signal could be detected (**Figure *4.14*** B). Most of the glycodelin signal was found in the tumor tissue and overlapped with panCK staining. However, some cells in the surrounding stroma revealed a glycodelin signal, as well. In general, tissue punches were found to be either positive for glycodelin or iNOS.

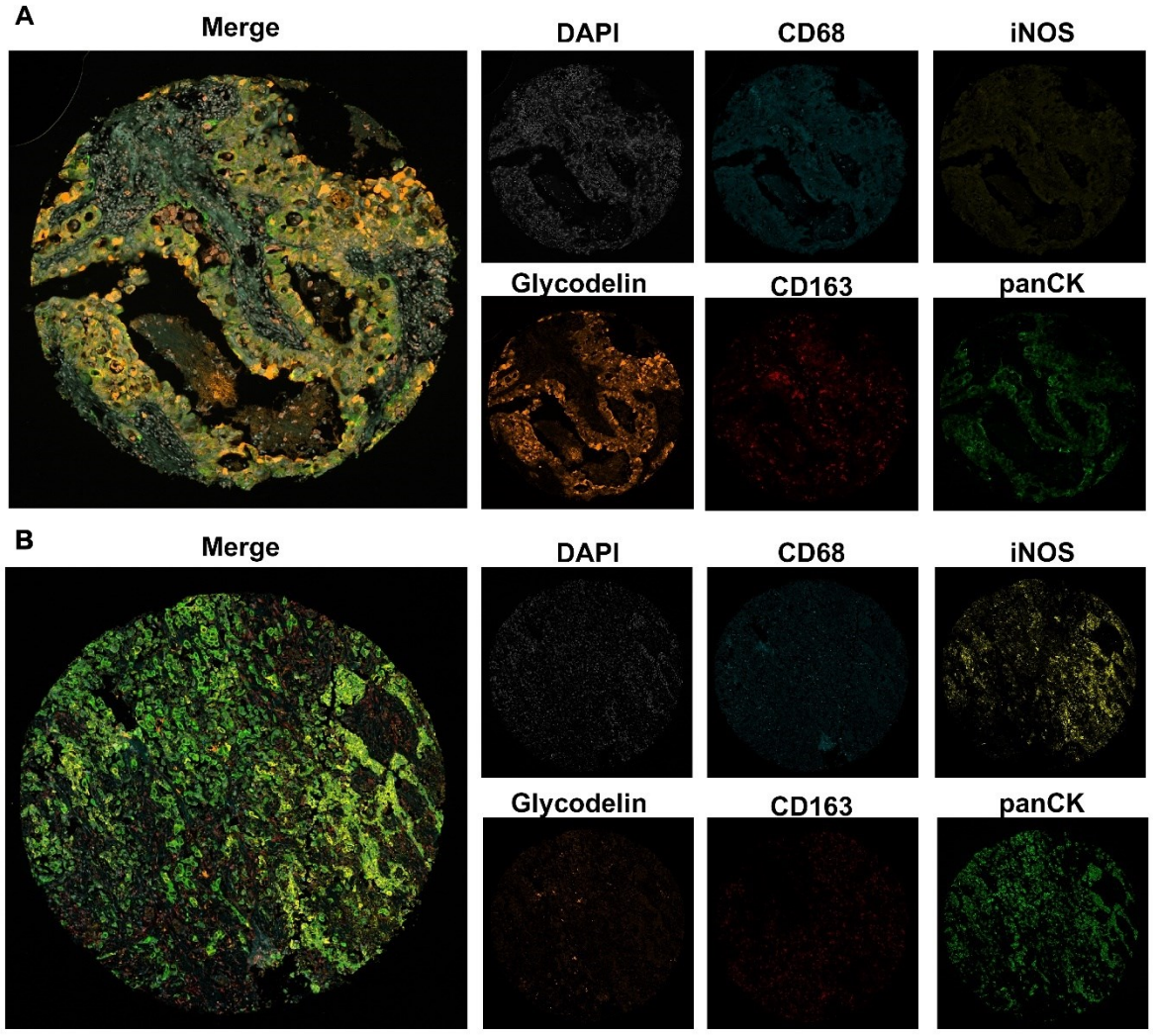

Figure 4.14: Examples of two punches stained with the macrophage panel (6.4x zoom). TMAs were stained with a 5-plex covering CD68, iNOS, glycodelin, CD163, and panCK. Cell nuclei were stained with DAPI. A) Example of a punch positive for glycodelin. B) Example of a punch with high iNOS signal.

I have further processed and analyzed the data by using the PhenoptR R package to obtain information about cell densities in distinct tissue areas and signal combinations that are of interest for the project. As expected, high cell numbers were found in the tumor tissue that were positive for panCK and glycodelin, while glycodelin positive cells were also detected in the stroma. A large proportion of tissue punches was found to be positive for iNOS in the tumor region, whereas the majority of CD163+ M2 macrophages was situated in the stroma. CD68+ macrophages were found in both areas, but also mostly in the surrounding stroma

(**Figure *4.15*** A). The analysis of cells that were detected in a combination of panCK and glycodelin showed that the majority of cell in the tumor are either positive for both markers or for panCK alone, while the combination of panCK-/glycodelin+ was significantly rarer. In the stroma, the opposite was observed, with panCK-/glycodelin+ cells accounting for the largest proportion of the investigated combinations (**Figure *4.15*** B). Regarding the different macrophage markers, it could be examined that the pattern of the different combinations appears the same in tumor and stroma. Cells triple positive for CD163, glycodelin, and CD68 were detected significantly less than cells that were only positive for CD163 and glycodelin. Still, CD163+/glycodelin- macrophages represented the largest group in tumor and especially in stromal areas (**Figure *4.15*** C). Probably the most apparent effect could be seen regarding the combination of iNOS and glycodelin. Hardly any cells were detected double positive in any of the tissue regions (**Figure *4.15*** D).

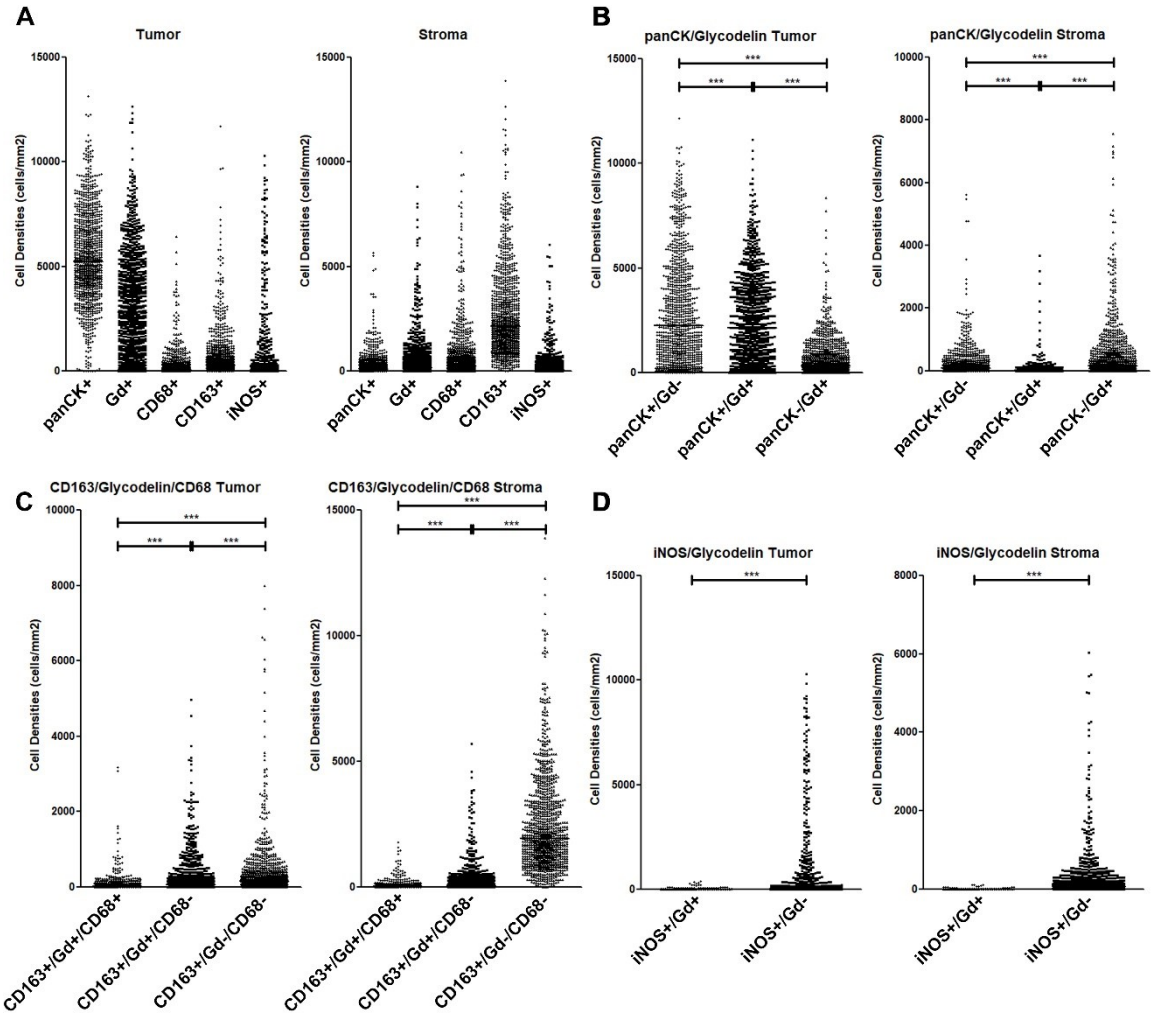

Figure 4.15: Cell densities of all phenotypes and specific combinations in the macrophage panel stained TMAs. Cell counts were normalized to the detected area and are displayed as cells/mm^2. A) Total cell densities of panCK, glycodelin, CD68, CD163, and iNOS positive cells in tumor and stroma. B) Comparison of cells positive for panCK and/or glycodelin in tumor and stroma. C) Comparison of cells positive for CD163 and positive or negative for CD68 and positive or negative for glycodelin in tumor and stroma. D) Comparison of cells positive for iNOS and positive or negative glycodelin in tumor and stroma. *** p-value < 0.0001, n.s. = not significant

By performing a Spearman correlation analysis with the results of the macrophage panel, the previous conclusions were further confirmed. The combination of glycodelin and CD163 in tumor remained below a correlation coefficient of 0.5. while cells positive for glycodelin nearly reached a correlation with CD163+ macrophages in the stroma (**Figure *4.16*** B). Nevertheless, correlation coefficients were close to 0.5 for glycodelin and CD68 ranging from 0.34-0.42 (**Figure *4.16*** C and D). In contrast, cells positive for iNOS or glycodelin revealed a tendency towards an anti-proportional location in the tumor with r = -0.37, while in the stroma no connection could be examined (**Figure *4.16*** E and F).

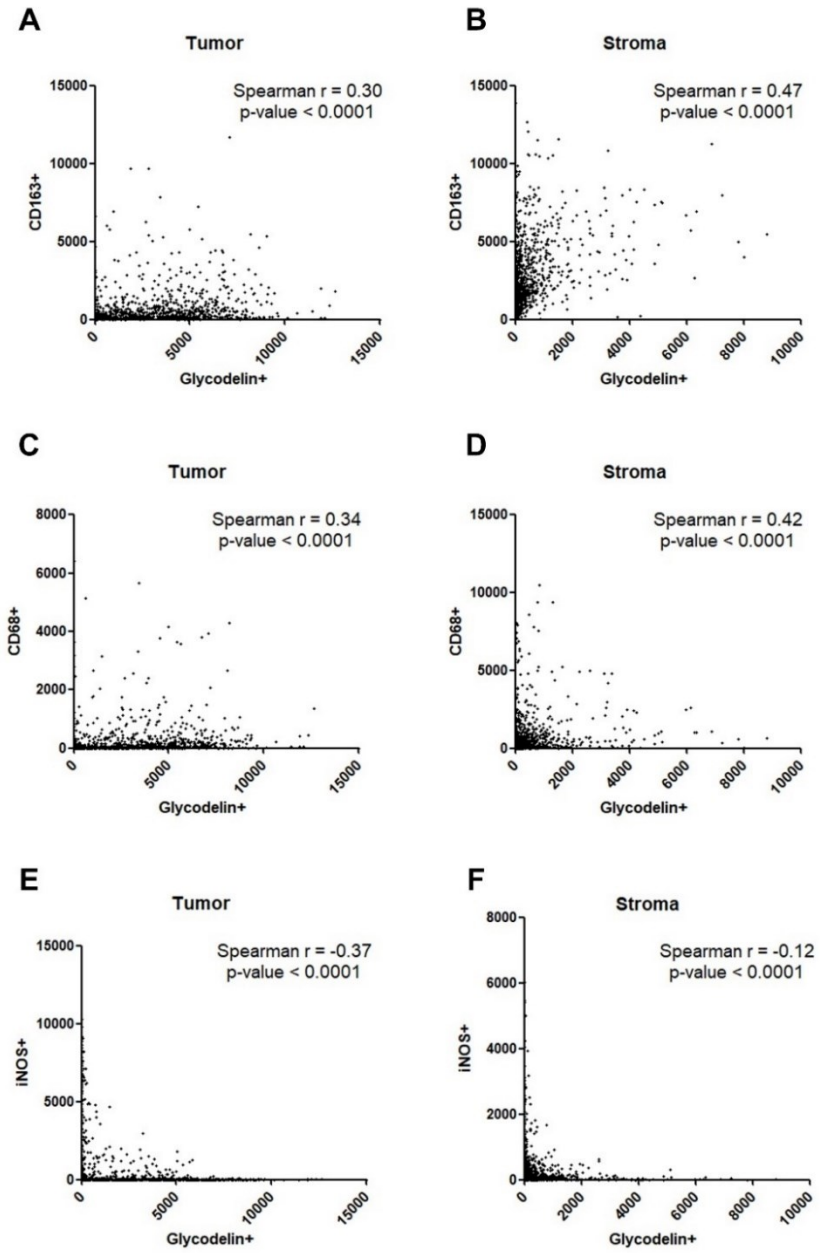

Figure 4.16: Spearman correlation analyses of macrophage markers and glycodelin in the analyzed TMAs. A) Graph depicts the normalized cell densities of glycodelin positive cells compared to CD163 positive cells in tumor and B) stroma. Spearman correlation coefficient r and p-value are displayed. The respective results for CD68 and iNOS are shown in the images C)-F).

The spatial analysis of the TMAs enabled a statistically robust insight into the interaction of glycodelin and different subsets of macrophages. Glycodelin seems to primarily bind to M2 macrophages, while it is rather negatively correlated with M1 macrophages.

4.4.4 Spatial analysis of glycodelin and T cells in NSCLC tumor microarrays

In addition to the evaluation of NSCLC glycodelin and macrophages, I have applied a T cell panel and stained the TMAs with antibodies against CD4, Granzyme B as a cytotoxic T cell marker, and CD8. Again, panCK was included as a tumor tissue marker.

As seen before, glycodelin signals were distributed heterogeneously across the tumor tissue, with some punches being highly positive while others showed a weak signal (**Figure *4.17*** A and B). Granzyme B positive T cells were rare in the investigated samples; however, successful staining could be confirmed and the marker was included in the analysis (**Figure *4.17*** B).

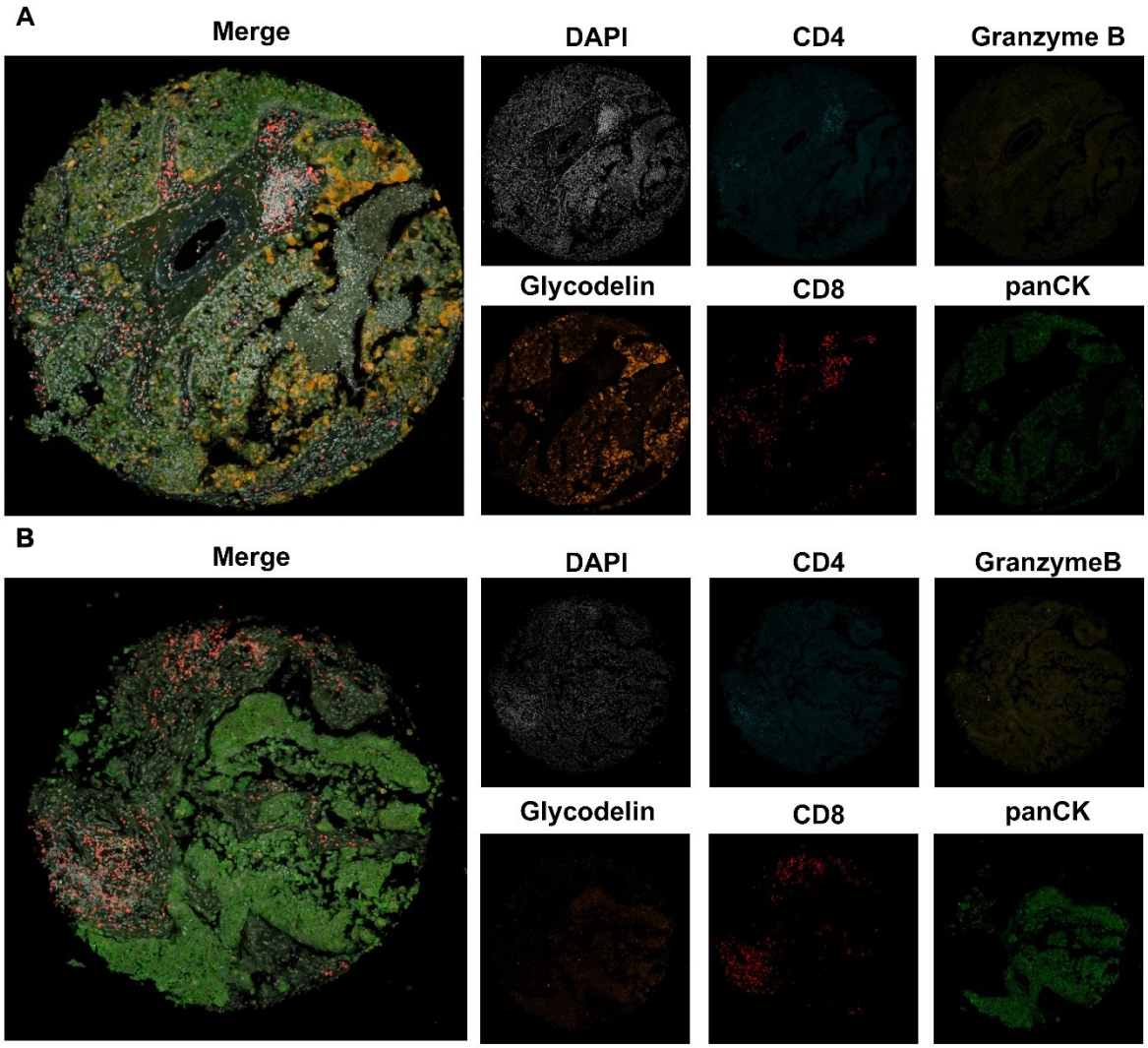

Figure 4.17: Examples of two punches stained with the T cell panel (6.8x zoom). TMAs were stained with a 5-plex covering CD4, Granzyme B, glycodelin, CD8, and panCK. Cell nuclei were stained with DAPI. A) Example of tissue positive for glycodelin. B) Example of a punch with cells positive for Granzyme B.

In line with the findings from the previous staining, panCK and glycodelin cell densities were high in tumor tissue and comparably high cell numbers positive for glycodelin were situated in the stroma. CD8 and CD4 positive T cells were apparent within the tumor region, but the majority was found in the surrounding stroma. Granzyme B signal was primarily detected outside of the tumor (**Figure *4.18*** A). Regarding the combination of panCK and glycodelin, the same conclusions could be drawn as before. Most of the cells in the tumor area are double positive for the two proteins, while in the stroma panCK-/glycodelin+ cells are more common than other combinations (**Figure *4.18*** B). The CD8 T cell subset in the tumor was highly double positive for glycodelin and the difference to CD8+/glycodelin- cells was not significant. The distribution in the stroma was slightly shifted towards CD8+/glycodelin- while a high proportion was also detected as CD8+/glycodelin+. Triple positive cells for CD8, glycodelin, and Granzyme B could neither be detected in the tumor nor in the stroma (**Figure *4.18*** C).

Regarding the interaction with CD4 T cells, double positive signals were detected for a small number of cells compared to CD4+/glycodelin- cells in tumor and in stroma (**Figure *4.18*** D).

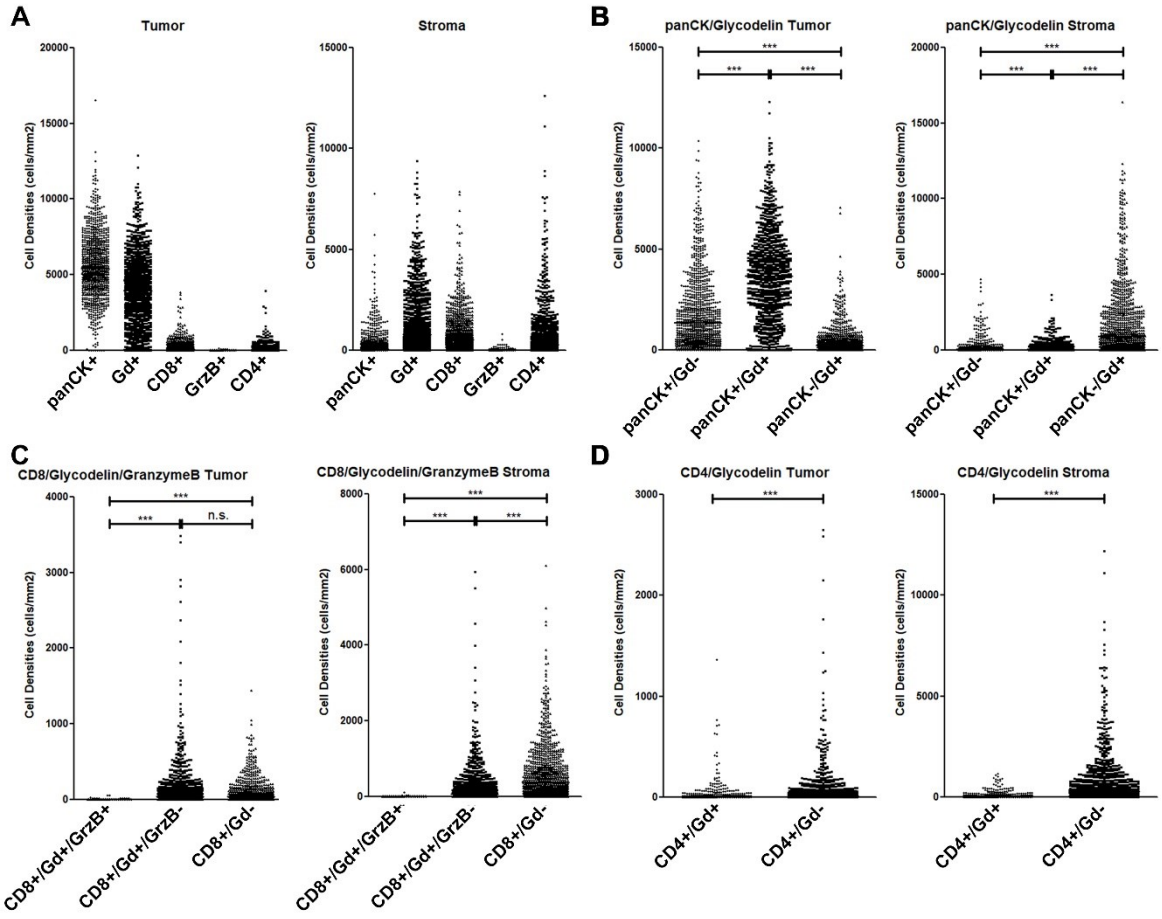

Figure 4.18: Cell densities of all phenotypes and specific combinations in the T cell panel stained TMAs. Cell counts were normalized to the detected area and are displayed as cells/mm^2. A) Total cell densities of panCK, glycodelin, CD8, Granzyme B, and CD4 positive cells in tumor and stroma. B) Comparison of cells positive for panCK and/or glycodelin in tumor and stroma. C) Comparison of cells positive for CD8 and positive or negative for Granzyme B and positive or negative for glycodelin in tumor and stroma. D) Comparison of cells positive for CD4 and positive or negative glycodelin in tumor and stroma. *** p-value < 0.0001, n.s. = not significant

In the T cell panel stained TMAs, CD8+ cells did not correlate with glycodelin signals in tumor tissue, but in the stroma with a Spearman coefficient of r = 0.51 (**Figure *4.19*** A and B). No correlation was observed between Granzyme B and glycodelin or CD4 and glycodelin (**Figure *4.19*** C-F).

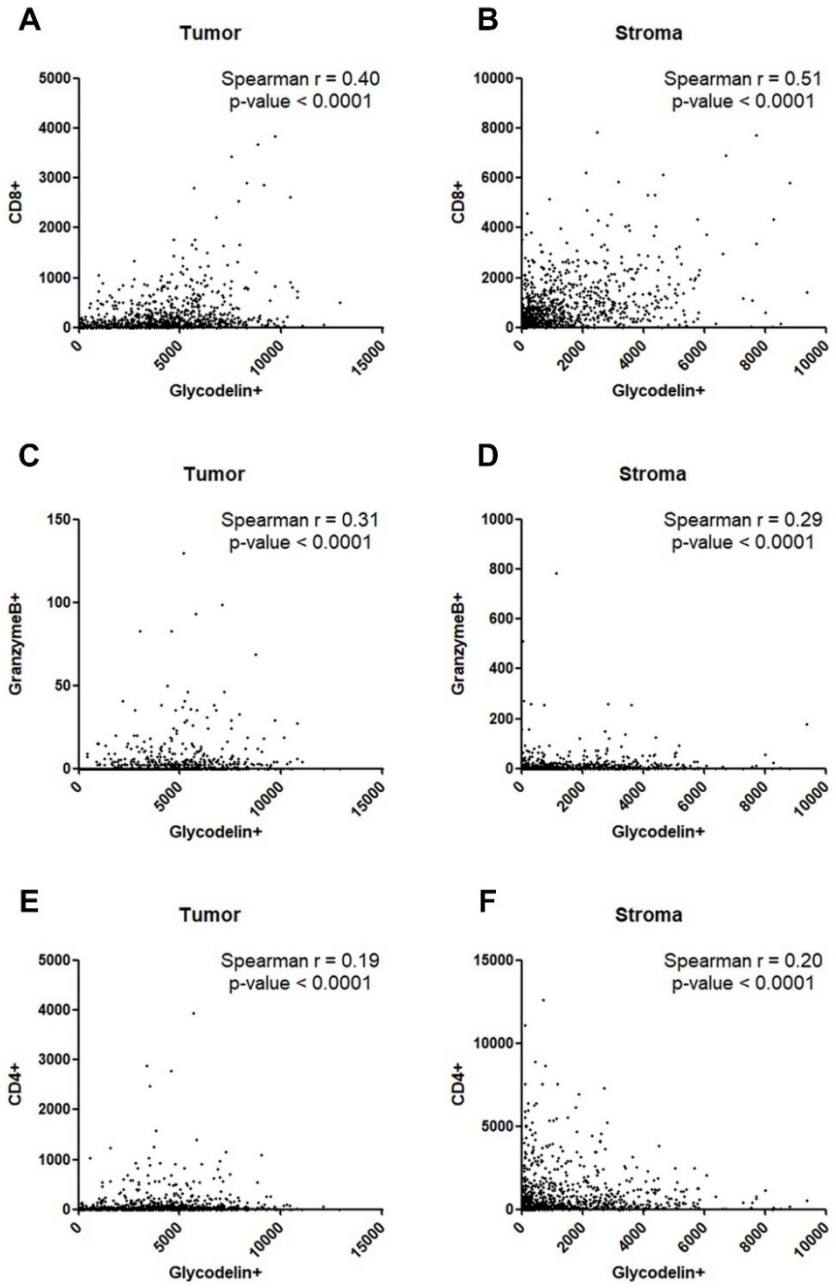

Figure 4.19. Spearman correlation analyses of T cell markers and glycodelin in the analyzed TMAs. A) Graph depicts the normalized cell densities of glycodelin positive cells compared to CD8 positive cells in tumor and B) stroma. Spearman correlation coefficient r and p-value are displayed. The respective results for Granzyme B and CD4 are shown in the images C)-F).

By applying a multiplex T cell panel on the TMAs, I could discover that glycodelin is binding to tumor infiltrating CD8 positive T cells and correlates with T cell densities in the surrounding stroma. Together with the conclusions drawn from the experiment with the macrophage panel, it can be stated that glycodelin expressed in NSCLC tumors can interact with specific immune cell subsets and might modulate the tumor environment. Further experiments should focus on characterizing these immune cells in detail and investigate possible connections with clinical parameters, such as progression-free survival, tumor stage, etc.

4.5 Glycodelin serum levels predict the clinical benefit of PD-1/PD-L1 therapy in female NSCLC patients

Immunotherapy for stage IV NSCLC patients is a promising approach that has led to effective results and increase of progression-free and overall survival for many patients. However, some patients do not benefit from this favorable treatment option and fail to respond without knowing the reason.

As the expression of the glycodelin encoding gene *PAEP* was already shown to have a negative influence on the overall survival of female NSCLC patients [91], I aimed to investigate glycodelin serum levels in a specific patient cohort and observe the progression-free survival (PFS) upon immunotherapy (**Table *4.2***). All patients in the study were diagnosed with stage IV NSCLC at the time point of investigation and were treated with anti-PD-1 or anti-PD-L1 antibodies.

Table 4.2: Clinical parameters of the investigated patient cohort
NOS = not otherwise specified, n.d. = no data, ECOG = Eastern Cooperative Oncology Group

Cohort characteristics					
Parameter	**n**	**(%)**	**Parameter**	**n**	**(%)**
Median Age	63 (38-85)		*Line Immuno-Therapy*		
Total	**139**		1	77	55
Gender			2	53	38
Male	81	58	3	6	4
Female	58	42	4	3	2
Histology			*mAb*		
Squamous	31	22	PD-1	114	82
Adeno	97	70	PD-L1	25	18
Large cell	3	2			
NOS	8	6	*ECOG*		
			0	57	41
PD-L1			1	74	53
<1 %	24	17	2	2	1
1-49 %	54	39	n.d.	6	4
>50 %	45	32			
n.d.	16	12			

Together with Dr. Marc Schneider, I have measured glycodelin serum levels *via* ELISA. Tumor progression was set as the primary endpoint (**Figure *4.20*** A). Dr. Schneider has processed the obtained data and kindly provided the results for my project and subsequent analyses.

The survival analyses revealed that high glycodelin serum concentrations led to a significantly worse PFS over all patients (**Figure *4.20*** B). However, this effect was not observed in male patients but only in female patients, where an elevated glycodelin level caused a highly

significant reduction of PFS (**Figure *4.20*** C and D). The same cutoff was applied for the analysis of the two different sexes to overcome any bias caused by cohort characteristics.

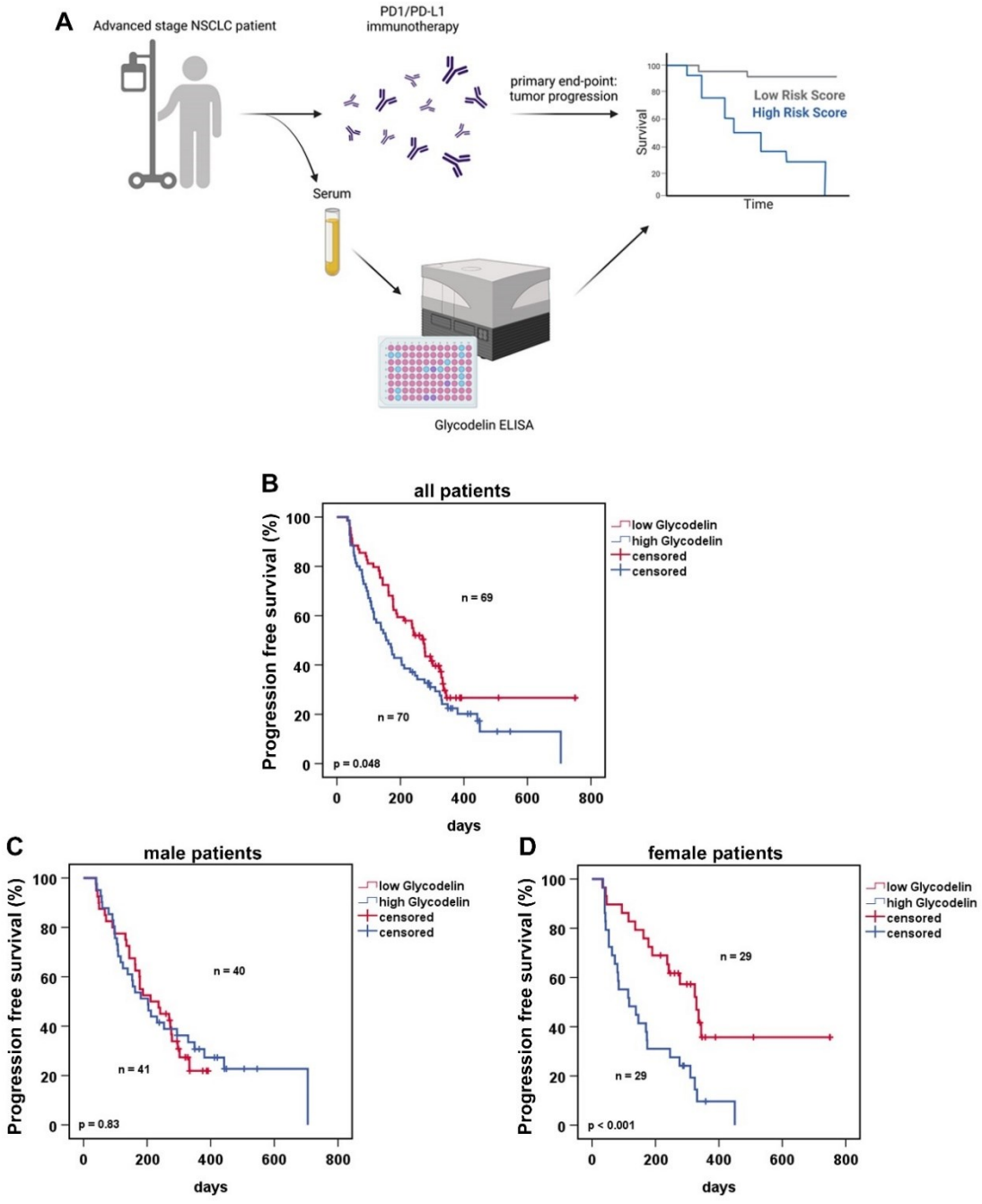

Figure 4.20: Glycodelin measurement in the serum of patients with advanced stage NSCLC. A) Schematic overview of the study. Patients with stage IV NSCLC were included and glycodelin levels in the serum was measured *via* ELISA before immunotherapy with anti-PD-1 or PD-L1 antibodies. Afterwards, glycodelin levels were analyzed with regard to progression free survival. The results are displayed in Kaplan-Meier plots for B) all patients, C) male patients, and D) female patients.

The results underlined that glycodelin might be a sex related predictor of therapy response and could have different functions in female patients that lead to an unfavorable outcome. Based on preliminary studies that have shown that progesterone among other hormones is a regulator of glycodelin, I have sent serum samples from 125 patients that were included in the glycodelin

measurements to the clinical diagnostics of the Heidelberg University Hospital. The laboratory offers diagnostic measurements of several hormones; thus, I have chosen to request estradiol, progesterone, human chorion gonadotropin (hCG), and testosterone to investigate any relation with glycodelin.

The concentration of glycodelin in the patients' serum varied highly and ranged from 0 to nearly 300 ng/ml (**Figure *4.21*** A). Estradiol levels also varied but most of the patients had levels around 20 mIE/ml, while some elevated values were located between 50-90 mIE/ml. Progesterone levels revealed a median at 0.3 ng/ml which corresponds to physiological conditions. Nevertheless, some patients showed higher concentrations of this hormone, as well. Normally, hCG is a common evidence for pregnancy. In the investigated patient cohort, only 39 out of the 125 patients had measurable amounts in their serum including some with elevated levels up to 11 pg/ml. Interestingly, testosterone was the only hormone that did not show any measurement outside of the physiological range. Spearman correlation analysis did not reveal a relation between glycodelin and any of the observed hormones (**Figure *4.21*** B).

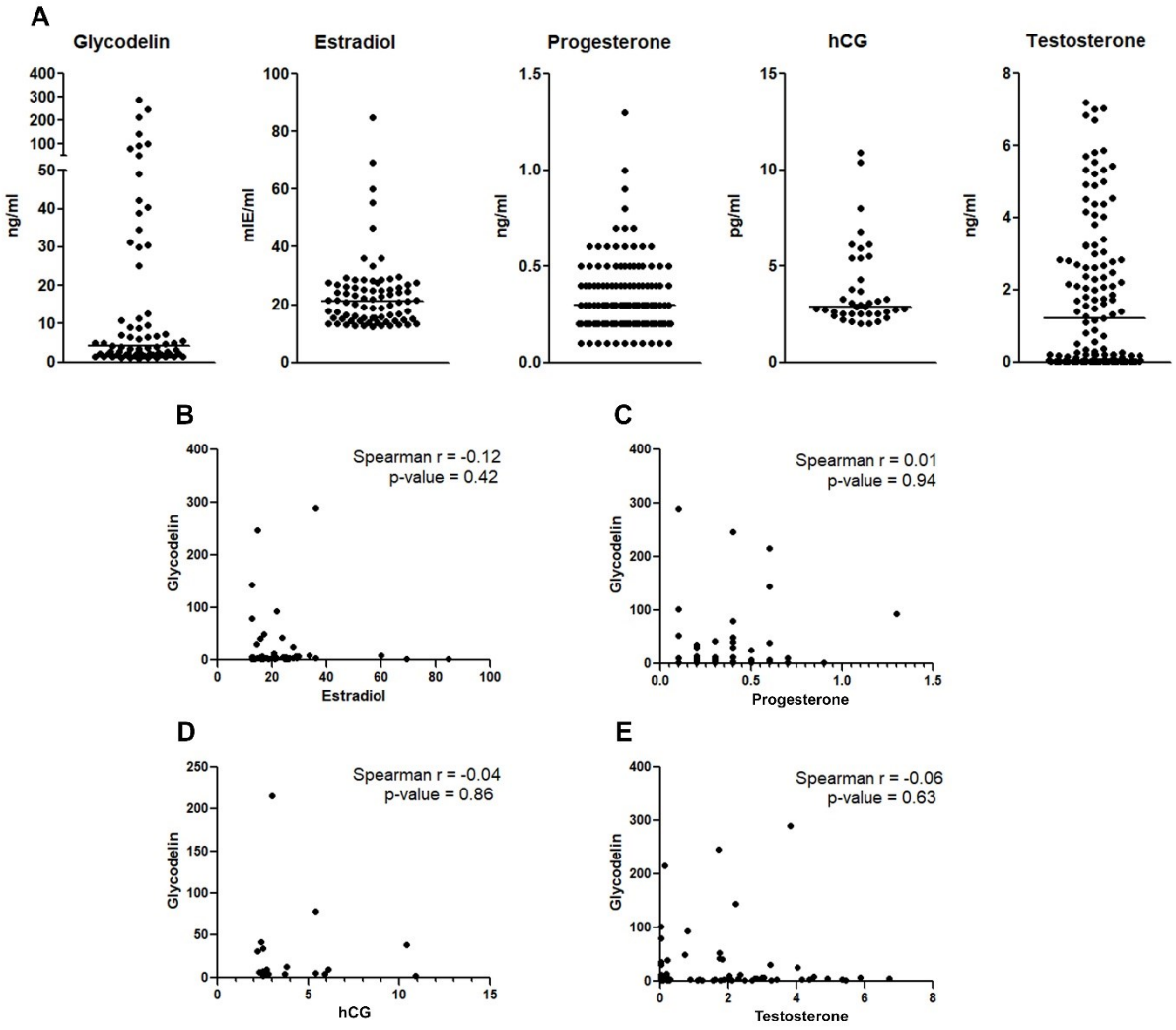

Figure 4.21: Comparison of glycodelin serum levels and hormones. A) Measurement of glycodelin, estradiol, progesterone, hCG, and testosterone in the serum of patients. Median is displayed as a line. B9-E) Spearman correlation analyses of glycodelin and the different hormones with respective coefficient and p-value.

A possible connection of glycodelin and the different hormones was further investigated as a combination could serve as a robust panel of two independent markers in NSCLC therapy prognosis. Dr. Marc Schneider has implemented the generated data into a Kaplan Meier analysis to examine prognostic effects. Progesterone was the only hormone having a significant impact on the PFS of male patients when elevated concentrations were found in the serum (**Figure *4.22*** A). In combination with glycodelin serum levels, the effect was lost (**Figure *4.22*** B). For female patients, progesterone alone did not have an impact on the PFS but showed to be a significant marker for a worse PFS in combination with glycodelin (**Figure *4.22*** C and D). However, the patient group was relatively small (7 patients) and the effect was not as strong as for elevated glycodelin alone (**Figure *4.20*** D).

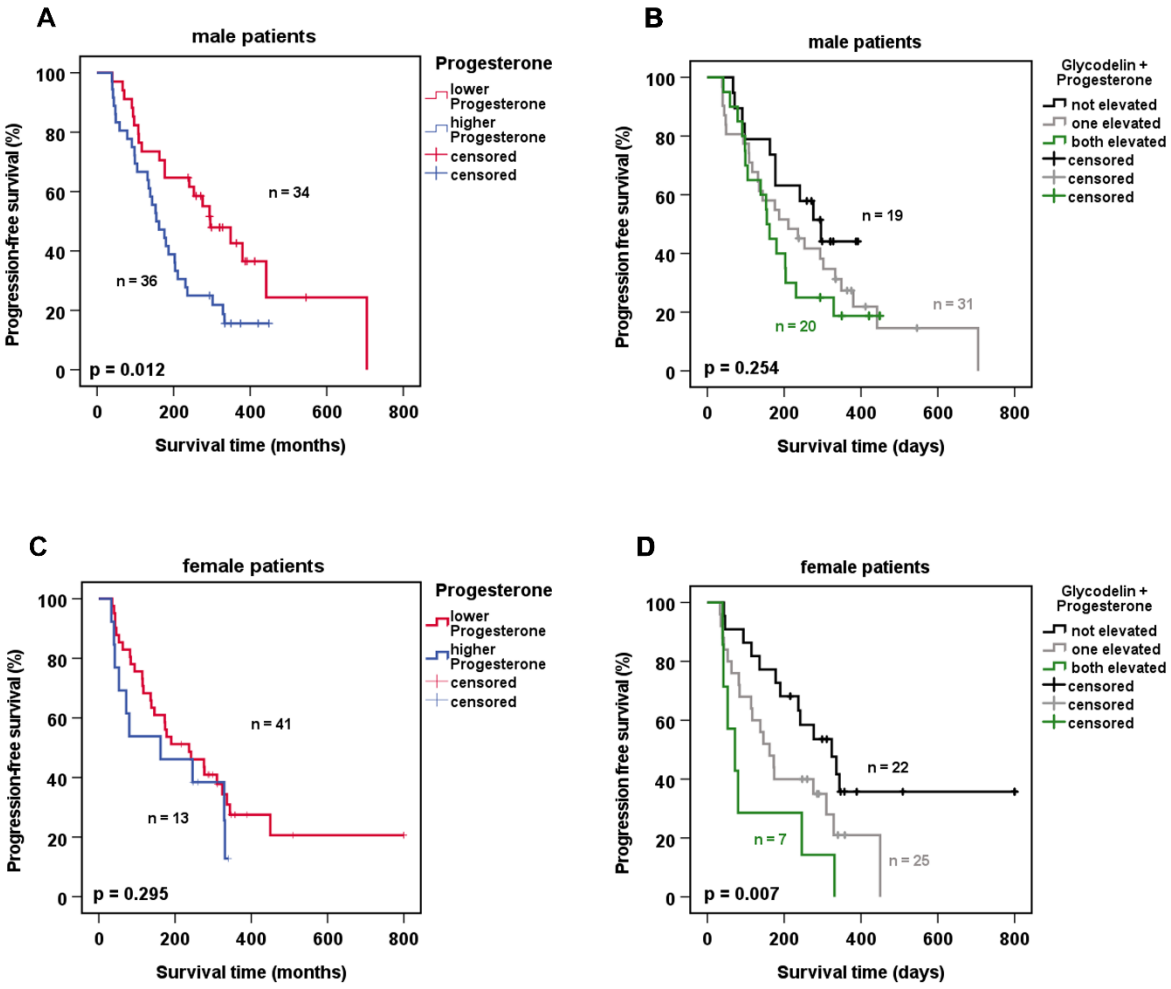

Figure 4.22: Kaplan-Meier plots reveal the impact of progesterone and glycodelin serum levels on progression-free survival. A) Kaplan Meier plot indicating the effect of lower and higher progesterone serum levels on the PFS of male patients. B) Effect of the combination of elevated progesterone and glycodelin serum concentrations on PFS in male patients. C) and D) show the respective Kaplan-Meier plots for female patients.

To conclude, the patient data has given valuable insights into the potential of glycodelin being a predictive marker for therapy outcome in female patients. It cannot be related to serum hormone levels and might be regulated locally at the tumor site. In addition, it is not clear how glycodelin interferes with PD-1/PD-L1 immunotherapies which needs to be further clarified.

4.6 **Inhibition of glycodelin binding by using a monoclonal anti-glycodelin antibody in vitro**

The different approaches in the herein presented thesis have demonstrated the high potential of the pregnancy associated protein glycodelin to be a novel target in immuno-oncology. Its characteristics resemble the immunosuppressive glycodelin A and seem to drive interaction and modulation of immune cells.

One way to target proteins efficiently, is by blocking them with specific monoclonal antibodies. In an *in vitro* approach, I have tested the ability of several antibodies available in our laboratory to inhibit glycodelin binding to the immune cells Jurkat, THP1, and KHYG-1. Subsequent western blot analysis and signal quantification have shown a reduction of glycodelin signal with increasing antibody concentrations when being pre-incubated with a monoclonal antibody prior to immune cell treatment (**Figure *4.23***). Further validations will be needed to prove the inhibition and to evaluate its effect.

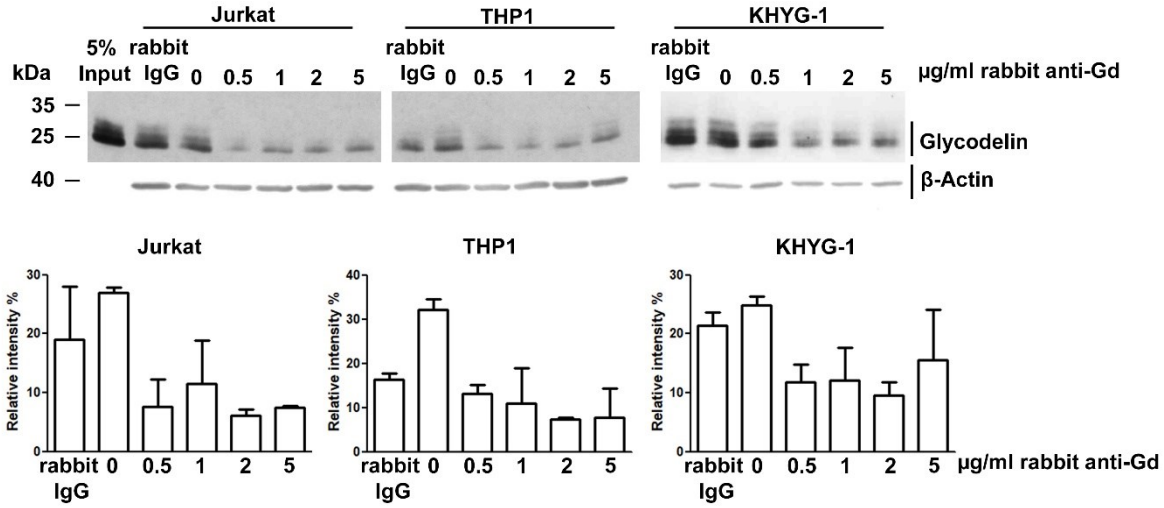

Figure 4.23: Glycodelin binding inhibition *in vitro*. Western blot and corresponding signal quantification representing an approach to inhibit glycodelin binding to immune cells by using a monoclonal anti-glycodelin antibody.

5 Discussion

Lung cancer treatment has experienced enormous improvements after the first applications of monoclonal antibodies that target the PD-1/PD-L1 axis [109]–[111]. Nevertheless, overall survival remains low for patients diagnosed at advanced stages and there is an unmet clinical need for effective biomarkers and novel targets.

Glycodelin is a protein well characterized in the context of pregnancy, encoded by the *PAEP* gene and primarily expressed and secreted by endometrial cells [45], [112]. The four different glycosylation forms glycodelin A, C, F, and S share the same protein backbone, but differ in their function based on the distinct sugar residues. Glycodelin A was shown to act highly immunosuppressive by interacting with various leukocytes at feto-maternal interface [48], [51].

Aberrant expression of *PAEP* and glycodelin were discovered in some cancer types, including NSCLC. Gene and protein expression were found nearly exclusively in tumor cells while the corresponding normal lung tissue did not reveal any signal. In female patients, a high *PAEP* gene expression was shown to lead to a worse overall survival and the question arose which function the pregnancy-associated protein might have in NSCLC [91].

In the frame of the herein presented thesis, I have investigated the hypothesis whether NSCLC-derived glycodelin shares functionality with the immunosuppressive glycodelin A known from pregnancy and hence, might be a possible target for future immunotherapies.

5.1 The glycosylation pattern of NSCLC-derived glycodelin

Since the functionality of pregnancy-associated glycodelin is dependent on the glycosylation structure at the two modification sites, I have applied a lectin-based enrichment of the protein from cell culture supernatant to characterize this feature. The protocol is adapted from Hautala et al. [88], who has used the same 22 lectins in an ELISA based approach in addition to a mass spectrometric analysis. In the study it was concluded that glycodelin expressed by a human endometrium carcinoma cell line has an altered glycosylation compared to normal human glycodelin A. In contrast to this work, I have investigated endogenous glycodelin secreted by the NSCLC cell lines 4950T and 170162T as I wanted to overcome possible structural changes based on an overexpression system. Besides, I have used western blots to detect unbound and bound protein. For effective enrichment of glycodelin and to reduce the amount of competing glycans in the solution, the supernatants were filtered through a 100 kDa centrifugal filter.

The evaluation has revealed several interesting results: i) Although expected differences were detected between glycodelin A and NSCLC-derived glycodelin, the proteins shared major

structural similarities like a mannose and glucose rich glycosylation; ii) Glycodelin secreted by 4950T cancer cells was highly sialylated which is the main driver of the immunomodulating functions of glycodelin A; iii) The cell line 170162T, which was isolated from the tumor tissue of a male patient, expressed glycodelin with lower affinity to sialyl binding lectins. Consequently, the cell lines seem to secrete slightly different glycosylation forms which might be based on the sex of the donor; and iv) The western blots have revealed that within the same sample, specific proportions of protein could be bound by a lectin while the rest could be only found in the flowthrough. This might be either due to a mixture of glycosylated forms, like glycodlein S, C, or F[60], in the samples, specific modifications in only one part of the proteins, or accessibility to sugar residues depending on structural conformation, protein aggregation, and interaction with other partners in the solution.

To sum up, the lectin assay enabled a quick and reliable insight into the structure of NSCLC-derived glycodelin. It showed that the cell lines 4950T and 170162T produce glycodelin which highly resembles the immunosuppressive glycodelin A from pregnancy. The amount of sialylation, the main functional driver, might be dependent on the sex of the patient. As glycodelin A is normally expressed by endometrial cells, the protein is not found in men with the specific glycan residues. Here, glycodelin S is contained in the seminal plasma which is high in fucose and lacks any sialyl residues [48], [113]. However, this finding needs to be further investigated in additional patient samples.

5.2 Glycodelin secreted by NSCLC cells interacts with immune cells *in vitro*

I have further investigated the ability of NSCLC-derived glycodelin to interact with immune cells *in vitro*. For this, I have performed several experiments that included the immortalized immune cell lines Jurkat, THP1, and KHYG-1 which cover three different leukocyte phenotypes. For all treatments, I have used the cell culture supernatant of the NSCLC cell line 4950T as it secretes the highest amount of the protein compared to any other cell line used in our laboratory.

From previous studies it was known that endometrial glycodelin interacts with various immune cells to modulate the surrounding immune environment into a tolerant state [51]. In the cell culture experiments, I validated a fast and specific binding and internalization of glycodelin for all immune cells. This effect could be observed for native glycodelin as well as for the deglycosylated protein.

As I have worked with cell culture supernatants that contain glycodelin, it is not clear whether other proteins like carriers are needed for this process. Glycodelin is structured as a nonpolar barrel which could facilitate membrane transition [61]. Despite numerous approaches from several members of the group, an efficient purification of endogenous glycodelin from NSCLC cell culture supernatant was not successful. The fact that glycodelin in the supernatant is

retained by a 100 kDa centrifugal filter indicates that the glycoprotein forms larger complexes or that it is bound to other proteins in the solution. In the serum of pregnant women, pregnancy zone protein (PZP) and α2-Macroglobulin were identified as carriers and modulators of glycodelin [114], [115]. In addition, several leukocyte specific receptors have shown to bind pregnancy-related glycodelin, i.e. CD45, CD7, Siglec-6, or L-selectin [64], [70], [101], [116], [117]. In contrast, the *in vitro* binding assay that I have performed with a subsequent acidic wash at different temperatures did not give hints regarding a possible receptor-dependent endocytosis. Here, a more straightforward approach would be to stain immune cells after treatment and enable localization by immunofluorescence imaging. Together with the antibody core facility at the German Cancer Research Center (DKFZ), I have screened over 600 clones of monoclonal antibodies specific for glycodelin. One of the clones has recognized overexpressed glycodelin specifically in immunofluorescence experiments. After further protocol optimizations, this antibody could be applied in future approaches to visualize glycodelin *in vitro*.

In general, the cell culture experiments confirmed an interaction of glycodelin from NSCLC cell culture supernatant and all observed immune cell lines. Therefore, additional functional studies were performed.

5.3 Transcriptome analysis of monocyte like and natural killer cells after glycodelin treatment

To further examine whether the interaction of NSCLC-derived glycodelin with immune cells is connected to a functional response, I have treated the samples with control and knockdown cell culture supernatant of 4950T cells. Glycodelin A concentrations vary during the menstrual cycle and in the course of a pregnancy. In the serum of women who were not pregnant, circulating glycodelin levels of around 100 ng/ml were measured at the end of a menstrual cycle [57]. In pregnancy, the level of glycodelin in the serum peaked between week 6 and 12 with values of 2200 ng/ml and reached concentrations of 232 µg/ml in amniotic fluid [50]. Early unpublished work from Dr. Marc Schneider has shown that glycodelin concentrations in the lysates of NSCLC tumor tissue can also reach 1-150 µg/ml, while in cell culture the cell line 4950T secretes the highest amounts of the glycoprotein with 50-100 ng/ml. Therefore, I have condensed the supernatants and finally applied 200 ng/ml for treatment and 60 ng/ml for comparison. In the work of Schneider *et al.* [91] a *PAE*P overexpression could be detected in more than 80 % of the tumors compared to the normal lung tissue. Nevertheless, common NSCLC tumor cell lines like H838 or A549 do not express any glycodelin while concentrations are very low from cells that do secrete glycodelin. Glycodelin expression might thus be regulated by the tumor environment and cannot be easily translated into cell culture systems.

With the mentioned conditions, no effect on immune cell viability could be detected. Glycodelin A purified from amniotic fluid was shown to induce apoptosis in T cells and monocyte like cells, more specifically in Jurkat and THP1 cells [118], [119]. In the studies, glycodelin concentrations of at least 5 µg/ml were used. Here, it is interesting to mention that these studies had contrary conclusions regarding the capability of apoptosis induction in specific immune cell types. Thus, it seems like that the experimental setup, proper concentration determination, and storage solution might be important factors for the functionality of glycodelin. As large amounts of NSCLC cell culture supernatants have to be heavily concentrated, other techniques will be needed for accurate dose-response analyses.

Nevertheless, significant genetic alterations could be detected in THP1 after 3, 8, and 24 h and in KHYG-1 after 24 h incubation. Genes related to inflammatory responses and tumor microenvironment pathway were activated and the expression of major regulators including *TNF*, *CCL4*, or *ICAM1* was increased. Various studies have investigated the effect of glycodelin on the expression of distinct genes. Tee et al. [78] have shown that the pro-apoptotic genes *Bad, Bax*, and *TNF-R1* were upregulated, whereas expression of *Bcl-2A1* and a proliferation-inducing ligand (*APRIL*) were reduced by recombinant glycodelin. In the generated data from my experiment, the affected genes were predominantly related to (hyper)inflammation which might be based on the treatment with endogenous NSCLC-derived glycodelin. In natural killer cells, it was reported that treatment with 5 µg/ml glycodelin converted peripheral NK cells into a decidual phenotype [70]. Transcriptomic data is not available, but increased secretion of vascular endothelial growth factor (VEGF) and insulin-like growth factor-binding protein 1 (IGFBP-1) was observed. Corresponding gene alterations were not detected in the data of treated KHYG-1. Again, (hyper)inflammation was an affected pathway along with cell-cycle control and cell-to-cell interaction. In addition, one of the transcriptional networks was associated with cancer.

To conclude, the transcriptional analysis of the immune cell lines revealed that glycodelin from 4950T supernatant has a significant impact on the gene regulation in THP1 and KHYG-1 cells. The results are made from a new perspective as the immune cells were not treated with physiological amounts of glycodelin but were still affected by it. Nonetheless, these cells are also only mimicking human leukocytes and interpretation of the data cannot be fully translated into realistic interpretations. Consequently, experiments are needed that include human primary immune cells or peripheral blood mononuclear cells to gain detailed and robust understanding of NSCLC associated glycodelin and its regulatory function on the transcriptome of leukocytes.

5.4 Spatial analysis of glycodelin in NSCLC tissue reveals interaction and relation with CD163+ M2 macrophages and CD8+ T cells

Multiplex immunofluorescence staining represents a robust tool to detect numerous different proteins of interest in the same FFPE tissue sample. In combination with machine-learning analysis, large cohorts can be screened for specific cell compositions, correlations, or interactions. The spatial analysis of glycodelin in around 700 tissue punches was performed with a macrophage and a T cell panel to get insight on the interaction of glycodelin and the tumor microenvironment *in vivo*.

The macrophage panel consisted of CD68 as a general macrophage marker, iNOS as an M1 macrophage marker, and CD163 representing M2 macrophages. Depending on the surrounding cytokine milieu within the tumor microenvironment, the phenotype of tumor-associated macrophages can polarize towards a pro-inflammatory M1 or an anti-inflammatory M2 state. While M1 macrophages have shown to be highly important in the recognition and destruction of cancer cells, M2 macrophages are considered to support tumor growth and metastasis [120], [121]. In NSCLC, elevated M2 ratio (CD163+/CD68+) was significantly associated with a worse overall survival [122] and impaired PFS in patients receiving immunotherapy [123]. In the investigated TMAs, glycodelin and CD163 double positive cells were found in the tumor and stroma region, while hardly any cells were detected with signals for glycodelin and iNOS. In contrast, cell densities of glycodelin positive and iNOS positive showed a tendency of a negative correlation in tumor sites. For CD163 and CD68, spearman correlation coefficients were close to 0.5 with glycodelin in the stroma. The results indicate an interaction of glycodelin with M2 macrophages and the modulation of the tumor environment towards an anti-inflammatory and pro-tumorigenic surrounding.

The T cell panel used markers to detect CD4+, CD8+, and Granzyme B+ T cells. CD4+ T cells are crucial for the development of CD8+ T cell immunity and act as a coordinator of immune response [124]–[126]. Granzyme B is a marker for activated CD8+ T cells but was rarely detected in the examined TMAs [127]. Activated CD8+ T cells have effector functions and are the main targets of immune checkpoint inhibitors in order to reactivate an anti-tumor cytotoxic CD8+ T lymphocyte response [128], [129]. One feature of tumors to avoid T cell recognition is to mediate T cell exhaustion which represents a specific type of T cell dysfunction [129]. Exhausted T cells have a loss of their effector functions, a dysregulated metabolism, and a reduced ability of homeostatic self-renewal [130]. The evaluation of the TMAs indicated a high proportion of double positive glycodelin/CD8 cells in the tumor and glycodelin containing cells correlated with CD8+ T cells in the stroma. As Granzyme B positive cells were hardly detected, it cannot be stated whether the observed CD8+ T cells were activated or not. Some CD4+ T

cells were also double positive with glycodelin but in a smaller proportion compared to the CD8+ T cells.

Taken together, the multiplex analysis confirms the ability of glycodelin to interact with specific subsets of immune cells in NSCLC tumor tissue and the surrounding stroma. Based on the observed relations, glycodelin might act as a modulator of the tumor microenvironment towards a pro-tumorigenic state and by this inhibit immune surveillance. For additional analyses, clinical parameters of the stained tissue punches should be included to examine whether specific cell densities and immune cells positive for glycodelin might lead to prognostic estimations. Further information could underline the high potential of glycodelin as an immuno-modulator in NSCLC.

5.5 Glycodelin is an independent predictor of PD-1/PD-L1 immunotherapy in female NSCLC patients

Immune checkpoint inhibition (ICI) represents a promising treatment option for patients who have advanced tumors negative for driver genes and are not eligible for targeted therapy. Treatments of these patients with platinum-based chemotherapy results in a poor PFS of 4-6 months and OS of 10-12 months [131], [132]. Since the first ICI approval in 2015, anticancer therapy has experienced major breakthroughs. Nivolumab was the first monoclonal antibody against PD-1 for third-line therapy of patients suffering from squamous cell carcinoma [110]. Present approaches exploit the two immune related pathways CTLA-4/B7 and PD-1/PD-L1 by inhibiting immunosuppressive signaling and reactivating an immune response against cancer cells. Activated T cells develop an increased expression of immunosuppressive signaling receptors like PD-1, CTLA-4, LAG-3, TIGIT, or TIM-3 [133]. The stimulation of coinhibitory pathways modulates the strength and duration of T cell mediated immune responses and prevents damage due to hyperinflammation. These regulatory pathways are exploited by cancer cells to overcome immune surveillance [134]. By blocking the suppressive T cell receptors, ICIs can regain anti-tumor immune response [135]. Today, monoclonal antibodies targeting PD-1, PD-L1, or CTLA-4 are also approved for combination first-line therapies in NSCLC, as the efficacy was shown to be higher in advanced stage disease compared to previous treatments with chemotherapy alone [110], [136]–[138]. However, not all patients benefit from this promising treatment option and especially women tend to have a significantly worse response to ICI monotherapy [139]. Combination therapies can only be extended to a certain amount as the treatment leads to high activation of the immune system and can cause severe adverse sight effects. Therefore, novel cancer specific targets are needed to overcome off-target effects [140]. Moreover, a detailed analysis of biomarkers should build the basis of therapeutic approaches towards the best option for each patient.

In cell culture experiments it was reported that glycodelin and PD-L1 expression might be related [91]. Moreover, an elevated *PAEP* gene expression in the tumor tissue of female NSCLC patients led to a worse OS, suggesting a sex dependent effect that favors cancer cell progression. In the frame of my project, I have further investigated possible effects of glycodelin in NSCLC patients. The measurement of glycodelin serum levels in stage IV NSCLC patients has revealed that again only female patients experience an enormous disadvantage when glycodelin concentrations are elevated. Under PD-1/PD-L1 immunotherapy, their PFS was significantly impaired, while in men no effect could be observed. Glycodelin in female NSCLC patients seems to interfere with the therapy response and is predictive for their PFS.

Sex differences in drug-response have been reported regarding the benefit of female patients when treated with EGFR-TKIs [141]. With regard to ICI, contrary results were reported in different studies. Additional factors that influence a therapy response also include patient characteristics like ethnicity, body mass index (BMI) or the disease-context. For female cancer patients, a benefit in treatment could be observed in combination therapies of ICIs and chemotherapy, while ICI alone failed to achieve a comparable response. Despite these data, the implementation of sex as a factor to apply the best possible treatment is still rare in current practice and might need to be implemented stronger in future clinical trial settings [142]–[145].

Glycodelin seems to be one major factor that influences the benefit of a PD-1/PD-L1 immunotherapy in female patients. In pregnancy, the expression of the glycoprotein is regulated by different hormones, including progesterone and hCG [48], [57]. Therefore, I have compared and analyzed glycodelin serum concentrations with estradiol, progesterone, hCG, and testosterone to investigate possible dependencies. None of the hormones was correlated with glycodelin concentrations, thus elevated serum concentrations of glycodelin represent an independent variable related to the PFS of female patients. Interestingly, progesterone levels were negatively associated with the PFS of the male patients and led to a significantly worse PFS in female patients only in combination with increased levels of glycodelin. Progesterone interacts with specific progesterone receptors. Activation of the receptor stimulates tissue differentiation and inhibits cell proliferation. However, studies referring to the receptor functions in the lung show contrary results and need to be further investigated [146], [147]. In a previous study from our group, it could be shown that glycodelin expression is regulated by the canonical TGF-β pathway in SQCC and the PKC signal cascade in ADC [94]. At the tumor site, locally elevated amounts of specific hormones, cytokines or other regulators might influence the function of glycodelin and lead to the significant deterioration of ICI treatment in female patients.

Glycodelin in NSCLC could serve as an easily accessible independent biomarker to predict therapy response and adapt treatment options in order to apply the best fit for every patient. It

is not yet clear, why elevated levels interfere with an ICI therapy response only in female patients. As glycodelin was shown to be regulated by pathways that are targets of current TKI treatments in NSCLC, it would be interesting to compare PFS in patients that are treated with combination therapies. In addition, future therapies targeting glycodelin in NSCLC could not only improve the therapy response itself but also circumvent hyperinflammation and adverse side effects based on the fact that glycodelin is not expressed in normal lung tissue [91].

5.6 Glycodelin inhibition by using a monoclonal antibody – tool for future therapy?

Glycodelin is not a target of any treatment, yet. Therefore, I have started with the first experiments to screen for antibodies that can inhibit the binding of glycodelin to immune cells and by this block subsequent regulatory effects. One of the antibodies showed efficient inhibitory effects and could reduce glycodelin signal in immune cells. The investigated cell lines represent cell models and are therefore altered in comparison to human primary leukocytes which needs to be considered in data interpretation. Furthermore, THP1 expresses Fc receptors on the cell surface which might interact with antibodies in the solution [148]. The glycodelin inhibition experiments might thus be repeated in approaches with primary immune cells to get a reliable and realistic insight.

In addition, novel monoclonal antibodies might be available that could recognize and target glycodelin more efficiently. In cooperation with the DKFZ antibody core facility, namely Ilse Hofmann and Claudia Tessmer, I have generated mAbs specific for NSCLC-derived glycodelin and validated them by using ELISA, immunofluorescence, and western blot. Two clones could be identified that showed specific detection in the different assays and could serve for future applications. The commercial ELISA that I have used to measure glycodelin serum levels is not produced anymore, same as the antibody clone that was used for western blot analyses. Future investigations will need to implement alternative tools to confirm that glycodelin in NSCLC is targetable.

6 Conclusion and Outlook

In my project, I have investigated the hypothesis whether glycodelin in NSCLC is as immunosuppressive as glycodelin A in pregnancy and might represent a promising novel target for immunotherapy. The results have confirmed that NSCLC-derived glycodelin shares the glycosylation structure with glycodelin A, but might contain differences between sex. I could show that the protein does not only interact with immune cells but is also functional and leads to an altered gene expression that is associated with several immune related pathways. In NSCLC tissue, glycodelin interacts with CD163+ M2 macrophages and CD8+ T cells, modulating the tumor environment and influencing surrounding immune cells. The effect of glycodelin can be indirectly observed in female NSCLC patients who fail to respond to PD-1/PD-L1 immunotherapy when they have increased glycodelin serum levels. With newly generated mAbs, glycodelin could become a novel target in NSCLC therapy and improve the PFS and OS in female patients who suffer from therapy failures.

Future approaches should focus on some major follow-up questions. First, the difference in glycosylation between female and male patients needs further investigation and more samples. Instead of using 22 lectins, it could be sufficient to concentrate on some major binding specificities like sialic acid, fucose, and high mannose/glucose. Furthermore, *ex vivo* experiments could help to understand the function of glycodelin in NSCLC without the bias of model cell lines. Here, our group has recently established the implementation of Precision Cut Lung Slices (PCLS) that enable the cultivation of fresh NSCLC tumor tissue for several days. Consequently, the tumor microenvironment is conserved and surrounding immune cells can be investigated directly regarding their interaction with tumor cells. Together with Dr. Marc Schneider, Carmen Hoppstock, and Elizabeth Xu Meister, I have performed first glycodelin knockdown experiments in PCLS to observe whether contained immune cells might be reactivated and initiate tumor cell killing. Additional approaches could analyze cytokine composition, cell phenotypes, transcriptional changes and numerous other aspects to get a deep understanding of glycodelin associated tumor biology. Single-cell sequencing could be applied to get a deep understanding of regulatory mechanisms that are mediated by glycodelin. Multiplex immunofluorescence staining would be a suitable supplement to validate findings on the protein level. PCLS represent a valuable tool to examine glycodelin *ex vivo* as the gene *PAEP* is not expressed in mice which excludes mouse models for future approaches.

As an approach to characterize glycodelin in NSCLC patients, together with Dr. Piotr Zadora I have generated a glycodelin calibrator for mass spectrometric analyses. By this, patient cohorts can be easily screened for glycodelin and possible combination markers in blood

samples that might explain the function or serve as panel markers in survival studies. This would be a non-invasive and low-risk approach to evaluate a best possible treatment.

To conclude, the herein presented findings clearly underline that the immunosuppressive form glycodelin A is secreted by NSCLC cells and the potential of glycodelin in NSCLC to be a valuable target and biomarker. Clinical studies and efficient glycodelin screening and inhibition will be needed in the future to activate therapy response in former non-responders.

References

[1] F. Bray, J. Ferlay, I. Soerjomataram, R. L. Siegel, L. A. Torre, and A. Jemal, "Global cancer statistics 2018: GLOBOCAN estimates of incidence and mortality worldwide for 36 cancers in 185 countries," *CA. Cancer J. Clin.*, vol. 68, no. 6, pp. 394–424, 2018, doi: 10.3322/caac.21492.

[2] I. Globocan, "Cancer Today Data visualization tools for exploring the global cancer burden in 2020," 2020. [Online]. Available: https://gco.iarc.fr/today/home.

[3] F. Islami *et al.*, "Proportion and number of cancer cases and deaths attributable to potentially modifiable risk factors in the United States," *CA. Cancer J. Clin.*, vol. 68, no. 1, pp. 31–54, Jan. 2018, doi: 10.3322/caac.21440.

[4] M. J. Thun *et al.*, "50-Year Trends in Smoking-Related Mortality in the United States," *N. Engl. J. Med.*, vol. 368, no. 4, pp. 351–364, Jan. 2013, doi: 10.1056/NEJMsa1211127.

[5] D. R. Youlden, S. M. Cramb, and P. D. Baade, "The International Epidemiology of Lung Cancer: Geographical Distribution and Secular Trends," *J. Thorac. Oncol.*, vol. 3, no. 8, pp. 819–831, Aug. 2008, doi: 10.1097/JTO.0b013e31818020eb.

[6] A. Jemal, M. M. Center, C. DeSantis, and E. M. Ward, "Global Patterns of Cancer Incidence and Mortality Rates and Trends," *Cancer Epidemiol. Biomarkers Prev.*, vol. 19, no. 8, pp. 1893–1907, Aug. 2010, doi: 10.1158/1055-9965.EPI-10-0437.

[7] J. H. A. Van der Heyden *et al.*, "Socioeconomic inequalities in lung cancer mortality in 16 European populations," *Lung Cancer*, vol. 63, no. 3, pp. 322–330, Mar. 2009, doi: 10.1016/j.lungcan.2008.06.006.

[8] S. Walters *et al.*, "Lung cancer survival and stage at diagnosis in Australia, Canada, Denmark, Norway, Sweden and the UK: a population-based study, 2004–2007," *Thorax*, vol. 68, no. 6, pp. 551–564, Jun. 2013, doi: 10.1136/thoraxjnl-2012-202297.

[9] Robert Koch-Institut, "Zentrum für Krebsregisterdaten," 2018. [Online]. Available: https://www.krebsdaten.de/Krebs/DE/Datenbankabfrage/datenbankabfrage_stufe1_node.html. [Accessed: 23-Jul-2022].

[10] S. Couraud, G. Zalcman, B. Milleron, F. Morin, and P.-J. Souquet, "Lung cancer in never smokers – A review," *Eur. J. Cancer*, vol. 48, no. 9, pp. 1299–1311, Jun. 2012, doi: 10.1016/j.ejca.2012.03.007.

[11] R. Miech, L. Johnston, P. M. O'Malley, J. G. Bachman, and M. E. Patrick, "Trends in Adolescent Vaping, 2017–2019," *N. Engl. J. Med.*, vol. 381, no. 15, pp. 1490–1491, Oct. 2019, doi: 10.1056/NEJMc1910739.

[12] L. F. Chun, F. Moazed, C. S. Calfee, M. A. Matthay, and J. E. Gotts, "Pulmonary toxicity of e-cigarettes," *Am. J. Physiol. Cell. Mol. Physiol.*, vol. 313, no. 2, pp. L193–L206, Aug. 2017, doi: 10.1152/ajplung.00071.2017.

[13] J. Shim, L. Brindle, M. Simon, and S. George, "A systematic review of symptomatic diagnosis of lung cancer," *Fam. Pract.*, vol. 31, no. 2, pp. 137–148, Apr. 2014, doi: 10.1093/fampra/cmt076.

[14] M. Alexander, S. Y. Kim, and H. Cheng, "Update 2020: Management of Non-Small Cell Lung Cancer," *Lung*, vol. 198, no. 6, pp. 897–907, Dec. 2020, doi: 10.1007/s00408-020-00407-5.

[15] B. O'Sullivan *et al.*, "The TNM classification of malignant tumours—towards common understanding and reasonable expectations," *Lancet Oncol.*, vol. 18, no. 7, pp. 849–851, Jul. 2017, doi: 10.1016/S1470-2045(17)30438-2.

[16] E. Duhig *et al.*, "The 2015 World Health Organization Classification of Lung Tumors," *J. Thorac. Oncol.*, vol. 10, no. 9, pp. 1243–1260, 2015, doi: 10.1097/jto.0000000000000630.

[17] M. S. Tsao, A. G. Nicholson, J. J. Maleszewski, A. Marx, and W. D. Travis, "Introduction to 2021 WHO Classification of Thoracic Tumors," *J. Thorac. Oncol.*, vol. 17, no. 1, pp. e1–e4, 2022, doi: 10.1016/j.jtho.2021.09.017.

[18] W. D. Travis *et al.*, "The 2015 World Health Organization Classification of Lung Tumors," *J. Thorac. Oncol.*, vol. 10, no. 9, pp. 1243–1260, 2015, doi: 10.1097/jto.0000000000000630.

[19] J.-P. Pignon *et al.*, "Lung Adjuvant Cisplatin Evaluation: A Pooled Analysis by the LACE Collaborative Group," *J. Clin. Oncol.*, vol. 26, no. 21, pp. 3552–3559, Jul. 2008, doi: 10.1200/JCO.2007.13.9030.

[20] P. Goldstraw *et al.*, "The IASLC Lung Cancer Staging Project: Proposals for Revision of the TNM Stage Groupings in the Forthcoming (Eighth) Edition of the TNM Classification for Lung Cancer," *J. Thorac. Oncol.*, vol. 11, no. 1, pp. 39–51, Jan. 2016, doi: 10.1016/j.jtho.2015.09.009.

[21] F. R. Hirsch *et al.*, "Lung cancer: current therapies and new targeted treatments," *Lancet*, vol. 389, no. 10066, pp. 299–311, Jan. 2017, doi: 10.1016/S0140-6736(16)30958-8.

[22] R. Timmerman, "Stereotactic Body Radiation Therapy for Inoperable Early Stage Lung Cancer," *JAMA*, vol. 303, no. 11, p. 1070, Mar. 2010, doi: 10.1001/jama.2010.261.

[23] R. L. Siegel, K. D. Miller, H. E. Fuchs, and A. Jemal, "Cancer Statistics, 2021," *CA. Cancer J. Clin.*, vol. 71, no. 1, pp. 7–33, Jan. 2021, doi: 10.3322/caac.21654.

[24] J.-C. Soria *et al.*, "Osimertinib in Untreated EGFR -Mutated Advanced Non–Small-Cell Lung Cancer," *N. Engl. J. Med.*, vol. 378, no. 2, pp. 113–125, Jan. 2018, doi: 10.1056/NEJMoa1713137.

[25] Y.-L. Wu *et al.*, "Osimertinib in Resected EGFR -Mutated Non–Small-Cell Lung Cancer," *N. Engl. J. Med.*, vol. 383, no. 18, pp. 1711–1723, Oct. 2020, doi: 10.1056/NEJMoa2027071.

[26] J. V. Heymach *et al.*, "Design and Rationale for a Phase III, Double-Blind, Placebo-Controlled Study of Neoadjuvant Durvalumab + Chemotherapy Followed by Adjuvant Durvalumab for the Treatment of Patients With Resectable Stages II and III non-small-cell Lung Cancer: The AEGEAN Tr," *Clin. Lung Cancer*, vol. 23, no. 3, pp. e247–e251, May 2022, doi: 10.1016/j.cllc.2021.09.010.

[27] J. D. Bradley *et al.*, "Long-Term Results of NRG Oncology RTOG 0617: Standard- Versus High-Dose Chemoradiotherapy With or Without Cetuximab for Unresectable Stage III Non–Small-Cell Lung Cancer," *J. Clin. Oncol.*, vol. 38, no. 7, pp. 706–714, Mar. 2020, doi: 10.1200/JCO.19.01162.

[28] K. S. Albain *et al.*, "Radiotherapy plus chemotherapy with or without surgical resection for stage III non-small-cell lung cancer: a phase III randomised controlled trial," *Lancet*, vol. 374, no. 9687, pp. 379–386, Aug. 2009, doi: 10.1016/S0140-6736(09)60737-6.

[29] S. I. Rothschild *et al.*, "SAKK 16/14: Durvalumab in Addition to Neoadjuvant Chemotherapy in Patients With Stage IIIA(N2) Non–Small-Cell Lung Cancer—A Multicenter Single-Arm Phase II Trial," *J. Clin. Oncol.*, vol. 39, no. 26, pp. 2872–2880, Sep. 2021, doi: 10.1200/JCO.21.00276.

[30] J. S. Temel *et al.*, "Early Palliative Care for Patients with Metastatic Non–Small-Cell Lung Cancer," *N. Engl. J. Med.*, vol. 363, no. 8, pp. 733–742, Aug. 2010, doi: 10.1056/NEJMoa1000678.

[31] N. I. Lindeman *et al.*, "Updated Molecular Testing Guideline for the Selection of Lung Cancer Patients for Treatment With Targeted Tyrosine Kinase Inhibitors: Guideline From the College of American Pathologists, the International Association for the Study of Lung Cancer, and the," *Arch. Pathol. Lab. Med.*, vol. 142, no. 3, pp. 321–346, Mar. 2018, doi: 10.5858/arpa.2017-0388-

CP.

[32] J. M. Taube *et al.*, “Colocalization of Inflammatory Response with B7-H1 Expression in Human Melanocytic Lesions Supports an Adaptive Resistance Mechanism of Immune Escape,” *Sci. Transl. Med.*, vol. 4, no. 127, Mar. 2012, doi: 10.1126/scitranslmed.3003689.

[33] Z. Y. Xu-Monette, M. Zhang, J. Li, and K. H. Young, “PD-1/PD-L1 Blockade: Have We Found the Key to Unleash the Antitumor Immune Response?,” *Front. Immunol.*, vol. 8, Dec. 2017, doi: 10.3389/fimmu.2017.01597.

[34] T. Inozume *et al.*, “Selection of CD8+PD-1+ Lymphocytes in Fresh Human Melanomas Enriches for Tumor-reactive T Cells,” *J. Immunother.*, vol. 33, no. 9, pp. 956–964, Nov. 2010, doi: 10.1097/CJI.0b013e3181fad2b0.

[35] D. M. Pardoll, “The blockade of immune checkpoints in cancer immunotherapy,” *Nature Reviews Cancer*, vol. 12, no. 4. pp. 252–264, 2012, doi: 10.1038/nrc3239.

[36] I. Le Mercier *et al.*, “VISTA Regulates the Development of Protective Antitumor Immunity,” *Cancer Res.*, vol. 74, no. 7, pp. 1933–1944, Apr. 2014, doi: 10.1158/0008-5472.CAN-13-1506.

[37] J. D. Wolchok *et al.*, “Nivolumab plus Ipilimumab in Advanced Melanoma,” *N. Engl. J. Med.*, vol. 369, no. 2, pp. 122–133, Jul. 2013, doi: 10.1056/NEJMoa1302369.

[38] L. Bracci, G. Schiavoni, A. Sistigu, and F. Belardelli, “Immune-based mechanisms of cytotoxic chemotherapy: implications for the design of novel and rationale-based combined treatments against cancer,” *Cell Death Differ.*, vol. 21, no. 1, pp. 15–25, Jan. 2014, doi: 10.1038/cdd.2013.67.

[39] P. Kvistborg *et al.*, “Anti–CTLA-4 therapy broadens the melanoma-reactive CD8 + T cell response,” *Sci. Transl. Med.*, vol. 6, no. 254, Sep. 2014, doi: 10.1126/scitranslmed.3008918.

[40] T. F. Gajewski, H. Schreiber, and Y.-X. Fu, “Innate and adaptive immune cells in the tumor microenvironment,” *Nat. Immunol.*, vol. 14, no. 10, pp. 1014–1022, Oct. 2013, doi: 10.1038/ni.2703.

[41] M. D. Hellmann *et al.*, “Nivolumab plus ipilimumab as first-line treatment for advanced non-small-cell lung cancer (CheckMate 012): results of an open-label, phase 1, multicohort study,” *Lancet Oncol.*, vol. 18, no. 1, pp. 31–41, Jan. 2017, doi: 10.1016/S1470-2045(16)30624-6.

[42] M. Provencio-Pulla *et al.*, “Neoadjuvant chemo/immunotherapy for the treatment of stages IIIA resectable non-small cell lung cancer (NSCLC): A phase II multicenter exploratory study—NADIM study-SLCG.,” *J. Clin. Oncol.*, vol. 36, no. 15_suppl, pp. 8521–8521, May 2018, doi: 10.1200/JCO.2018.36.15_suppl.8521.

[43] D. D. Petrunin, I. M. Griaznova, I. A. Petrunina, and I. S. Tatarinov, “[Immunochemical identification of human placental organ specific alpha2-globulin and its concentration in amniotic fluid].,” *Biull. Eksp. Biol. Med.*, vol. 82, no. 7, pp. 803–4, Jul. 1976.

[44] S. G. Joshi, K. M. Ebert, and D. P. Swartz, “Detection and synthesis of a progestagen-dependent protein in human endometrium,” *Reproduction*, vol. 59, no. 2, pp. 273–285, Jul. 1980, doi: 10.1530/jrf.0.0590273.

[45] S. C. Bell, S. Patel, M. W. Hales, P. H. Kirwan, and J. O. Drife, “Immunochemical detection and characterization of pregnancy-associated endometrial α1- and α2-globulins secreted by human endometrium and decidua,” *J. Reprod. Fertil.*, vol. 74, no. 1, pp. 261–270, 1985.

[46] M. L. Huhtala, M. SeppÃ¤lÃ¤, A. NÃ¤rvÃ¤nen, P. PalotmÃ¤ki, M. Julkunen, and H. Bohn, “Amino acid sequence homology between human placental protein 14 and Î²-lactoglobulins from

various species," *Endocrinology*, vol. 120, no. 6, pp. 2620–2622, Jun. 1987, doi: 10.1210/endo-120-6-2620.

[47] H. Bohn, W. Kraus, and W. Winckler, "New soluble placental tissue proteins: their isolation, characterization, localization and quantification.," *Placenta. Suppl.*, vol. 4, pp. 67–81, 1982.

[48] M. Seppälä, H. Koistinen, and R. Koistinen, "Glycodelins," *Trends in Endocrinology and Metabolism*, vol. 12, no. 3. pp. 111–117, 2001, doi: 10.1016/S1043-2760(00)00365-9.

[49] J. Garde, S. C. Bell, and I. C. Eperon, "Multiple forms of mRNA encoding human pregnancy-associated endometrial alpha 2-globulin, a beta-lactoglobulin homologue.," *Proc. Natl. Acad. Sci.*, vol. 88, no. 6, pp. 2456–2460, Mar. 1991, doi: 10.1073/pnas.88.6.2456.

[50] M. JULKUNEN, E. -M RUTANEN, A. KOSKIMIES, T. RANTA, H. BOHN, and M. SEPPÄLÄ, "Distribution of placental protein 14 in tissues and body fluids during pregnancy," *BJOG An Int. J. Obstet. Gynaecol.*, vol. 92, no. 11, pp. 1145–1151, 1985, doi: 10.1111/j.1471-0528.1985.tb03027.x.

[51] C. L. Lee *et al.*, "The Pleiotropic Effect of Glycodelin-A in Early Pregnancy," *American Journal of Reproductive Immunology*, vol. 75, no. 3. pp. 290–297, 2016, doi: 10.1111/aji.12471.

[52] P. C. N. Chiu *et al.*, "Glycodelin-A interacts with fucosyltransferase on human sperm plasma membrane to inhibit spermatozoa-zona pellucida binding," *J. Cell Sci.*, vol. 120, no. 1, pp. 33–44, 2007, doi: 10.1242/jcs.03258.

[53] M. Seppälä, H. Koistinen, R. Koistinen, P. C. N. Chiu, and W. S. B. Yeung, "Glycosylation related actions of glycodelin: Gamete, cumulus cell, immune cell and clinical associations," *Hum. Reprod. Update*, vol. 13, no. 3, pp. 275–287, 2007, doi: 10.1093/humupd/dmm004.

[54] K. K. W. Lam *et al.*, "Glycodelin-A as a modulator of trophoblast invasion," *Hum. Reprod.*, vol. 24, no. 9, pp. 2093–2103, 2009, doi: 10.1093/humrep/dep205.

[55] M. Seppälä, H. Koistinen, R. Koistinen, L. Hautala, P. C. Chiu, and W. S. Yeung, "Glycodelin in reproductive endocrinology and hormone-related cancer," *European Journal of Endocrinology*, vol. 160, no. 2. pp. 121–133, 2009, doi: 10.1530/EJE-08-0756.

[56] H. Uchida, T. Maruyama, S. Nishikawa-Uchida, K. Miyazaki, H. Masuda, and Y. Yoshimura, "Glycodelin in reproduction," *Reprod. Med. Biol.*, vol. 12, no. 3, pp. 79–84, 2013, doi: 10.1007/s12522-013-0144-2.

[57] N. A. Bersinger, M. H. Birkhäuser, M. Yared, and D. M. Wunder, "Serum glycodelin pattern during the menstrual cycle in healthy young women," *Acta Obstet. Gynecol. Scand.*, vol. 88, no. 11, pp. 1215–1221, 2009, doi: 10.3109/00016340903294264.

[58] M. Seppälä, R. N. Taylor, H. Koistinen, R. Koistinen, and E. Milgrom, "Glycodelin: A major lipocalin protein of the reproductive axis with diverse actions in cell recognition and differentiation," *Endocrine Reviews*, vol. 23, no. 4. pp. 401–430, 2002, doi: 10.1210/er.2001-0026.

[59] P. C. N. Chiu *et al.*, "Cumulus oophorus-associated glycodelin-C displaces sperm-bound glycodelin-A and -F and stimulates spermatozoa-zona pellucida binding," *J. Biol. Chem.*, vol. 282, no. 8, pp. 5378–5388, 2007, doi: 10.1074/jbc.M607482200.

[60] C. L. Lee *et al.*, "Effects of differential glycosylation of glycodelins on lymphocyte survival," *J. Biol. Chem.*, vol. 284, no. 22, pp. 15084–15096, 2009, doi: 10.1074/jbc.M807960200.

[61] A. Schiefner, F. Rodewald, I. Neumaier, and A. Skerra, "The dimeric crystal structure of the human fertility lipocalin glycodelin reveals a protein scaffold for the presentation of complex

glycans," *Biochem. J.*, vol. 466, pp. 95–104, 2015, doi: 10.1042/BJ20141003.

[62] R. Jayachandran, M. S. Shaila, and A. A. Karande, "Analysis of the Role of Oligosaccharides in the Apoptotic Activity of Glycodelin A," *J. Biol. Chem.*, vol. 279, no. 10, pp. 8585–8591, Mar. 2004, doi: 10.1074/jbc.M310480200.

[63] D. Ponnalagu and A. A. Karande, "Mapping the apoptosis inducing domain of an immunomodulatory protein: glycodelin A," *Mol. Cell. Biochem.*, vol. 377, no. 1–2, pp. 131–141, May 2013, doi: 10.1007/s11010-013-1578-x.

[64] A. Dixit and A. A. Karande, "Glycodelin regulates the numbers and function of peripheral natural killer cells," *J. Reprod. Immunol.*, vol. 137, no. January 2019, p. 102625, 2020, doi: 10.1016/j.jri.2019.102625.

[65] Y. B. L. Hansen, V. Myrhøj, and S. Sørensen, "Glycodelin is internalized by peripheral monocytes," *J. Reprod. Immunol.*, vol. 138, no. September 2019, p. 103102, 2020, doi: 10.1016/j.jri.2020.103102.

[66] P. C. N. Chiu *et al.*, "Glycodelin-S in human seminal plasma reduces cholesterol efflux and inhibits capacitation of spermatozoa," *J. Biol. Chem.*, vol. 280, no. 27, pp. 25580–25589, 2005, doi: 10.1074/jbc.M504103200.

[67] N. Gneist, G. Keck, A. Zimmermann, I. Trinkaus, E. Kuhlisch, and W. Distler, "Glycodelin binding to human ejaculated spermatozoa is correlated with sperm morphology," *Fertil. Steril.*, vol. 88, no. 5, pp. 1358–1365, Nov. 2007, doi: 10.1016/j.fertnstert.2006.12.069.

[68] R. Yanagimachi, "Fertility of mammalian spermatozoa: Its development and relativity," *Zygote*, vol. 2, no. 4, pp. 371–372, Nov. 1994, doi: 10.1017/S0967199400002240.

[69] P. C. N. Chiu, R. Koistinen, H. Koistinen, M. Seppala, K.-F. Lee, and W. S. B. Yeung, "Binding of Zona Binding Inhibitory Factor-1 (ZIF-1) from Human Follicular Fluid on Spermatozoa," *J. Biol. Chem.*, vol. 278, no. 15, pp. 13570–13577, Apr. 2003, doi: 10.1074/jbc.M212086200.

[70] C. L. Lee *et al.*, "Glycodelin-A stimulates the conversion of human peripheral blood CD16-CD56 bright NK cell to a decidual NK cell-like phenotype," *Hum. Reprod.*, vol. 34, no. 4, pp. 689–701, 2019, doi: 10.1093/humrep/dey378.

[71] N. OKAMOTO *et al.*, "Suppression by Human Placental Protein 14 of Natural Killer Cell Activity," *Am. J. Reprod. Immunol.*, vol. 26, no. 4, pp. 137–142, 1991, doi: 10.1111/j.1600-0897.1991.tb00713.x.

[72] C. L. Lee *et al.*, "Glycodelin-A as a paracrine regulator in early pregnancy," *J. Reprod. Immunol.*, vol. 90, no. 1, pp. 29–34, 2011, doi: 10.1016/j.jri.2011.04.007.

[73] U. Jeschke *et al.*, "Human Amniotic Fluid Glycoproteins Expressing Sialyl Lewis Carbohydrate Antigens Stimulate Progesterone Production in Human Trophoblasts in vitro," *Gynecol. Obstet. Invest.*, vol. 58, no. 4, pp. 207–211, 2004, doi: 10.1159/000080073.

[74] U. Jeschke *et al.*, "Stimulation of hCG and inhibition of hPL in isolated human trophoblast cells in vitro by glycodelin A," *Arch. Gynecol. Obstet.*, vol. 268, no. 3, pp. 162–167, Aug. 2003, doi: 10.1007/s00404-002-0360-1.

[75] G. Mishan-Eisenberg, Z. Borovsky, M. C. Weber, R. Gazit, M. L. Tykocinski, and J. Rachmilewitz, "Differential Regulation of Th1/Th2 Cytokine Responses by Placental Protein 14," *J. Immunol.*, vol. 173, no. 9, pp. 5524–5530, Nov. 2004, doi: 10.4049/jimmunol.173.9.5524.

[76] C. Soni and A. A. Karande, "Glycodelin A suppresses the cytolytic activity of CD8+ T lymphocytes," *Mol. Immunol.*, vol. 47, no. 15, pp. 2458–2466, Sep. 2010, doi:

10.1016/j.molimm.2010.06.008.

[77] C. Soni and A. A. Karande, “Glycodelin-A interferes with IL-2/IL-2R signalling to induce cell growth arrest, loss of effector functions and apoptosis in T-lymphocytes,” *Hum. Reprod.*, vol. 27, no. 4, pp. 1005–1015, Apr. 2012, doi: 10.1093/humrep/der477.

[78] M. K. Tee, J.-L. Vigne, J. Yu, and R. N. Taylor, “Natural and recombinant human glycodelin activate a proapoptotic gene cascade in monocyte cells,” *J. Leukoc. Biol.*, vol. 83, no. 4, pp. 843–852, 2008, doi: 10.1189/jlb.0406291.

[79] J.-L. Vigne, D. Hornung, M. D. Mueller, and R. N. Taylor, “Purification and Characterization of an Immunomodulatory Endometrial Protein, Glycodelin,” *J. Biol. Chem.*, vol. 276, no. 20, pp. 17101–17105, May 2001, doi: 10.1074/jbc.M010451200.

[80] R. E. Miller, J. D. Fayen, S. Chakraborty, M. C. Weber, and M. L. Tykocinski, “A receptor for the lipocalin placental protein 14 on human monocytes,” *FEBS Lett.*, vol. 436, no. 3, pp. 455–460, 1998, doi: 10.1016/S0014-5793(98)01184-3.

[81] C. Scholz *et al.*, “Glycodelin a induces a tolerogenic phenotype in monocyte-derived dendritic cells in vitro,” *Am. J. Reprod. Immunol.*, vol. 60, no. 6, pp. 501–512, 2008, doi: 10.1111/j.1600-0897.2008.00647.x.

[82] A. Erlebacher, “Immunology of the Maternal-Fetal Interface,” *Annu. Rev. Immunol.*, vol. 31, no. 1, pp. 387–411, Mar. 2013, doi: 10.1146/annurev-immunol-032712-100003.

[83] E. Yaniv, Z. Borovsky, G. Mishan-Eisenberg, and J. Rachmilewitz, “Placental protein 14 regulates selective B cell responses,” *Cell. Immunol.*, vol. 222, no. 2, pp. 156–163, 2003, doi: 10.1016/S0008-8749(03)00129-1.

[84] H. O. D. Critchley *et al.*, “Role of the ovary in the synthesis of placental protein-14,” *J. Clin. Endocrinol. Metab.*, vol. 75, no. 1, pp. 97–100, 1992, doi: 10.1210/jcem.75.1.1619035.

[85] M. Tulppala, M. Julkunen, A. Tiitinen, U.-H. Stenman, and M. Seppälä, “Habitual abortion is accompanied by low serum levels of placental protein 14 in the luteal phase of the fertile cycle**Supported by grants from The Academy of Finland, the Finnish Cultural Foundation and the Maud Kuistila Foundation, Helsinki, Finland.,” *Fertil. Steril.*, vol. 63, no. 4, pp. 792–795, Apr. 1995, doi: 10.1016/S0015-0282(16)57483-4.

[86] R. Focarelli *et al.*, “Dysregulation of GdA Expression in Endometrium of Women With Endometriosis: Implication for Endometrial Receptivity,” *Reprod. Sci.*, vol. 25, no. 4, pp. 579–586, 2018, doi: 10.1177/1933719117718276.

[87] H. Koistinen, L. C. Hautala, M. Seppälä, U. H. Stenman, P. Laakkonen, and R. Koistinen, “The role of glycodelin in cell differentiation and tumor growth,” *Scand. J. Clin. Lab. Invest.*, vol. 69, no. 4, pp. 452–459, 2009, doi: 10.1080/00365510903056023.

[88] L. C. Hautala *et al.*, “Altered glycosylation of glycodelin in endometrial carcinoma,” *Lab. Investig.*, vol. 100, no. 7, pp. 1014–1025, 2020, doi: 10.1038/s41374-020-0411-x.

[89] M. Kämäräinen *et al.*, “Normal human ovary and ovarian tumors express glycodelin, a glycoprotein with immunosuppressive and contraceptive properties,” *Am. J. Pathol.*, vol. 148, no. 5, pp. 1435–1443, 1996.

[90] M. A. Schneider *et al.*, “Glycodelin as a serum and tissue biomarker for metastatic and advanced NSCLC,” *Cancers (Basel).*, vol. 10, no. 12, pp. 1–12, 2018, doi: 10.3390/cancers10120486.

[91] M. A. Schneider *et al.*, “Glycodelin: A new biomarker with immunomodulatory functions in non-small cell lung cancer,” *Clin. Cancer Res.*, vol. 21, no. 15, pp. 3529–3540, 2015, doi:

10.1158/1078-0432.CCR-14-2464.

[92] C. Kunert-Keil, F. Steinmüller, U. Jeschke, T. Gredes, and T. Gedrange, “Immunolocalization of glycodelin in human adenocarcinoma of the lung, squamous cell carcinoma of the lung and lung metastases of colonic adenocarcinoma,” *Acta Histochem.*, vol. 113, no. 8, pp. 798–802, 2011, doi: 10.1016/j.acthis.2010.11.009.

[93] M. A. Schneider *et al.*, “The pregnancy associated protein glycodelin as a follow-up biomarker in a male non-small cell lung cancer patient,” *Cancer Treat. Commun.*, vol. 4, pp. 139–142, 2015, doi: 10.1016/j.ctrc.2015.09.005.

[94] R. Weber *et al.*, “Pathways regulating the expression of the immunomodulatory protein glycodelin in non-small cell lung cancer,” *Int. J. Oncol.*, vol. 54, no. 2, pp. 515–526, 2019, doi: 10.3892/ijo.2018.4654.

[95] A. Alok and A. A. Karande, “The role of glycodelin as an immune-modulating agent at the feto-maternal interface,” *J. Reprod. Immunol.*, vol. 83, no. 1–2, pp. 124–127, 2009, doi: 10.1016/j.jri.2009.06.261.

[96] S. A. Bustin *et al.*, “The MIQE guidelines:Minimum Information for publication of quantitative real-time PCR experiments,” *Clin. Chem.*, vol. 55, no. 4, pp. 611–622, 2009, doi: 10.1373/clinchem.2008.112797.

[97] A. Warth *et al.*, “The novel histologic International Association for the Study of Lung Cancer/American Thoracic Society/European Respiratory Society classification system of lung adenocarcinoma is a stage-independent predictor of survival,” *J. Clin. Oncol.*, vol. 30, no. 13, pp. 1438–1446, 2012, doi: 10.1200/JCO.2011.37.2185.

[98] A. Krämer, J. Green, J. Pollard, and S. Tugendreich, “Causal analysis approaches in Ingenuity Pathway Analysis,” *Bioinformatics*, vol. 30, no. 4, pp. 523–530, Feb. 2014, doi: 10.1093/bioinformatics/btt703.

[99] M. Seppälä, R. N. Taylor, H. Koistinen, R. Koistinen, and E. Milgrom, “Glycodelin: A major lipocalin protein of the reproductive axis with diverse actions in cell recognition and differentiation,” *Endocr. Rev.*, vol. 23, no. 4, pp. 401–430, 2002, doi: 10.1210/er.2001-0026.

[100] M. Seppälä, H. Koistinen, R. Koistinen, P. C. N. Chiu, and W. S. B. Yeung, “Glycosylation related actions of glycodelin: Gamete, cumulus cell, immune cell and clinical associations,” *Human Reproduction Update*, vol. 13, no. 3. pp. 275–287, 2007, doi: 10.1093/humupd/dmm004.

[101] E. Ish-Shalom *et al.*, “α2,6-Sialylation promotes binding of placental protein 14 via its Ca2+-dependent lectin activity: Insights into differential effects on CD45RO and CD45RA T cells,” *Glycobiology*, vol. 16, no. 3, pp. 173–183, 2006, doi: 10.1093/glycob/cwj053.

[102] L. Sawyer, “β-Lactoglobulin and Glycodelin: Two Sides of the Same Coin?,” *Front. Physiol.*, vol. 12, no. May, pp. 1–18, 2021, doi: 10.3389/fphys.2021.678080.

[103] A. Sorkin and G. Carpenter, “Interaction of Activated EGF Receptors with Coated Pit Adaptins,” *Science (80-.).*, vol. 261, no. 5121, pp. 612–615, Jul. 1993, doi: 10.1126/science.8342026.

[104] J. C. Chow, G. Condorelli, and R. J. Smith, “Insulin-like Growth Factor-I Receptor Internalization Regulates Signaling via the Shc/Mitogen-activated Protein Kinase Pathway, but Not the Insulin Receptor Substrate-1 Pathway,” *J. Biol. Chem.*, vol. 273, no. 8, pp. 4672–4680, Feb. 1998, doi: 10.1074/jbc.273.8.4672.

[105] R. A. Heller-Harrison, M. Morin, and M. P. Czech, “Insulin Regulation of Membrane-associated Insulin Receptor Substrate 1,” *J. Biol. Chem.*, vol. 270, no. 41, pp. 24442–24450, Oct. 1995, doi: 10.1074/jbc.270.41.24442.

[106] S. G. Penheiter, H. Mitchell, N. Garamszegi, M. Edens, J. J. E. Doré, and E. B. Leof, "Internalization-Dependent and -Independent Requirements for Transforming Growth Factor β Receptor Signaling via the Smad Pathway," *Mol. Cell. Biol.*, vol. 22, no. 13, pp. 4750–4759, Jul. 2002, doi: 10.1128/MCB.22.13.4750-4759.2002.

[107] J. Rachmilewitz, G. J. Riely, and M. L. Tykocinski, "Placental protein 14 functions as a direct T-cell inhibitor," *Cell. Immunol.*, vol. 191, no. 1, pp. 26–33, 1999, doi: 10.1006/cimm.1998.1408.

[108] H. Koistinen *et al.*, "Glycodelin from seminal plasma is a differentially glycosylated form of contraceptive glycodelin-A," *Mol. Hum. Reprod.*, vol. 2, no. 10, pp. 759–765, 1996, doi: 10.1093/molehr/2.10.759.

[109] T. Okazaki and T. Honjo, "PD-1 and PD-1 ligands: From discovery to clinical application," *International Immunology*, vol. 19, no. 7. pp. 813–824, 2007, doi: 10.1093/intimm/dxm057.

[110] M. Steins *et al.*, "Nivolumab versus Docetaxel in Advanced Nonsquamous Non–Small-Cell Lung Cancer," *N. Engl. J. Med.*, vol. 373, no. 17, pp. 1627–1639, 2015, doi: 10.1056/nejmoa1507643.

[111] S. M. Goldberg *et al.*, "Safety and Activity of Anti–PD-L1 Antibody in Patients with Advanced Cancer," *N. Engl. J. Med.*, vol. 366, no. 26, pp. 2455–2465, 2012, doi: 10.1056/nejmoa1200694.

[112] M. Julkunen, R. Koistinen, J. Sjöberg, E. M. Rutanen, T. Wahlström, and M. SeppäLä, "Secretory endometrium synthesizes placental protein 14," *Endocrinology*, vol. 118, no. 5, pp. 1782–1786, 1986, doi: 10.1210/endo-118-5-1782.

[113] H. R. Morris *et al.*, "Gender-specific Glycosylation of Human Glycodelin Affects Its Contraceptive Activity," *J. Biol. Chem.*, vol. 271, no. 50, pp. 32159–32167, Dec. 1996, doi: 10.1074/jbc.271.50.32159.

[114] E. L. Skornicka, N. Kiyatkina, M. C. Weber, M. L. Tykocinski, and P. H. Koo, "Pregnancy zone protein is a carrier and modulator of placental protein-14 in T-cell growth and cytokine production," *Cell. Immunol.*, vol. 232, no. 1–2, pp. 144–156, 2004, doi: 10.1016/j.cellimm.2005.03.007.

[115] G. J. Riely, J. Rachmilewitz, P. H. Koo, and M. L. Tykocinski, "alpha2-macroglobulin modulates the immunoregulatory function of the lipocalin placental protein 14.," *Biochem. J.*, vol. 351 Pt 2, pp. 503–8, Oct. 2000.

[116] S. SundarRaj, C. Soni, and A. A. Karande, "Glycodelin A triggers T cell apoptosis through a novel calcium-independent galactose-binding lectin activity," *Mol. Immunol.*, vol. 46, no. 16, pp. 3411–3419, 2009, doi: 10.1016/j.molimm.2009.07.013.

[117] K. K. W. Lam *et al.*, "Glycodelin-A protein interacts with Siglec-6 protein to suppress trophoblast invasiveness by down-regulating extracellular signal-regulated kinase (ERK)/c-jun signaling pathway," *J. Biol. Chem.*, vol. 286, no. 43, pp. 37118–37127, 2011, doi: 10.1074/jbc.M111.233841.

[118] D. Mukhopadhyay, S. Sundereshan, C. Rao, and A. A. Karande, "Placental Protein 14 Induces Apoptosis in T Cells but Not in Monocytes," *J. Biol. Chem.*, vol. 276, no. 30, pp. 28268–28273, Jul. 2001, doi: 10.1074/jbc.M010487200.

[119] A. Alok, D. Mukhopadhyay, and A. A. Karande, "Glycodelin A, an immunomodulatory protein in the endometrium, inhibits proliferation and induces apoptosis in monocytic cells," *Int. J. Biochem. Cell Biol.*, vol. 41, no. 5, pp. 1138–1147, May 2009, doi: 10.1016/j.biocel.2008.10.009.

[120] P. Sinha, V. K. Clements, and S. Ostrand-Rosenberg, "Reduction of Myeloid-Derived Suppressor Cells and Induction of M1 Macrophages Facilitate the Rejection of Established Metastatic Disease," *J. Immunol.*, vol. 174, no. 2, pp. 636–645, Jan. 2005, doi:

10.4049/jimmunol.174.2.636.

[121] J. Yan, X. Wu, J. Yu, Y. Zhu, and S. Cang, “Prognostic Role of Tumor Mutation Burden Combined With Immune Infiltrates in Skin Cutaneous Melanoma Based on Multi-Omics Analysis,” *Front. Oncol.*, vol. 10, no. November, pp. 1–13, 2020, doi: 10.3389/fonc.2020.570654.

[122] I. Hwang *et al.*, “Tumor-associated macrophage, angiogenesis and lymphangiogenesis markers predict prognosis of non-small cell lung cancer patients,” *J. Transl. Med.*, vol. 18, no. 1, p. 443, Dec. 2020, doi: 10.1186/s12967-020-02618-z.

[123] L. Li *et al.*, “Low Infiltration of CD8+ PD-L1+ T Cells and M2 Macrophages Predicts Improved Clinical Outcomes After Immune Checkpoint Inhibitor Therapy in Non-Small Cell Lung Carcinoma,” *Front. Oncol.*, vol. 11, Jun. 2021, doi: 10.3389/fonc.2021.658690.

[124] D. Y. Oh *et al.*, “Intratumoral CD4+ T Cells Mediate Anti-tumor Cytotoxicity in Human Bladder Cancer,” *Cell*, vol. 181, no. 7, pp. 1612-1625.e13, 2020, doi: 10.1016/j.cell.2020.05.017.

[125] B. J. Laidlaw, J. E. Craft, and S. M. Kaech, “The multifaceted role of CD4+ T cells in CD8+ T cell memory,” *Nat. Rev. Immunol.*, vol. 16, no. 2, pp. 102–111, Feb. 2016, doi: 10.1038/nri.2015.10.

[126] S. R. M. Bennett, F. R. Carbone, F. Karamalis, J. F. A. P. Miller, and W. R. Heath, “Induction of a CD8+ Cytotoxic T Lymphocyte Response by Cross-priming Requires Cognate CD4+ T Cell Help,” *J. Exp. Med.*, vol. 186, no. 1, pp. 65–70, Jul. 1997, doi: 10.1084/jem.186.1.65.

[127] X. Cao *et al.*, “Granzyme B and Perforin Are Important for Regulatory T Cell-Mediated Suppression of Tumor Clearance,” *Immunity*, vol. 27, no. 4, pp. 635–646, Oct. 2007, doi: 10.1016/j.immuni.2007.08.014.

[128] J. Gong, A. Chehrazi-Raffle, S. Reddi, and R. Salgia, “Development of PD-1 and PD-L1 inhibitors as a form of cancer immunotherapy: a comprehensive review of registration trials and future considerations,” *J. Immunother. Cancer*, vol. 6, no. 1, p. 8, Dec. 2018, doi: 10.1186/s40425-018-0316-z.

[129] R. A. M. Wilson, T. R. J. Evans, A. R. Fraser, and R. J. B. Nibbs, “Immune checkpoint inhibitors: new strategies to checkmate cancer,” *Clin. Exp. Immunol.*, vol. 191, no. 2, pp. 133–148, Jan. 2018, doi: 10.1111/cei.13081.

[130] A. De Sousa Linhares, J. Leitner, K. Grabmeier-Pfistershammer, and P. Steinberger, “Not All Immune Checkpoints Are Created Equal,” *Front. Immunol.*, vol. 9, Aug. 2018, doi: 10.3389/fimmu.2018.01909.

[131] L. G. Paz-Ares *et al.*, “PARAMOUNT: Final Overall Survival Results of the Phase III Study of Maintenance Pemetrexed Versus Placebo Immediately After Induction Treatment With Pemetrexed Plus Cisplatin for Advanced Nonsquamous Non–Small-Cell Lung Cancer,” *J. Clin. Oncol.*, vol. 31, no. 23, pp. 2895–2902, Aug. 2013, doi: 10.1200/JCO.2012.47.1102.

[132] M. A. Socinski *et al.*, “Weekly nab -Paclitaxel in Combination With Carboplatin Versus Solvent-Based Paclitaxel Plus Carboplatin as First-Line Therapy in Patients With Advanced Non–Small-Cell Lung Cancer: Final Results of a Phase III Trial,” *J. Clin. Oncol.*, vol. 30, no. 17, pp. 2055–2062, Jun. 2012, doi: 10.1200/JCO.2011.39.5848.

[133] Y. Cheng, T. Zhang, and Q. Xu, “Therapeutic advances in non-small cell lung cancer: Focus on clinical development of targeted therapy and immunotherapy,” *MedComm*, vol. 2, no. 4, pp. 692–729, Dec. 2021, doi: 10.1002/mco2.105.

[134] G. L. Beatty and W. L. Gladney, “Immune Escape Mechanisms as a Guide for Cancer Immunotherapy,” *Clin. Cancer Res.*, vol. 21, no. 4, pp. 687–692, Feb. 2015, doi: 10.1158/1078-0432.CCR-14-1860.

[135] M. A. Postow, M. K. Callahan, and J. D. Wolchok, “Immune Checkpoint Blockade in Cancer Therapy,” *J. Clin. Oncol.*, vol. 33, no. 17, pp. 1974–1982, Jun. 2015, doi: 10.1200/JCO.2014.59.4358.

[136] L. Paz-Ares *et al.*, “First-line nivolumab plus ipilimumab combined with two cycles of chemotherapy in patients with non-small-cell lung cancer (CheckMate 9LA): an international, randomised, open-label, phase 3 trial,” *Lancet Oncol.*, vol. 22, no. 2, pp. 198–211, Feb. 2021, doi: 10.1016/S1470-2045(20)30641-0.

[137] L. Paz-Ares *et al.*, “Pembrolizumab plus Chemotherapy for Squamous Non–Small-Cell Lung Cancer,” *N. Engl. J. Med.*, vol. 379, no. 21, pp. 2040–2051, Nov. 2018, doi: 10.1056/NEJMoa1810865.

[138] R. S. Herbst *et al.*, “Atezolizumab for First-Line Treatment of PD-L1–Selected Patients with NSCLC,” *N. Engl. J. Med.*, vol. 383, no. 14, pp. 1328–1339, Oct. 2020, doi: 10.1056/NEJMoa1917346.

[139] Y. Huang, H. J. Cho, B. E. Stranger, and R. S. Huang, “Sex dimorphism in response to targeted therapy and immunotherapy in non-small cell lung cancer patients: a narrative review,” *Transl. Lung Cancer Res.*, vol. 11, no. 5, pp. 920–934, May 2022, doi: 10.21037/tlcr-21-1013.

[140] S. Zhu *et al.*, “Combination strategies to maximize the benefits of cancer immunotherapy,” *J. Hematol. Oncol.*, vol. 14, no. 1, p. 156, Dec. 2021, doi: 10.1186/s13045-021-01164-5.

[141] J. Xiao, L. Zhou, B. He, and Q. Chen, “Impact of Sex and Smoking on the Efficacy of EGFR-TKIs in Terms of Overall Survival in Non-small-Cell Lung Cancer: A Meta-Analysis,” *Front. Oncol.*, vol. 10, Aug. 2020, doi: 10.3389/fonc.2020.01531.

[142] F. Conforti *et al.*, “Cancer immunotherapy efficacy and patients’ sex: a systematic review and meta-analysis,” *Lancet Oncol.*, vol. 19, no. 6, pp. 737–746, Jun. 2018, doi: 10.1016/S1470-2045(18)30261-4.

[143] C. J. D. Wallis *et al.*, “Association of Patient Sex With Efficacy of Immune Checkpoint Inhibitors and Overall Survival in Advanced Cancers,” *JAMA Oncol.*, vol. 5, no. 4, p. 529, Apr. 2019, doi: 10.1001/jamaoncol.2018.5904.

[144] F. Conforti *et al.*, “Sex-Based Heterogeneity in Response to Lung Cancer Immunotherapy: A Systematic Review and Meta-Analysis,” *JNCI J. Natl. Cancer Inst.*, vol. 111, no. 8, pp. 772–781, Aug. 2019, doi: 10.1093/jnci/djz094.

[145] F. Conforti *et al.*, “Sex-based differences in response to anti-PD-1 or PD-L1 treatment in patients with non-small-cell lung cancer expressing high PD-L1 levels. A systematic review and meta-analysis of randomized clinical trials,” *ESMO Open*, vol. 6, no. 5, p. 100251, Oct. 2021, doi: 10.1016/j.esmoop.2021.100251.

[146] D. C. Marquez-Garban *et al.*, “Progesterone and estrogen receptor expression and activity in human non-small cell lung cancer,” *Steroids*, May 2011, doi: 10.1016/j.steroids.2011.04.015.

[147] C. L. Clarke and R. L. Sutherland, “Progestin regulation of cellular proliferation,” *Endocr. Rev.*, vol. 11, no. 2, pp. 266–301, May 1990, doi: 10.1210/edrv-11-2-266.

[148] S. Tsuchiya, M. Yamabe, Y. Yamaguchi, Y. Kobayashi, T. Konno, and K. Tada, “Establishment and characterization of a human acute monocytic leukemia cell line (THP-1),” *Int. J. Cancer*, vol. 26, no. 2, pp. 171–176, Aug. 1980, doi: 10.1002/ijc.2910260208.

Publications, Posters, and Talks during my PhD studies

Publications

Theobald, V.; Benjamin, N.; Seyfarth, H.-J.; Halank, M.; Schneider, M.A.; **Richtmann, S.**; Hinderhofer, K.; Xanthouli, P.; Egenlauf, B.; Seeger, R.; Hoeper, M.M.; Jonigk, D.; Grünig, E.; Eichstaedt, C.A. Reduction of *BMPR2* mRNA Expression in Peripheral Blood of Pulmonary Arterial Hypertension Patients: A Marker for Disease Severity? *Genes* **2022**, *13*, 759. https://doi.org/10.3390/genes13050759

Schneider MA, **Richtmann S**, Gründing AR, Wrenger S, Welte T, Meister M, Kriegsmann M, Winter H, Muley T, Janciauskiene S. Transmembrane serine protease 2 is a prognostic factor for lung adenocarcinoma. Int J Oncol. 2022 Apr;60(4):39. doi: 10.3892/ijo.2022.5329. Epub 2022 Feb 25. PMID: 35211754; PMCID: PMC8878627.

Küster MM, Schneider MA, Richter AM, **Richtmann S**, Winter H, Kriegsmann M, Pullamsetti SS, Stiewe T, Savai R, Muley T, Dammann RH. Epigenetic Inactivation of the Tumor Suppressor *IRX1* Occurs Frequently in Lung Adenocarcinoma and Its Silencing Is Associated with Impaired Prognosis. Cancers (Basel). 2020 Nov 26;12(12):3528. doi: 10.3390/cancers12123528. PMID: 33256112; PMCID: PMC7760495.

Ercetin E, **Richtmann S**, Delgado BM, Gomez-Mariano G, Wrenger S, Korenbaum E, Liu B, DeLuca D, Kühnel MP, Jonigk D, Yuskaeva K, Warth A, Muley T, Winter H, Meister M, Welte T, Janciauskiene S, Schneider MA. Clinical Significance of *SERPINA1* Gene and Its Encoded Alpha1-antitrypsin Protein in NSCLC. Cancers (Basel). 2019 Sep 4;11(9):1306. doi: 10.3390/cancers11091306. PMID: 31487965; PMCID: PMC6770941.

Richtmann S, Wilkens D, Warth A, Lasitschka F, Winter H, Christopoulos P, Herth FJF, Muley T, Meister M, Schneider MA. FAM83A and FAM83B as Prognostic Biomarkers and Potential New Therapeutic Targets in NSCLC. Cancers (Basel). 2019 May 11;11(5):652. doi: 10.3390/cancers11050652. PMID: 31083571; PMCID: PMC6562954.

Talks and Posters

05/22	German Center for Lung Research (DZL) Mobility Grant
01/22	Translational Lung Research Center (TLRC) lecture series; **Talk**
11/21	DZL Academy Lecture; **Chair**
09/21	World Conference on Lung Cancer (virtual event); **E-Poster**
06/21	International PhD student Cancer Conference; **Talk**
01/20	DZL, Annual Meeting; **Poster and Teaser Presentation**
10/2019	World Conference on Lung Cancer; Barcelona, Spain; **E-Poster**
01/2019	DZL, Annual Meeting; **Poster and Teaser Presentation**

Danksagung

Zunächst möchte ich Prof. Dr. Ursula Klingmüller dafür danken, dass sie mich mit einem eher fremden Projekt als Doktorandin sofort angenommen und mich jederzeit in meiner Arbeit unterstützt hat. Der gesamten Gruppe B200 inklusive ehemaliger Mitglieder möchte ich für die herzliche, hilfsbereite Atmosphäre danken, die ich jedes Mal spüren durfte, wenn ich im DKFZ gearbeitet habe.

Prof. Dr. Holger Sültmann möchte ich dafür danken, dass er das Zweitgutachten übernommen hat und mich in meinen TAC Meetings mit ruhiger und freundlicher Bestimmtheit immer „Back on Track“ bringen konnte.

Bei Dr. Thomas Muley und Dr. Michael Meister bedanke ich mich sehr herzlich, dass ich in der Sektion Translationale Forschung an dem Projekt arbeiten durfte und dadurch so unglaublich viel dazulernen konnte. Dem gesamten Team der STF, insbesondere Carmen Hoppstock, Sabine Wessels, Martin Fallenbüchel und Liz Meister, möchte ich für die enorme Unterstützung (im Labor und mental) danken. Ich hatte in der STF eine wunderbare Zeit, die ich sehr genossen habe.

Ein besonderer Dank geht an Dr. Marc Schneider. Ich hätte mir keinen besseren Betreuer für meine Arbeit wünschen können, vielen Dank für jedes Gespräch, die Hilfe, den Spaß, die Unterstützung, das Vertrauen, die Akzeptanz, das Miteinander auf Augenhöhe, und und und! Ich bin so froh, dass ich mich damals zu diesem Thermomix Erlebnisabend gequält habe und dadurch zufällig an mein Praktikum in der STF gekommen bin. Oh mann, ich werde euch alle vermissen…

Ein großes Dankeschön geht an meine Mutter und meine Schwester, die mich immer unterstützen und für mich da sind. Ich hab euch lieb. Danke auch an meinen Papa, den ich gerne nochmal stolz mache und dafür alles gebe. Hab dich auch lieb.

Ich möchte mich auch bei all meinen Freunden bedanken, besonders bei Johanna für ihre mentale Unterstützung und einfach dafür, dass sie immer da ist, wenn ich sie brauche.

Außerdem danke ich natürlich Paul. Wir sind als fröhliches junges Paar hierhergezogen und ziehen als fröhliche, 9 Jahre ältere Eheleute weiter und ich bin so froh, dass du das einfach alles mitmachst und auch noch Spaß daran hast! Das ist viel wert und macht mich sehr glücklich. Und Rika <3